A HETEROGENEOUS APPROACH TO UNDERSTANDING THE MECHANISMS FOR REENTRY

A Dissertation

Presented to the Faculty of the Graduate School

of Cornell University

In Partial Fulfillment of the Requirements for the Degree of

Doctor of Philosophy

by

Frederick Barrett von Stein

August 2012

ABSTRACT

A HETEROGENEOUS APPROACH TO UNDERSTANDING THE MECHANISMS FOR REENTRY

Frederick B. von Stein, Ph.D

Cornell University 2012

This thesis presents the continuing research effort towards understanding the mechanisms in cardiac tissue that facilitate reentry, the process which is generally agreed upon to cause ventricular fibrillation. Fibrillation is an abnormal rhythm disorder where the heart does not contract in a coordinated manner to pump blood, but instead exhibits chaotic, dyssynchronous contraction characterized by the uncontrolled quivering or twitching of the muscle fibers; when it occurs in the lower chambers of the heart is it called ventricular fibrillation, which can rapidly progress to sudden cardiac death. Sudden cardiac death is the leading cause of death in the western, industrialized world, it is not fully understood and there is no known cure.

However, in recent years, the use of new technology called optical mapping has provided some interesting clues, one of which is the phenomena of cardiac muscle activation waves, responsible for contraction and which normally spread in a synchronous fashion across the surface of the heart, break into a dyssynchronous spread during ventricular fibrillation. This break in activation waves can cause the formation of spiral waves which re-activate tissue at a faster rate of uncoordinated contraction than would normally occur.

The first part of this thesis presents a useful tool for understanding cardiac wave dynamics by examining a well-known chemical oscillator: the Belousov-Zhabotinsky, or BZ, reaction. The BZ reaction serves as a chemical model of non-equilibrium thermodynamics present in biological processes such as in cardiac tissue. The chemical substrate of the BZ reaction is excitable, and can form activation waves just as those seen in the heart. These

waves can also be perturbed to form spiral waves. This visual teaching exercise was presented to students of various backgrounds and degrees of education to understand cardiac wave dynamics and elicit interest in cardiac research, and it resulted in the paper **Teaching cardiac electrophysiology modeling to undergraduate students: laboratory exercises and GPU programming for the study of arrhythmias and spiral wave dynamics**. *Adv Physiol Educ* 35: 427–437, 2011;

One prominent theory on the mechanism of fibrillation is the process of reentry, which could be facilitated by heterogeneity within the muscle itself. The second part of this thesis presents the use of silicon microprobes with ultrasonic PZT actuators to reduce penetration force to measure action potential duration in canine left ventricular tissue. Platinum electrodes patterned on the microprobe transduce intramural membrane potentials to measure action potential duration and assess the degree of heterogeneity within the ventricle wall. This technique differs from other techniques that have been used to study intramural electrophysiology in that the mid-myocardial tissue remains in a syncytium that does not electrically decouple the tissue, such as with previous studies by sharp electrode impalement, optical mapping, or patch-clamp study which require sectioning the tissue with a dermatome, or dissociation into individual cells.

The third part of this thesis examines the role that the Purkinje fiber network itself may play in participating in or initiating reentry. It is popularly held that the structure of the Purkinje network is fractal, to maximize signal transmittance in a limited volume. But closer examination shows that this is not the case, and incorporation of a fractal network into computer models to simulate the cause of fibrillation could yield a different result than a network that incorporates loop structures.

BIOGRAPHICAL SKETCH

Frederick Barrett von Stein was born to Frederick JC, and Janet E. von Stein, in April of 1979, in Mt Kisco, NY. He grew up with his two younger brothers, and later younger sister, along with many pets- dogs, cats, birds, fish, hamsters, ferrets, rabbits, and even spiders - along the way. Needless to say, he became very comfortable around animals.

He enrolled at Union College, in Schenectady, NY, where he decided to pursue his interests in physical science, taking courses in physics, biology and chemistry, while minoring in Mathematics and graduating in 2001 with a BS in Physics.

After graduation he became a research scientist at Kansas State University in the laboratory of Dr Lisa Freeman. It was here that he gained an appreciation for research, working with other scientists and graduate students. He learned a variety of experimental research techniques, and developed an interest in electrophysiology. His primary project was studying ion channels in granulosa cells by patch clamp.

Eventually, he would decide to go on to graduate school, and apply to and subsequently be accepted by the department of Biological Sciences, at Cornell University, in Ithaca NY, for a Ph.D program in Physiology in the fall of 2004.

He began work on a project in the laboratory of Dr Robert Gilmour to better understand the underlying mechanism causing ventricular fibrillation. While at Cornell, under the guidance of Dr Gilmour and others, he was able to explore many aspects of his projects, and build interdisciplinary skills: from material science and photolithography, electrical engineering and circuit design, computer science and programming to electrophysiology and optical mapping.

His future direction is to continue his interests in research, combining his skills in various disciplines and to work with others on solving problems using interdisciplinary tools.

To Zazzy, for always being there to greet me with a smile, and reminding me to stay curious, and that every day is a gift.

ACKNOWLEDGEMENTS

I would like to acknowledge Dr Lisa Freeman, for taking me into her lab and teaching me to enjoy research. Dr Robert Gilmour, for accepting me into his lab, having the patience to give me the freedom to explore my interests, and his guidance to make sure that I stayed on track and graduated. Dr Andy Zygmunt, for first teaching me in Kansas how to patch-clamp cells, and later troubleshooting technical issues with my project in Ithaca. Dr Bruce Kornreich, for company during long nights, for our great conversations, and listening. Dr Flavio Fenton, for all the help on my projects, for his humor and support, which kept me going through the years. Dr Elizabeth Cherry, for assistance with Matlab, remembering birthdays, and baking. Dr Niels Otani, for helping me over many hurdles along the way. Mark Riccio, for his help with microCT. Rupinder and Ayesa Sinha, for social excursions, their friendship, and help and support through a PhD. Nathan Ellis, for after-hours access to the physics machine shop, and his ever-cheerful attitude. Youssef el Fassy Fihry, for providing a sounding board to complain about life, sharing a viewpoint that I am not alone in my madness, and distractions keeping me sane. My brother, Richard, for too many things to list. My family, for all their support and love. My friends in Ithaca, many of whom are no longer in Ithaca, for laughing, dancing, and for all the great memories. And Mabel Thomas, for her patience and support, and believing in me.

TABLE OF CONTENTS

LIST OF ABBREVIATIONS

SCD = Sudden Cardiac Death

AHA = American Heart Association

NIH = National Institute of Health

CDC = Center for Disease Control

VF = ventricular fibrillation

ICD = implantable cardioverter-defibrillator

SA = sinoatrial

AV = atrioventricular

AP = action potential

APD = action potential duration

DI = diastolic interval

BCL = basic cycle length

CV = conduction velocity

BZ = Belousov-Zhabotinsky

MAP = monophasic action potential

LPCVD = low pressure chemical vapor deposition

PECVD = plasma-enhanced chemical vapor deposition

PZT = piezoelectric lead zirconate titanate

PCB = printed circuit board

RC = resistor-capacitor

BDM = -2,3-butanedione monoxime

HPS = His-Purkinje system

PMJ = Purkinje-muscle junction

MI = myocardial infarction

PF = Purkinje fiber

VT = ventricular tachycardia

PREFACE

1.1 – SCD & VF

Sudden cardiac death (SCD) is an unexpected death in a person with cardiac disease, caused by a loss of heart function (sudden cardiac arrest) that prevents the heart from effectively pumping oxygenated blood to the brain and body. Although mortality due to cardiac disease is in decline(Roger, Go, Lloyd-Jones, & Adams, 2011) according to recently released statistics from the American Heart Association (AHA), the Center for Disease Control (CDC) and the National Institute of Health (NIH), it remains the leading cause of death in the United States, accounting for more than 25% of all deaths. While heart disease manifests its symptoms in various forms, SCD is responsible for more than half of all heart disease deaths.

Ventricular fibrillation (VF) is the most common life-threatening rhythm disorder and is a direct cause of SCD(Zheng, Croft, Giles, & Mensah, 2001). Treatment of this fatal rhythm disorder remains difficult, largely due to an incomplete understanding of its underlying mechanism. During VF, the ventricles of the heart, normally responsible for pumping blood to the lungs and the body do not work in a coordinated fashion. Instead of contracting in unison, they dis-synchronously quiver or flutter and oxygenated blood is not delivered to the body. In the first few minutes following the onset of VF the greatest concern is that blood supply to the brain will be reduced so drastically that the person will lose consciousness. Death follows unless emergency treatment is begun immediately. Treatment of VF is the delivery of a massive electrical shock (defibrillation) via external paddles or via an implantable cardioverter-defibrillator (ICD) until normal heart rhythm resumes.

While arrhythmias such as VF are characterized as mechanical events, they are directly related to electrical malfunctions. It is these disturbances in the regular control mechanisms of electrical signal transduction that trigger the initiation of lethal arrhythmias such as VF. The primary objective of the work described in this thesis is to identify the factors responsible for the initiation and maintenance of VF, to better understand its cause so we can better prevent its occurrence.

1.2 – Reentry

In humans and large animals, the heart is comprised of four chambers: two atria, which receive blood into the heart and pre-load the ventricles, and two ventricles, which forcibly pump blood out of the heart to the lungs and the body. A specialized region of self-depolarizing cells known as the sinoatrial (SA) node is located in the right atrium. This structure is the primary pacemaker of the heart. Under normal circumstances, the SA node depolarizes a small area of tissue in the atria and this depolarization spreads over the atria, causing them to contract and pump blood into the ventricles. The atria are electrically decoupled from the ventricles except at the atrioventricular (AV) node, where the electrical signal passes into the His-Purkinje system and rapidly conducts to the ventricles. The ventricles are then activated at specific locations and contract in uniform coordination to pump the blood out of the heart. The electrical signal initiated by the SA node activates the entire heart once, before a subsequent signal is generated to repeat the process.

During normal heart rhythm the electrical impulse initiated by the SA node propagates across the tissue as a wave and elevates the voltage at each cell, producing an action potential (AP), at the same time causing the cell to contract. An action potential is characterized by the depolarization of a cell that is at rest, from a negative resting membrane potential, to a more positive potential. The transition from the rest state to the active state is followed by a third state, known as the inactive

state, before the cell can return to rest again. In this inactive, or refractory state, the cell is unable to be activated again, even if a subsequent electrical stimulus is applied.

Because of this protective feature, the propagation of an action potential wave is normally in an antegrade direction from the site of initiation, and never in a retrograde direction, because it cannot activate an area more than once until the tissue has recovered. However, in some cases a single action potential wavefront can (re)activate neighboring tissue by re-entering a region that was previously activated and has now recovered or that was not activated initially, a process known as reentry. Reentrant excitation occurs when the propagating impulse does not die out after complete activation of the heart, as is normally the case, but persists to re-excite the tissue after the expiration of the refractory period(El-Sherif, 1988). In this case, the tissue that is re-activated may have a wavefront travelling in a different direction and synchronization with the surrounding tissue, interfering with normal contraction rhythm, and causing wavebreak. While it is generally agreed that reentry is responsible for the maintenance of VF, the mechanism for the initiation and perpetuation of reentry remains uncertain.

1.3 – Excitable media, spiral waves

Reentry is not unique to cardiac arrhythmia – a similar phenomenon has been observed in other biological systems(Jalife, Delmar, & Davidenko, 1999). The common feature of all of these systems is the property of excitability, where just as in myocardial tissue, a local excitation above a threshold results in the initiation of a propagating wave akin to the cardiac action potential. These systems are called excitable media and are governed by a set of mathematical equations and provide a useful experimental technique to understand wave dynamics as well as model wave activity in cardiac tissue.

It has been demonstrated in many types of excitable media that a particular perturbation of the excitation wave can result in self-organizing patterns, with the resultant appearance of spiral wave activity. The Belousov-Zhabotinsky (BZ) reaction is an example of such a system. The BZ reaction is an oscillatory chemical reaction occurring in non-equilibrium conditions(Nagy-Ungvarai, Ungvarai, & Müller, 1993; Petrov, Crowley, & Showalter, 1994; Vanag, Yang, Dolnik, Zhabotinsky, & Epstein, 2000). It is basically a catalytic oxidation of an organic substrate (malonic acid) by bromate ions, where ferroin acts as an indicator of the process and changes from blue to red as the reaction progresses.

Like other excitable media, the BZ reaction can exist as an oscillator that changes color periodically, or it can be perturbed from a quiescent state to an excited state, as occurs when a silver wire is dipped into the reaction to trigger an outwardly propagating concentric circular blue wave. Perturbing the blue wavefront with the silver wire initiates a stable period of two counter rotating reentrant spiral waves of constant period.

1.4 – Wave break and reentry

The two-dimensional projection of rotors seen on the surface of the heart as spiral waves has been observed on both epicardial and endocardial surfaces of mammalian hearts. During *in vitro* experiments the reentrant spiral waves were seen to lead to tachycardia(Allessie, Bonke, & Schopman, 1973; Davidenko, Pertsov, Salomonsz, Baxter, & Jalife, 1992; Efimov, Sidorov, & Cheng, 1999) and fibrillation(Bonometti et al., 1995; J. Chen, Mandapati, Berenfeld, Skanes, & Jalife, 2000; Holden, Mironov, & Pertsov, 1999; Witkowski, Leon, Penkoske, & Giles, 1998). However, surface spiral waves are not always visible during fibrillation, or are only seen transiently, alluding to the

possibility that the rotors could exist beneath the surface of the heart, where they are shielded from view(Holden et al., 1999).

Substantial experimental data have bolstered the hypothesis that the onset of VF in large mammalian hearts is associated with the breakup of a single spiral wave or a pair of counter-rotating spiral waves into multiple wavelets(Karma, 1994; Riccio, Koller, & Gilmour, 1999; Weiss, Garfinkel, Karagueuzian, Qu, & Chen, 1999). Yet the mechanism by which spiral waves break and cause VF is not yet fully understood. It has been proposed that the breakup of spiral waves is precipitated by a period doubling bifurcation of action potential duration (APD), known as electrical alternans, which can be seen in cardiac tissue(Koller, Riccio, & Gilmour, 1998). Previously it has been shown by our lab(Fox, Riccio, Hua, Bodenschatz, & Gilmour, 2002a; Fox, Gilmour, & Bodenschatz, 2002b; Gilmour, 2004) and others(Echebarria & Karma, 2002; Xie et al., 2004) that alternans can occur when the relationship between the APD and the diastolic interval, known as the restitution relationship, is steeply sloped: that is, greater than one, but a steep slope does not guarantee the existence of alternans(Cherry & Fenton, 2004).

Complicating the issue is that the ventriclular wall is not a homogenous layer of cells, and may not exhibit a common APD restitution. Differences in restitution can be caused by differences in local electrophysiology within the heart, causing dispersion in refractoriness and dispersion in APD.

Dispersion of refractoriness and APD refer to the non-uniform electrical dynamics of working myocardium. Dispersion of APD would represent non-uniform action potential duration such that some areas of myocardium would have longer action potential duraction, while neighboring areas would have shorter duration. Similarly, dispersion of refractoriness would

indicate that some areas have longer refractory periods while adjacent areas are shorter. The net result of this difference in electrophysiological properties is that there is non-uniform behavior in the time-scale of the myocardium in response to a depolarization eliciting an action potential and the subsequent recovery period, therefore dictating that the myocardium will have non-uniform behavior. This can directly affect the propagation wave of excitation across the myocardium.

Therefore heterogeneity in the tissue can affect the normal propagation of electrical wavefronts, and thus alter the mechanical efficacy of the heart to work in a coordinated effort.

1.5 – Heterogeneity : Differences in Epicardium, Endocardium & M cells

It has been well established that the electrical and pharmacological properties of the epicardium differ from those of the endocardium in human and canine hearts under normal conditions: epicardium has a greater amount of the transient outward current (I_{to}) which is responsible for the characteristic spike-and-dome morphology of the epicardial action potential(Gilmour & Zipes, 1980; Sicouri & Antzelevitch, 1991; Zicha et al., 2004). Epicardium also exhibits more pronounced changes in monophasic action potentials(Taggart et al., 1988) and greater prolongation of conduction time and refractory period(Scherlag, El-Sherif, Hope, & Lazzara, 1974) than does endocardium during acute ischemia.

In addition, as you transition from the epicardial surface of the ventricle wall to the endocardial surface, recent evidence indicates there exists a sub-population of cells in the deep sub-epicardium with altered action potential kinetics(Sicouri & Antzelevitch, 1991; Solberg, Singer, Eick, & Duffin, 1974). These cells, termed M-cells, display spike-and-dome morphology similar to epicardial cells, but a maximal upstroke velocity greater than either epicardial or endocardial cells.

They also are characterized by a greater rate dependence on action potential duration(Antzelevitch & Shimizu, 1999).

One hypothesis put forth has been that differing electrical properties of the various layers through the cardiac wall produces a heterogeneous environment that can create a pro-arrhythmic environment. Because of dispersion of refractoriness and APD at various layers in the ventricle wall, a pro-arrhythmic environment may exist where some areas with shorter APD or refractory periods may no longer be refractory and would therefore be susceptible to triggered activity by after-depolarizations, while on the other hand areas with longer APD and/or refractory periods may block activation and cause reentry.

The existence and relevance of these M-cells, however, is controversial, since studying them usually requires creating "wedge preparations" (Akar & Rosenbaum, 2003; Fast, Sharifov, Cheek, Newton, & Ideker, 2002; Sharifov & Fast, 2003), whereby the wall is sectioned into layers using a dermatome. This approach is often criticized as possibly altering electrophysiological properties and augmenting or changing tissue coupling and conduction by causing damage and/or decoupling cells from their neighbors. Further, M-cells are not always observed to be present by this method.

1.6 – Silicon microprobes

To measure the intramural differences in APD while avoiding the shortcomings of the wedge preparation approach, other researchers have looked to plunge-style needle electrodes with wires threaded into them to various depths which can record from multiple sites through the cardiac wall(P. S. Chen et al., 1988). This method unfortunately causes heavy tissue damage possibly affecting normal conduction and the mechanism of ventricular vulnerability to initiation of VF. However, by this method of study, researchers concluded that the 5-mm inter-electrode

distance was inadequate to map interactions between Purkinje fibers and ventricular myocytes, which may be important in the maintenance of reentry after the onset of VF.

Silicon based microprobes have been reported for recording 3-D electrical activity in neural tissue. Recently, these neural probes have been adapted using an ultrasonically driven piezo-electric to reduce penetration force, allowing their use to probe electrical activity from dog myocardium. This reduction in penetration force allows the probes to maintain small size (40μm wide x 140μm thick) minimizing damage to the tissue while still being capable of resisting structural buckling during insertion into the muscle, penetrating the entire ventricle wall (1cm deep) and measuring extracellular local voltages. This method provides for high spatial and temporal resolution of intramural action potentials to characterize the extent of heterogeneity in intact tissue with minimal damage.

1.7 – Role of Purkinje network

Another hypothesis concerning the mechanism for initiation and maintenance of VF is that Purkinje network is not a passive component, but plays an active role in either triggering VF, and/or maintaining it. The His-Purkinje network, begins with the bundle of His which terminates at the AV node, and runs down the septum of the heart to the apex, and branches out in the Purkinje network which runs over and into the endocardium. The Purkinje network is electrically decoupled from the surrounding tissue, except at key locations known as Purkinje Muscle Junctions (PMJ) at the end of the Purkinje network. It is at these locations that electrical signal passes out of the Purkinje network and into the muscle, depolarizing it and causing a ventricular activation sequence. The activation sequence is usually orthodromic, that is, it passes out of the Purkinje fibers (PF),

across the PMJ, and into the muscle, but experimental evidence exists that show antidromic, or retrograde, activation of the Purkinje conduction system is also possible as well under certain conditions.

This retrograde activation is believed to be one method by which the Purkinje network can participate in either initiating, or maintaining arrhythmia in the heart. Other evidence that the Purkinje network plays a role in initiation of arrhythmia is that ablating the sites where Purkinje potentials are first seen to trigger VF causes the loss of Purkinje potentials and prevents the onset of Ventricular fibrillation.

Also, treating the endocardium with Lugols or Phenol has been shown to kill the Purkinje network, which raises the threshold for the onset of VF, though not preventing it entirely, while also decreasing the time to spontaneous termination of VF. Further evidence that the Purkinje network may play a role in maintaining VF is the observation that the Purkinje fibers are less sensitive to ischemia than the surrounding muscle(Friedman, Stewart, & Wit, 1973a), and are likely to be more electrically active during the global ischemia seen during long duration VF. Lastly, in dogs, where PMJs are near the endocardial surface, activation wavefronts during VF proceed from Endocardium to Epicardium, yet in pigs, where PMJs are dispersed from Endocardium to Epicardium, activation wavefronts during VF are distributed uniformly.

BACKGROUND

2.1 – History of VF

The initiation of ventricular fibrillation (VF) may well depend on several pre-existing intrinsic conditions, such as the size of the heart, as well as on dynamic conditions, such as the timing of electrical impulses. While existing conditions can be determined using specific tests, the anticipation of dynamic events is more difficult.

It has been observed that small hearts such as those of the mouse, rabbit, and cat are not as susceptible to persistent VF as larger hearts, such as in dogs and humans. In the late 1800's, McWilliam observed that "spontaneous recovery may take place readily in the hearts of the cat, rabbit, rat, mouse, hedgehog, and fowl,(McWilliam, 1888)" while the ventricles of dogs do not usually recover spontaneously from fibrillation, except in rare instances. In 1912 Erlanger published that large beef hearts fibrillate with relative ease, and that once initiated the arrhythmia seldom stops, either spontaneously or following a bolus perfusion of KCl solution. Walter Garrey noted in 1914 that "the hearts (ventricles) of large animals fibrillate with great ease and only rarely recover from the fibrillatory state, while small hearts rarely fail to recover.(Garrey, 1912)" Taking into account that fibrillation of the thin-walled atria usually is seen as transitory, while fibrillation in the thicker wall of the ventricle of the same animal is more prone to persist, he concluded that the size of the tissue involved must play a significant role; there must be a "*critical mass*" to permit the initiation and persistence of fibrillation.

The discovery of the vulnerable period of the ventricle by George Mines in 1914 unmasked one of the major electrical properties of the heart that predisposes to fibrillation. Mines identified a narrow window of time within electrical diastole during which the heart was extremely vulnerable to fibrillation. An external stimulus, or an ectopic stimulus generated from within the heart, if properly timed to fall within this window, could trigger a fatal arrhythmia and cause death. Mines also proposed the theoretical basis for the occurrence of such arrhythmias, which he called "reciprocating rhythm." Tragically, he confirmed his theory by conducting such an experiment on himself, causing ventricular fibrillation and sudden death. Drury subsequently described this arrhythmia in humans in 1924. Today, this reciprocating rhythm is called reentry.

2.2 – Reentry

The simplest form of reentry is modeled as a ring of tissue. In 1906 Mayer showed that stimulating tissue from a jellyfish initiated rhythmic contraction about the ring. When Garrey cut rings from the fibrillating ventricles of turtles he found that the fibrillation continued if the rings were broad, but ceased and gave way to regular contraction passing around the ring when the ring was narrow. He noticed that the contraction sometimes bypassed one part of the ring and other times bypassed a different part. From these observations he believed that the essential conditions of fibrillation were the occurrence of "blocks," i.e., portions of decreased conductivity and excitability occurring in alternating areas about the cut ventricle rings.

Mines conceived reentry as a mechanism for arrhythmias when he realized that reentrant arrhythmia arises from circular electrical pathways, often initiated by a blocked impulse. Reentry occurs when a propagating impulse fails to die out after normal activation of the heart and persists to re-excite the heart after the refractory period has ended. This is defined as a continuous repetitive propagation of an excitatory wave traveling in a circular path, returning to its site of origin to reactivate that site. Today reentry is believed to be the major mechanism underlying most lethal cardiac arrhythmia.

During normal cardiac muscle excitation, an electrical stimulus triggers a depolarization of tissue. This depolarization results in the opening of ion channels in the cell membrane that respond to changes in membrane voltage. The cascade of ion channel events allows current, as ions, to flow across the cell membrane, causing a signal cascade that results in the muscle contracting. This characteristic flow of charge is called an action potential. The period after an action potential is when the ion channels are in their rest states and available for re-activation, and is called the diastolic interval. The time encompassed by the action potential duration (APD) and diastolic interval (DI) is the basic cycle length (BCL). See Figure 2.1.

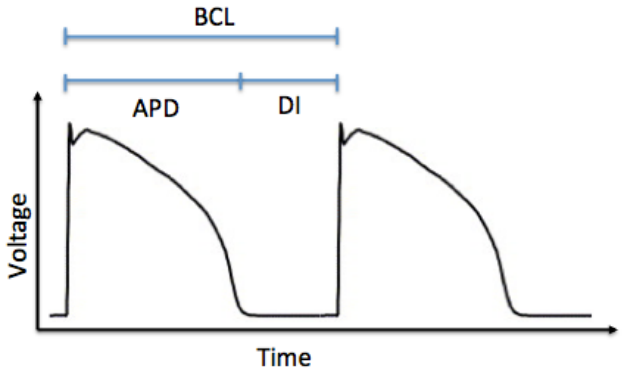

Figure 2.1 : Schematic depicting the relationship between action potential duration (APD), diastolic interval (DI), and the basic cycle length (BCL).

Crucial to the development of reentrant arrhythmias is the failure of a group of cells to activate during a depolarization wave. The initiation of a reentrant arrhythmia requires several electrophysiological characteristics of the myocardial tissue(Allessie et al., 1973; Allessie, Bonke, & Schopman, 1976; 1977), first outlined in 1920 by Lewis. Specifically, that adjacent tissue have different conduction velocity (CV) and refractoriness, such that propagation is non-uniform; the tissue must also be connected proximally and distally to form a circuit, and that both anterograde and retrograde conduction of an impulse along either pathway be possible. Because CV and refractoriness depend on many factors, these circuits may be fixed, such as around physical obstacles, or move within the tissue, due to dynamic changes in cellular electrical properties.

Due to heterogeneity of the electrophysiological properties of the myocardium, transient or permanent unidirectional block can occur within the circuit, secondary to either one of the electrical pathways having a prolonged refractory period or a prolonged repolarization time. Therefore, an electrical

impulse conducted to the proximal end of the circuit may be only able to travel down one pathway. If the conduction velocity in the normal, unblocked pathway is slow enough relative to the refractoriness of the blocked pathway to allow recovery in the blocked pathway, the impulse can then be conducted into the previously blocked pathway at the distal end of the circuit, and proceed in a retrograde direction. Lastly, to initiate reentry, retrograde conduction in the previously blocked pathway must be slow enough to allow the normal pathway to recover by the time the impulse reaches the proximal end. See Figure 2.2.

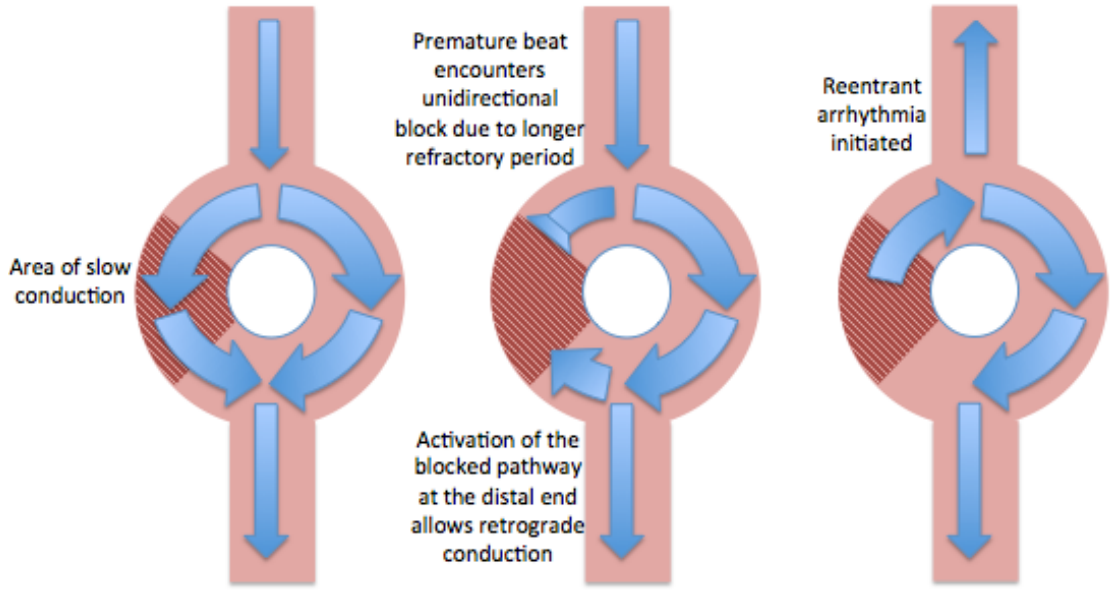

Figure 2.2 : Schematic showing a mechanism for initiation of reentry by unidirectional block

The manifestation of these reentrant circuits is seen on the surface of the heart as rotating waves of action potential, one manifestation of which is spiral waves.

2.3 – Spiral waves

In 1940 Wiggers noted the appearance of contraction waves on the surface of the heart that spread in opposing directions. In 1946 Wiener and Rosenblueth gave a theoretical description of the mechanism of initiation of fibrillation in cardiac muscle in the presence of anatomical obstacles that created a "block," as Garrey suggested. They hypothesized that wave rotation around a single or multiple obstacles was necessary to initiate and maintain fibrillation, which they assumed to be the result of a single reentrant mechanism. They also provided an explanation in the absence of such obstacles for how successive stimulation in a two-dimensional excitable sheet gave rise to a single wave propagating in one direction. Shortly thereafter, their model was modified by Selfridge in 1948 to show the formation of a persistent rotating wave in a two-dimensional medium in the absence of obstacles.

The connection between reentrant waves rotating about a site, causing re-excitation of muscle, and fibrillation seemed clear, and so scientists focused on understanding spiral wave behavior. Work done by Moe in the mid 1960's studying the mechanism of reentry initiation by shocks applied during the vulnerable phase suggested that fibrillation is a fundamentally turbulent and self-sustaining process, which takes place in a non-homogeneous excitable medium. Such a process could be initiated by an impulse propagating through the medium at a time when some of its components have recovered, while others remain partially or fully refractory as a

result of a preceding activation. Accordingly, some elements in the medium may be activated while their neighbors may not(Moe, 1964).

Moe postulated that maintenance of VF stems from the total disorganization of activity arising from randomly wandering wavefronts, ever changing direction and number. This idea of a multiple wavelet hypothesis suggests randomness in temporal and spatial distribution of membrane properties plays a role. Although the original multiple wavelet hypothesis was intended to explain atrial fibrillation, it was later assumed a similar mechanism applied to VF(Downar, Harris, Mickleborough, Shaikh, & Parson, 1988). However, today there is ample evidence that suggests wave propagation in the heart during VF is not entirely random(Garfinkel et al., 1997; Ideker et al., 1981).

Ideas regarding the spatiotemporal organization of VF have evolved since the advent of optical mapping techniques, which permit more precise characterization of wave propagation immediately preceeding and during fibrillation. In the late 1970s, Salama and Morad began pioneering work looking at voltage sensitive dyes capable of responding to changes in membrane potential, although the number of recording sites initially was limited. By the late 1980's they were able to record from 124 sites simultaneously, but they were only able to take a 'snapshot' of wave propagation. As technology advanced, high-speed cameras became available to visualize the emission spectra from the dye. Building on earlier work, Gray et al(Gray, Pertsov, & Jalife, 1998) used video imaging to record the dynamics of transmembrane potentials during fibrillation which showed the existence of spiral

waves during VF. By creating spatial phase maps, they determined that transmembrane signals at many sites exhibit a strong periodic component and revealed the sources of fibrillation in the form of phase singularities about which spiral waves rotated. Therefore, as opposed to Moe's theory on the existence of a completely chaotic state during VF, they concluded that a substantial amount of spatial and temporal organization underlies cardiac fibrillation in the heart.

It is also known that VF changes as it progresses with time(Tabereaux, Dosdall, & Ideker, 2009). Wiggers first proposed four distinct phases of VF based on epicardial motion visualized by high speed cinematography in dog hearts. His description of the four stages included an initial tachysystolic stage (<1s of VF), a convulsive incoordination stage (1-40s of VF), a tremulous incoordination stage (40s-3min of VF), followed by a progressive atonic incoordination stage (>3min of VF). Later, Huang et al performed an analysis of the epicardial activation sequence during the first 10 minutes of VF in dogs. They found that the data temporally clustered into 5 stages. Based on local VF dynamics recorded optically in pig hearts, Huizar et al(Huizar et al., 2007) classified the first 10 minutes of VF into 3 stages.

Whether the number of stages is 3, 4, 5, or some other number(Ideker, Rogers, & Huang, 2004), these distinct phases raise the possibility that there exist different mechanisms that change as VF is initiated and progresses through these stages.

The underlying mechanism(s) for fibrillation has been a matter of some debate for a number of years. Heterogeneity of refractoriness creates unidirectional

block, which is a prerequisite for reentry. Traditionally, it has been believed that unidirectional block requires an intrinsic difference in regional excitability, which is produced by electrophysiological and anatomical heterogeneities in the tissue, most often resulting from dispersion of action potential duration and refractoriness(Antzelevitch, 2000; Moe, 1964; Yan, Shimizu, & Antzelevitch, 1998). However, another theory is that heterogeneity of refractoriness and the induction of unidirectional block can arise in cardiac tissue comprised of cells having identical electrophysiological properties, secondary to the intrinsic dynamical properties of cardiac tissue(Echebarria & Karma, 2002; Fox et al., 2002a; Gelzer et al., 2008; Gilmour, 2004; 2009). Given that ample evidence exists for both theories, it seems likely that both mechanisms play key roles in the initiation and perpetuation of fibrillation(Xie, Qu, & Garfinkel, 2001).

Chemical Oscillators & Excitable Media

3.1 – The BZ reaction

Since the most life-threatening ventricular arrhythmias result from reentrant activity, which can occur around anatomic or functional obstacles, a basic grasp of the dynamics of spiral wave activity in excitable media is needed to understand reentrant activation.

The phenomena of spiral wave reentry is not unique to cardiac arrhythmia, and has been observed in other biological systems including brain, retina(Gorelova & Bures, 1983), as well as in chemical reactions. In that regard, in 1950, while studying the Krebs cycle in the USSR, B.P. Belousov discovered a chemical oscillator of citric acid and bromate that would periodically turn colorless and then return to yellow again for up to an hour. Chemical reactions do not generally display dynamic patterns or spatial order. Belousov's newly discovered chemical system showed spatial, periodic and wave properties that suggest that morphogenetic self-organization might follow similar pathways in both inorganic and organic systems - an idea that had far reaching implications on the origin of life. Consequently, his 1951 manuscript, as well as an expanded comprehensive analysis he submitted in 1957, were rejected, and never published because it opposed existing theory.

The knowledge of Belousov's reaction was not completely lost, however, and the information passed amongst scientists at various institutions. In 1962 A.M. Zhabotinsky began studying the mechanism of a citric acid reaction demonstration, unaware of the recipe's source or Belousov's work, and in 1968 he presented his

findings at the Symposium on Biological and Biochemical Oscillators in Prague. The Western literature that proceeded to study the "Zhabotinsky reaction" only later acknowledged the true origins, changing the name, and today the Belousov-Zhabotinsky (BZ) reaction is one of the most studied and well understood examples of an oscillatory chemical reaction.

The BZ reaction involves nothing more than chemical reaction and molecular diffusion. During the reaction, there is first a positive feedback effect so that a substance (bromic acid) stimulates its own formation, and an expanding volume of production spreads out. In the process, carbon dioxide is also produced, which inhibits the production of bromic acid. The BZ reaction is sufficiently complex in that it oscillates rather than settling down to equilibrium. In a flat petri dish, which models a two-dimensional space, propagating waves of bromic acid production are initiated from regions where the process gets a head start, often due to a bit of dust where the reactions are slightly accelerated, followed by a wave of inhibition. When coupled with an indicator of bromic acid production, such as Ferroin, these waves can be visualized as changes in color. See figure 3.1.

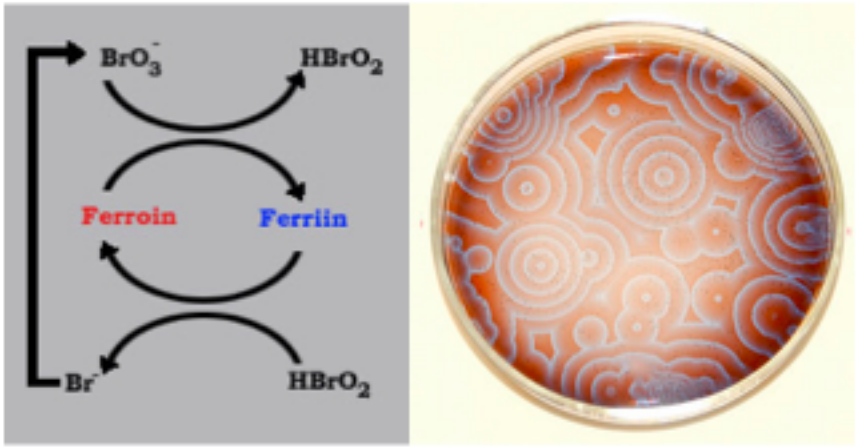

Figure 3.1 : Process by which Ferroin is converted to act as an indicator in the BZ reaction (left), and a dish with BZ fluid showing the color changes that occur within the solution as the reaction spreads (right).

The BZ reaction generates concentric rings that slowly travel outwards from centers that spontaneously arise. When expanding rings encounter one another they disappear, they do not form interference patterns, because bromic acid is inhibited behind the wave front and cannot immediately switch to production again. This situation is analogous in the heart, where cells in a refractory period are unable to be immediately activated again, and so collision of two waves leads to the annihilation of both.

If a slight shear is introduced by tipping the petri dish gently to one side, spiral waves will form and will tend to take over by displacing the concentric circles. Its initiator is a wave propagating around in a little circle at the center whose cycling time is the minimum time there can be between initiations. If the reagents are kept well-mixed by stirring, the whole system can change periodically from one state to another instantaneously, so that changes occur in time but are spatially

homogeneous. In this case, the BZ reaction settles into oscillations that make it a chemical clock, and is cited by Prigogine and Stengers as an example of self-organization.

However, if the system is not disturbed to enhance diffusion and homogenize the liquid, small heterogeneities in the mixture will result in some regions oscillating out of phase, so that some locations will change color before others. This is the principle behind propagating waves in space, where only part of the domain is excited, and the excited state advances by exciting the quiescent part of the domain adjacent to it.

3.2 – Materials & methods

To illustrate the propagation of waves a set of experiments were created using the Beluosov-Zhabotinsky (BZ) reaction(Belousov, 1959; Zhabotinsky, 1964), allowing visualization of wave propagation(Shakhashiri, 1989). The BZ reaction is made by combining three chemical solutions and an indicator to observe the formation of bromic acid. The first solution is made with sodium bromate in water to obtain a 0.23M concentration of bromate ions. The second solution is comprised of malonic acid and sodium bromide in water to a final volume equal to the first solution with a 0.31M concentration of malonic acid and a 59mM concentration of bromide. The third solution is made with cerium (IV) ammonium nitrate dissolved in 2.7M sulfuric acid to a final volume equal to the first solution to yield a concentration of cerium ammonium nitrate of 19mM.

To make the BZ reaction, the first solution is combined with second solution with the aid of a magnetic stir bar to mix. This solution will turn brown from the formation of

bromine. After the solution clears, the third solution is added along with sufficient Ferroin to reach a concentration of 0.5mM, and it can be observed that the solution will change from green, to blue, to violet, and then to red over a period of about a minute. These oscillations will persist for at least 20 minutes.

A simplistic model of a two-dimensional substrate is created by filling petri dishes with enough BZ solution to form a thin layer ~1 mm deep. Initiation of target waves due to small localized changes in concentrations can be observed. The sensitivity to initial conditions(Shinbrot et al., 1992) of chaotic systems, also known as the butterfly effect, can be noted by observation that each petri dish produces a completely different pattern, even though all petri dishes are started in a similar way.

In the heart, the propagation of electrical waves is normally initiated by the SA node or ectopic foci. This mechanism of initiation can be replicated in the BZ reaction by touching the BZ liquid with a silver wire to locally excite the system and generate propagating waves. The silver metal in the oxidizing solution forms Ag^{+}, which reacts with Br^{-} to form the precipitate AgBr. This reaction causes an excitation since Br^{-} is an inhibitor of autocatalysis. The resulting variation in concentration propagates by diffusion, and in a two-dimensional medium gives rise to an expanding annular wave, where the area of the annulus is a function of the diameter of the silver wire and the duration of time that it is in contact with the solution(Gomez-Gesteria & Fernández-Garcia, 1994).

Generation of spiral waves is also possible using a method similar to the initiation protocols for cardiac tissue known as the S1-S2 protocol or pinwheel protocol proposed by Winfree(Winfree, 2001), as modified for the BZ media. This method generates a wave

by an initial stimulus "S1," by touching the silver wire to one location of the petri dish. Then a second wave is created somewhere behind the first wave by a stimulus "S2", again using the silver wire. If this second wave is initiated at just the right distance from the wave-back of S1, it will encounter a vulnerable window(Shaw & Rudy, 1995; Starmer, 2007), where part of the system is excitable and part is refractory, which causes the second wave to propagate in only one direction initially. As the medium immediately behind the first wave recovers, the new wavefront curls, thereby initiating two counter-rotating spiral waves, as seen in Figure 3.2**.** These spiral waves will eventually take control of the system because the spiral waves have a rotational period faster than that of natural oscillation.

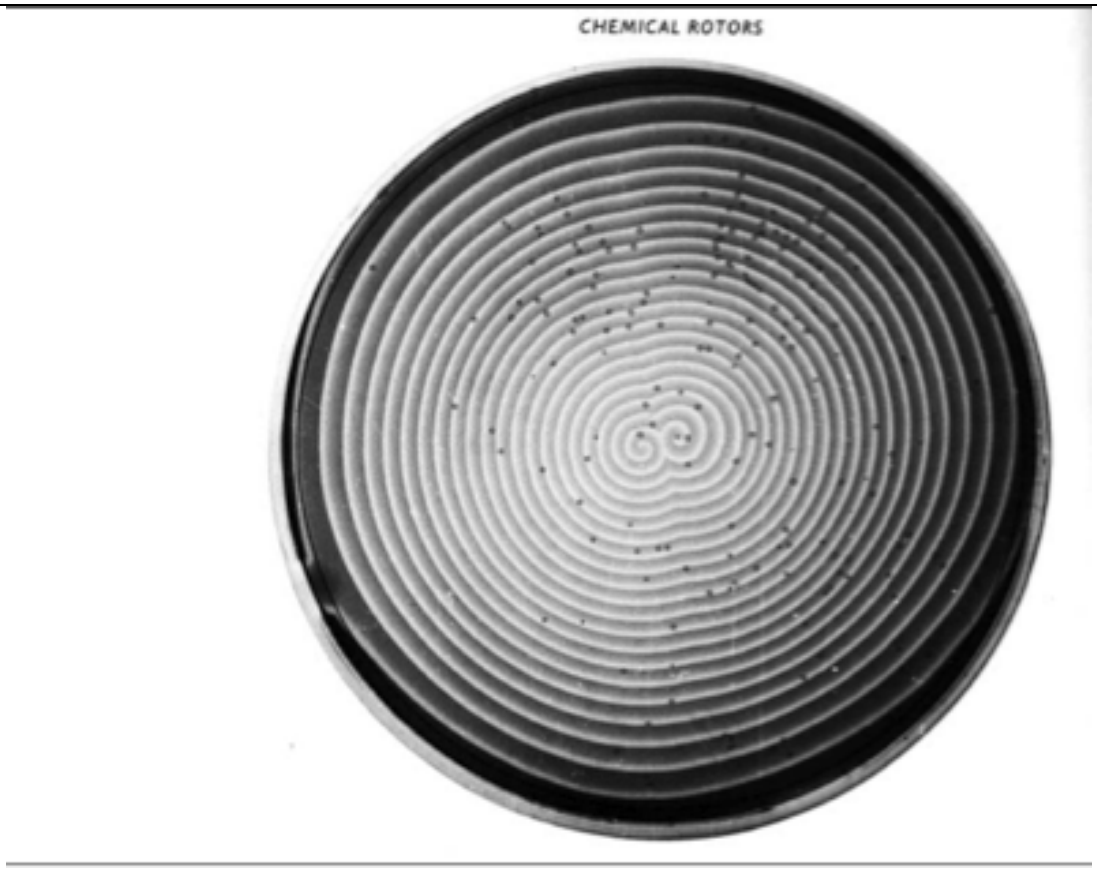

Figure 3.2 : Image from A.T. Winfree, *When Time Breaks Down*, showing a pair of mirror-image rotors expanding to fill the system.

3.3 – Results

Use of excitable media and chemical oscillators has been shown to be an effective, engaging, yet low-cost method for teaching students about excitable tissue, cardiac dynamics, wave propagation and cardiac rhythm disorders(Bartocci et al., 2011). In particular, an educational workshop module using excitable media was first given at Lehman College in the Bronx to 18 undergraduate students. Students were recruited from several campuses of The City University of New York (CUNY), of which Lehman College is one of several colleges. Although the module included some teaching of the basic theory behind complex systems from mathematical, physical, chemical, and biological points of view, most of the module centered on experiences in the lab exercises. The interdisciplinary theme of the module proved engaging for the students who themselves came from several disciplines (6 math, 4 biology, and 7 computer science majors). The module was then given to 50 masters level students majoring in engineering (30 biomedical and 20 chemical) at University Campus Bio-Medico di Roma in Italy, and then to three classes of 20 students each at the Ernie Davis Middle school in Elmira, NY.

After teaching students about simple oscillators, to demonstrate the high levels of complexity that emerge in space, chemical oscillators were used for demonstration. The use of the Briggs-Rauscher (BR) reaction was one such chemical system used that oscillates between two colors and whose period of oscillation can be changed by modifying the amount of hydrogen peroxide used in the initial conditions for the formulation of the reaction. As long as the liquid reaction remains homogenous by continuous mixing, the change in color occurs everywhere at the same time. However, if the liquid is not perturbed, small heterogeneities in the mixture will result in some

regions oscillating out of phase, so that some locations change color before others. This is the principle behind propagating waves in space, where only part of the domain is excited, and the excited state can advance by exciting the unexcited (quiescent) part of the domain. To further study wave propagation and pattern formation in excitable systems, the Belousov-Zhabotinsky (BZ) reaction was used, which is slower than that the BR reaction and lasts for several hours. The students were shown how to initiate propagating waves and even spiral waves and chaotic dynamics in two dimensional systems, as seen in Figures 3.3 through 3.5.

Figure 3.3 : Simple waves formed in a dish of BZ solution showing interference patterns.

Figure 3.4 : Complex wave behavior in BZ excitable media. Note the formation of counter-rotating spiral waves, and interference patterns.

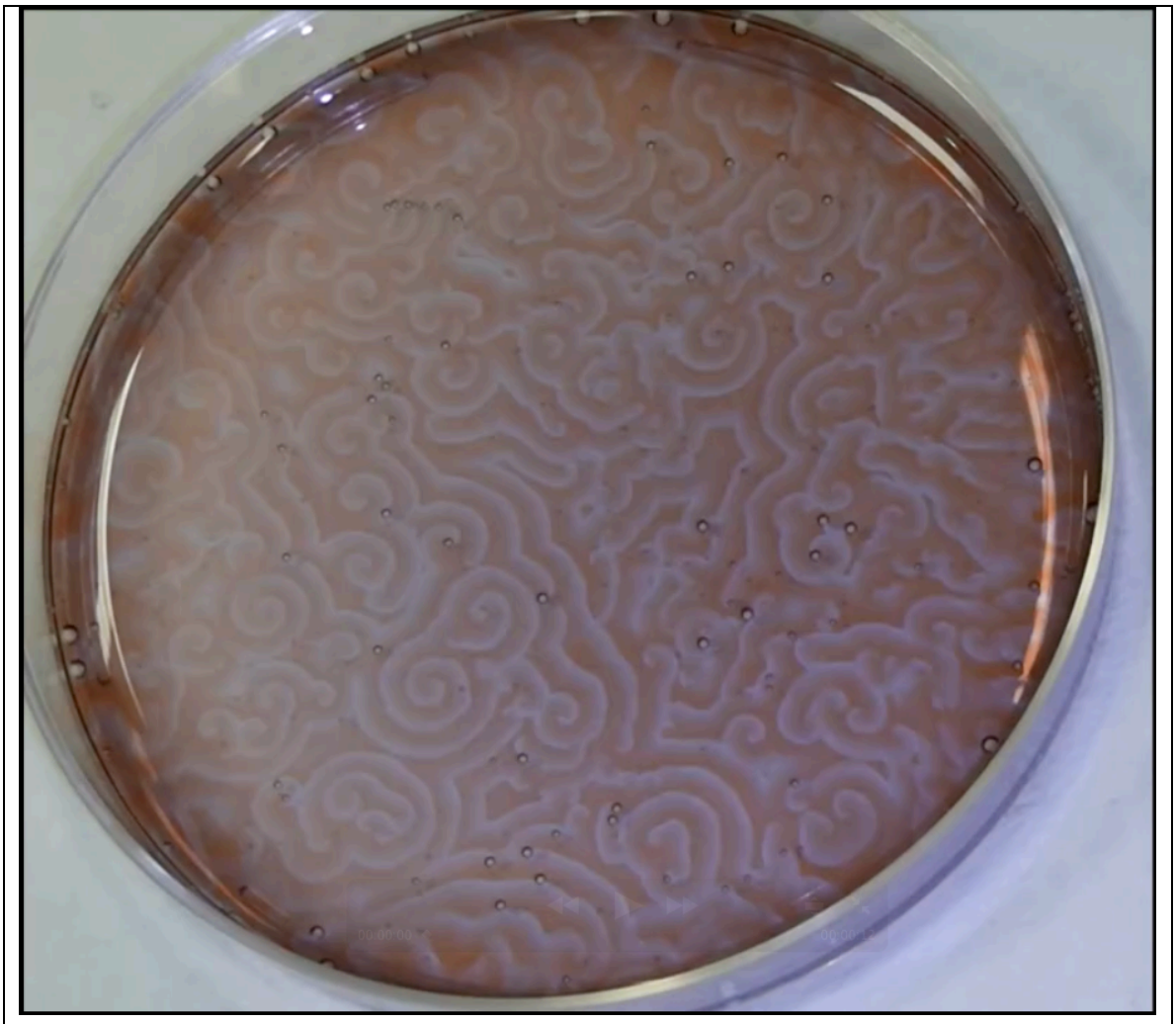

Figure 3.5 : Evolution into a more complex state. Multiple spiral waves causing wave break at many locations and chaotic interference patterns.

At the end of the chemical oscillator module students responded anonymously to a survey, the average results of which, from one of the workshops, is shown in Table 3.1 below. (1: strongly disagree; 5: strongly agree).

Table 3.1 : Average results of module as reported by students in an anonymous survey.

1. The workshop helped me to better understand dynamical systems.	4.26
2. The workshop helped me to understand the connection between the theory and the mathematics learned in class and systems that occur in real life.	4.11
3. The use of models and simulation improved my understanding of the studied biological processes.	4.11
4. The workshop helped me to understand how parameters changes influence the response of physical, chemical and biological systems.	4.42
5. Did you find the course module useful and how?	95% Yes
6. The course module made me more interested in continuing studying complex dynamical systems.	4.16
7. The course module helped me to understand how to formulate and examine scientific hypotheses.	4.2
8. I feel more confident of my ability to do scientific or technical work as a result of attending the course module.	5.0

Although the entire workshop also included other modules, including a section with a saline oscillator to understand excitable tissue and pacemaker functionality, and a section to learn about the relationship between spiral waves and arrhythmias using computer simulations, a feedback form from the students asked the following questions about the workshop in general, and the average results are shown (scored on a 5 point scale).

Table 3.2 : Average scores from entire workshop on excitable tissue as reported by students in an anonymous survey.

The workshop helped me to understand how atrial fibrillation happens.	4.21
The workshop helped me to understand how to analyze and use models of biological processes.	4.28
The use of models and simulation during the workshop improved my understanding of biological processes.	4.28
The workshop helped me to understand how to construct and use models of biological processes.	3.78
The workshop helped me to understand how to verify properties of biological processes.	3.92
The workshop helped me to understand how to formulate and examine scientific hypotheses.	4.07
I feel more confident of my ability to do scientific or technical work as a result of attending the workshop.	4.62
The workshop was a worthwhile way of spending my time.	4.85
I would be interesting in attending another such workshop.	4.92
Attending the workshop helped me to understand how scientific research works.	4.86
The workshop made me more interested in continuing my schooling in a scientific, technical, engineering, or mathematical field.	4.86

3.4 – Conclusion

Chemical oscillators can be used to demonstrate complex dynamics that are also found in cardiac systems. The excitable media and chemical oscillator workshop module used to demonstrate the dynamics found in cardiac tissue were both engaging and

informative to a range of academic levels, from middle school to a masters in engineering. Such a workshop module can be an effective teaching tool, piquing curiosity of and broadening interest in research and understanding cardiac arrhythmias.

MEASURING DISPERSION OF APD ACROSS INTACT CANINE VENTRICLE

4.1 – Intrinsic Heterogeneity

As described previously, closely co-localized areas with different action potential durations, which correspond to long and short refractory periods, may form the substrate for unidirectional block, a prerequisite for reentry. Dispersion of action potential duration and of refractory period therefore play a major role in arrhythmogenesis. Moreover, a short action potential duration may promote the occurrence of reentrant arrhythmias(Mines, 1914), whereas a long action potential duration underlies triggered arrhythmias induced by early afterdepolarizations(Verkerk, Tan, Kirkels, & Ravesloot, 2003). Therefore, heterogeneity of the myocardium with respect to conduction velocity, action potential duration, and refractory period could provide a substrate for reentrant arrhythmias.

It has been appreciated for several decades that electrical heterogeneity exists in ventricular tissue. Transmural dispersion of refractory periods in the canine ventricular wall was shown by Van Dam and Durrer(VANDAM & Durrer, 1961) as early as 1961. Work done by Solberg et al(Solberg et al., 1974) with glass microelectrodes on intramural papillary muscle in the mid 1970's showed that sectioned ventricle tissue displayed differing maximal rates of rise of the AP upstroke, as well as differing APD across the ventricle wall.

It has been well established that the electrical and pharmacological properties of the epicardium differ from those of the endocardium in human and canine hearts under normal and disease conditions. Recently, a third type of cell in the deep subepicardium with electrical properties that differ from those of either epicardium or endocardium has been identified(Sicouri, 1991). These midmyocardial cells, called M cells, exhibit substantially longer APD than epicardial or endocardial myocytes, a feature that has been attributed to their smaller I_{Ks} current, but larger late sodium and sodium/calcium exchanger currents(Antzelevitch et al., 1991b). The M cell has been proposed to underlie the electrophysiological basis for transmural dispersion of repolarization(Akar, Yan, Antzelevitch, & Rosenbaum, 2002). This stands in contrast to the existing belief that APD shortens monotonically in the direction of propagation (endocardium to epicardium).

The discovery of the M cell was accomplished by creating 'wedge' preparations by cutting the canine ventricle perpendicular to the surface to gain access to midmyocardial cells, from which transmembrane potentials could be measured using glass microelectrodes(Sicouri & Antzelevitch, 1991). It was noted initially that the maximal APD gradient consistently resided at the epicardial-midmyocardial surface, and maximum transmural APD difference was 30-50ms. Based on impalements from relatively sparse recording sites along the cut surface of a wedge of ventricular myocardium, it was suggested that the transmural APD profile was characterized by discrete midmyocardial zones possessing myocytes

with longer APD(Antzelevitch, Sicouri, & Litovsky, 1991a; Liu, Gintant, & Antzelevitch, 1993).

However, in intact myocardium, electrotonic coupling between myocytes was later predicted to smooth transmural gradients in APD(Viswanathan, Shaw, & Rudy, 1999). El-Sherif et al(El-Sherif, Caref, Yin, & Restivo, 1996) used sixty four 21-gauge plunge-needle electrodes to measure transmural activation recovery intervals (ARIs)- which can be used to determine APD. They showed that the transmural APD difference was also on the order of 30ms, but that the greatest gradient resided in the deep subendocardial region, between the endocardial-midmyocardial surface.

The first optical maps of the transmurally-cut surface to measure dispersion of APD were recently reported by Akar and Rosenbaum(Akar et al., 2002). They found that under disease conditions or heart failure, mean APD increased, but importantly showed that complex topographical patterns of M cells can occur; instead of forming bands across the midmyocardial region, M cells can form isolated islands or clusters, which was later confirmed in humans(Glukhov et al., 2010).

To date, the role of M cells in normal cardiac function has not been understood, but they provide a useful explanation for a mechanism that promotes pathologic heterogeneities of repolarization and arrhythmogenesis in disease(Wilson, Jennings, & Rosenbaum, 2011). The controversy over M cells is not on their existence, which has been well demonstrated to exist in human, canine and other mammalian hearts by multiple groups, but on their phenotypic expression in

the intact, electrically coupled myocardium, and their relative importance in determining dispersion of repolarization in the heart.

4.2 – Dynamic heterogeneity

The restitution hypothesis was first put forward by Nolasco and Dahlen(Nolasco & Dahlen, 1968) in 1968, where they intuitively explained the relationship between APD alternans and APD restitution slope. APD restitution refers to the relationship between APD and the previous DI, such that $APD_{n+1} = f(DI_n)$, where f is the function relating the new APD (APD_{n+1}) to the previous DI (DI_n). This relationship can be measured experimentally by pacing at a given cycle length (CL) and plotting APD versus DI as the heart rate increases. Drawing an analogy to electronic feedback circuits, Nolasco and Dahlen used a simple graphical method to demonstrate that sustained APD alternans is possible when APD restitution slope is greater than 1, whereas if the slope was less than 1, alternans was not possible.

Whether APD alternates at a given CL depends on whether this equilibrium point is stable or unstable. It can be shown(Nolasco & Dahlen, 1968) that if the slope of the APD restitution curve at its intersection with the CL line is <1, APD alternans will be transient and return to the stable equilibrium point over successive beats. However, if the slope is >1, the equilibrium point is unstable, and the amplitude of APD alternans will grow. This can either lead to 2:1 block or to stable APD alternans.

Although conceptually very useful and well supported by computer simulations, this analysis of APD alternans has several limitations when applied to real cardiac tissue because the cellular and molecular mechanisms of APD

restitution and APD alternans are multifactorial(Shiferaw, Chen, & Garfinkel, 2006), depending not only local state of the membrane, but also on the curvature of the wavefront, the state of the neighboring cells, and on the nature of the intercellular coupling. The assumption that APD is solely a function of the previous DI is an oversimplification because the pacing history is also important (termed short-term cardiac memory). Memory effects have been shown to limit the reliability of the APD restitution slope criterion in predicting the onset of APD alternans(Tolkacheva, Schaeffer, Gauthier, & Krassowska, 2003). However, it has been possible to predict a wide variety of rhythms exhibited by periodic stimulation of cardiac tissue from the unidimensional APD restitution relation(Chialvo, Michaels, & Jalife, 1990; Guevara, Alonso, & Jeandupeux, 1989; Jalife, 1990; Lewis & Guevara, 1990).

Cardiac alternans may be spatially concordant or discordant. During spatially concordant alternans all regions of the tissue alternate in phase with each other, while spatially discordant alternans display some regions of tissue alternating in a long-short-long pattern, whereas other regions simultaneously alternate in a short-long-short pattern. These out of phase regions are separated by a nodal line, in which no alternans is present(Shiferaw et al., 2006). At a nodal line, the spatial gradients in APD amplitude are the steepest, predisposing to localized conduction block, particularly during sustained high-frequency pacing(Qu, Shiferaw, & Weiss, 2007).

Spatially discordant APD alternans is more arrhythmogenic than concordant APD alternans(Qu, Garfinkel, & Chen, 2000). This is because discordant alternans

amplify dispersion of refractoriness, producing a favorable substrate for initiation of re-entry by an ectopic beat. If the tissue is heterogeneous so that some regions are more likely to develop APD alternans(Wan, Laurita, Pruvot, & Rosenbaum, 2005) then reentry can occur even in the absence of an ectopic beat(Cao, Qu, Kim, Wu, & Garfinkel, 1999). Reentry occurs because as APD alternans increases in magnitude, resulting in local conduction block of the subsequent wave (with short APD), while unblocked waves in adjacent regions with lower susceptibility to APD alternans can re-enter into the blocked region, producing reentry. This is the classic mechanism by which rapid pacing results in VF. Consequently, heterogeneity of APD restitution increases the occurrence of spatially discordant alternans, dynamically enhancing dispersion of refractoriness, which could play a significant role in the generation of reentrant arrhythmias.

In summary, heterogeneity of the electrical properties in myocardium can be intrinsic, or dynamic. Intrinsic heterogeneity of APD, CV, or refractoriness can create unidirectional conduction block, and facilitate the initiation of reentrant excitation. If the tissue is heterogeneous in APD restitution, then a dynamic contribution to dispersion of APD and refractoriness can contribute to the creation of block and re-entry.

- Hypothesis: Intrinsic heterogeneity of the electrical properties of ventricular tissue, secondary to the presence of cells in the mid-myocardium having different propensities for developing discordant APD alternans, renders the myocardium more susceptible to reentry.

To test this hypothesis, a minimally invasive method to measure transmural action potentials is required.

4.3 – Silicon microprobes

The first intramural recordings of cardiac electrical activation were made by Durrer and van der Tweel(Durrer & Van Der Tweel, 1953) in 1953. They used purpose-built hypodermic needle probes with which extracellular potentials were measured at sites along the needle via ultra-fine wires introduced through the needle lumen. This technique has since been used by a number of investigators(Kerber, Spencer, Kallok, & Birkett, 1994; Pope, Sands, Smaill, & LeGrice, 2008; Selvester, Kirk, & Pearson, 1970). By increasing the number of needles inserted through the heart wall, the transmural spread of electrical activation has been mapped in three dimensions, revealing details of normal and arrhythmic propagation(Arnar, Bullinga, & Martins, 1997; P. S. Chen et al., 1988; Frazier et al., 1988).

There are limitations, however, in relating extracellular potential signals to underlying cellular electrical activity. Extracellular signals represent the integrated effects of membrane currents over a relatively large volume, and distinguishing near from far electrical events is often difficult(Hooks, LeGrice, Harvey, & Smaill, 2001). As a consequence, activation and recovery, the two most basis characteristics of propagation, cannot be identified reliably at the site of recording from unipolar or bipolar electrograms for conditions other than uniform propagation(Steinhaus, 1989).

Since the early 1970s, when it was first demonstrated by Wise et al(Wise, Angell, & Starr, 1970), researchers have been interested in the use of microelectronic fabrication techniques for the manufacture of thin-film microelectrodes for use as transducers between tissue and electronic signals. Using photolithography technology pioneered in Silicon Valley for microchip design, silicon-based microprobes have been reported for 3D electrical activity recording in neural tissues(Ensell, Banks, Ewins, Balachandran, & Richards, 1996; Kewley, Hills, & Borkholder, 1997; Najafi, 1986; Najafi, Wise, & Mochizuki, 1985; Tae Hwan Yoon et al., 2000). Such probes provide high spatial resolution, reduced tissue damage, and easy integration with microelectronics.

Although the use of silicon microprobes for neural signal recording has gained in popularity, the application of silicon microprobes for use in cardiac tissue presents new challenges: neural tissue is much softer than cardiac muscle and increased resistance to penetration would necessitate larger, more durable probes capable of withstanding the increased forces exerted during impalement. Thicker probes will cause more damage and may disrupt the inherent electrophysiological activity of the tissue that one is attempting to measure.

More recently, researchers have extended the use of microfabricated silicon surgical tools by using ultrasonic actuation to reduce cutting force on biological tissues(Lal, 1998; Son, Lal, & Hubbard, 2001). Combining these technologies to create ultrasonically actuated silicon microprobes, researchers have further developed probes for extracellular transmural cardiac signal recording(X. Chen, Lal,

& Riccio, 2004; X. Chen, Lal, Riccio, & Gilmour, 2006) with a minimal width of 200µm, thickness of 60µm to 80µm, and length of 5mm (See Figure 4.1). In comparison, 32 gauge wire is roughly 200 microns in diameter, while 40 gauge wire is approximately 80 microns in diameter, and a 21 gauge needle used for plunge electrodes is 820 microns in diameter.

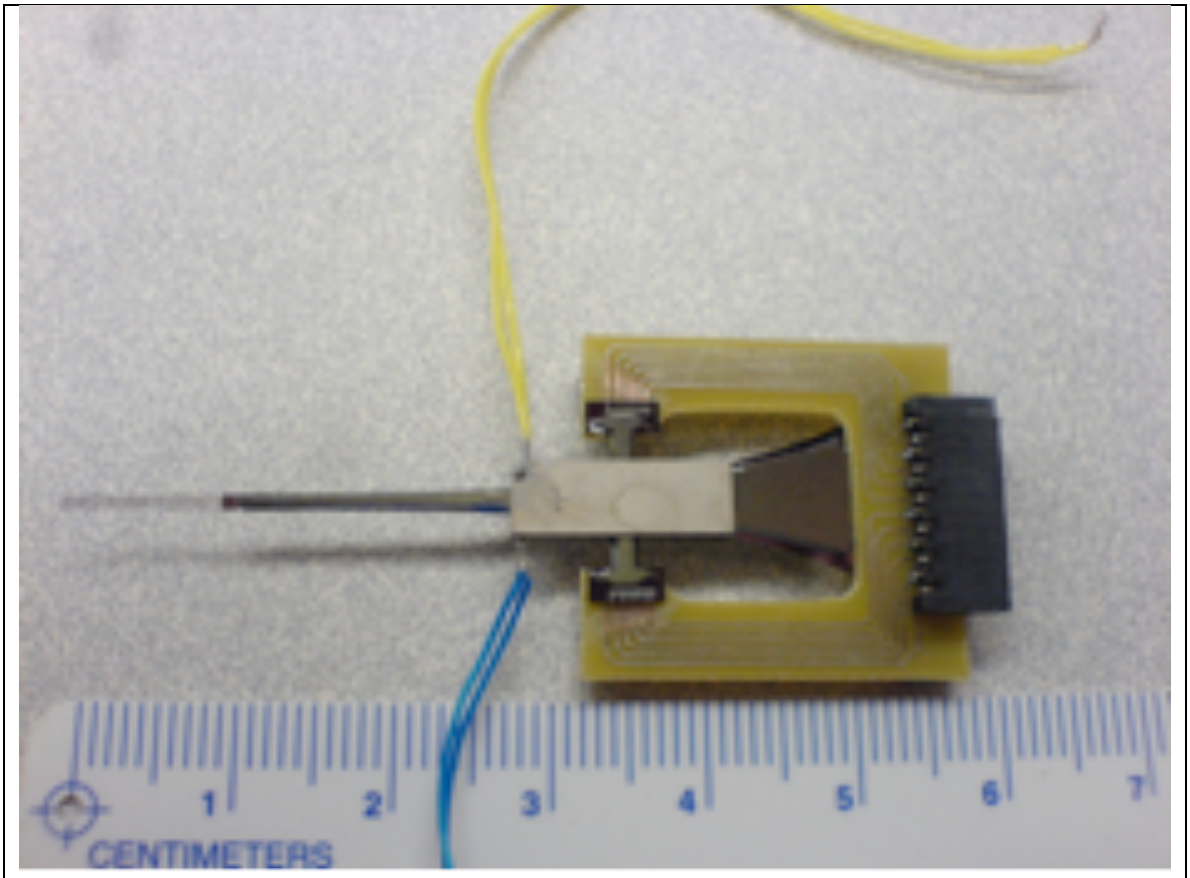

Figure 4.1: a completed, catenary horn-shaped silicon microprobe, with PZT-4 plates centered at the ½ wavelength node, and attached to a PCB with ribbon connector.

These ultrasonic silicon microprobes (USM) can be fabricated to penetrate the full thickness of the ventricle wall, with multiple sampling sites to record transmural monophasic action potentials with high spatial and temporal resolution,

while minimizing size to reduce disruption to the normal electrophysiological activity.

4.4 – History of MAP potentials

The basic function of electrodes for biological applications is to serve as transducers between physiologic and electronic systems(Kovacs, 1994). In the biological environment, bioelectric potentials are carried in electrolytic media in the form of ionic currents. The purpose of the electrode is to transduce these signals to and from electronic signals.

It has been observed that, when measuring the difference of potential between a small macerated cardiac area and an intact one, the injured region shows negativity in relation to the intact one. The resulting potential has been called an "injury potential" (Guyton, 1985). The probable explanation for the existence of this potential is that injury destroys the selective permeability of the cellular membrane, reducing the membrane's electrical resistance, so that an electrode placed in the injured region contacts the cellular cytoplasm through a fluid filled pathway of relatively low resistance. (Sperelakis, 1979)

In 1883, Burdon-Sanderson and Page published some of the earliest records of injury potentials, showing recordings of the potentials generated by frog heats(Burdon-Sanderson & Page, 1883). In one of their studies, when an electrode was placed on the intact surface of the heart and another on an injured region, a transitory monophasic potential (having only one polarity) was recorded despite the known transitory multiphase recordings (positive and negative polarities). This

was the origin of the term monophasic action potential (MAP), whose form was very similar to the cellular action potential later obtained using the cellular impalement technique with glass microelectrodes.

In the late 1930s, impaling giant squid axons with electrodes became a powerful experimental tool that provided a direct measurement of the electrical potential difference between the interior and exterior of a single cell. (Cole, 1939) In 1949 the cellular impalement technique was applied to cardiac cells by Coraboeuf and Wiedmann(Coraboeuf & Weidmann, 1949) and in 1950 by Woodbury et al(WOODBURY, Woodbury, & Hecht, 1950).

MAP recordings from suction electrodes and transmembrane potentials were compared as early as 1960(Hoffman & Cranefield, 1959), in perfused rabbit hearts, and it was found that although there were some quantitative differences between the two, the monophasic record provided an adequate representation of the voltage-time course of the plateau and phase 3 repolarization(Hoffman, 2000). Cardiac action potentials recorded from glass microelectrodes were compared with metal microelectrodes and it was determined that APD and slope of AP closely correlated, but metal microelectrodes were more stable for long-term recordings in vitro. (Omichi et al., 2000)

In 1966, Korsgren et al introduced a suction electrode that captured monophasic potentials, not requiring the production of a specific myocardial lesion. This technique was improved by Olsson(Olsson, 1971) as well as others(CHURNEY & OHSHIMA, 1964; Shabetai, Surawicz, & Hammill, 1968). In 1986, Franz et al

produced an electrode-catheter which could record a stable and high-quality MAP from myocardium with simple contact.(Franz, Burkhoff, Spurgeon, Weisfeldt, & Lakatta, 1986) The MAP was once again a useful technique for studying cardiac electrophysiology. However, despite the fact that these measurements have been used for many years, there is still controversy regarding the origin of the MAP signal. (Coronel et al., 2006)

The MAP is an extracellular recording and only records potentials that are generated by current flowing in the extracellular space, which is caused by differences in transmembrane potential generated during propagation of electrical impulse. As in every extracellular recording, the MAP reflects the potential difference between two recording sites, which are recorded by the exploring (or depolarizing/different) electrode and a reference (or indifferent) electrode. By convention, the exploring electrode is usually connected to the positive input of a differential amplifier and the indifferent electrode is connected to the negative input.

Recently, various papers have been published debating the question of which of the two electrode terminals used in the MAP catheter actually records the MAP(Franz, 2005; Kondo, Nesterenko, & Antzelevitch, 2004; Vigmond, 1999). A controversy exists about the site of origin of the monophasic complex in a MAP Some investigators believe that it is generated at the non-depolarized area if a KCL electrode is used as a 'reference' electrode connected to the positive input of the amplifier, allowing intramural MAP recordings. (WEISSENBURGER, NESTERENKO, & Antzelevitch, 2000)

To resolve this controversy, Coronel et al(Coronel et al., 2006) simultaneously recorded unipolar electrograms and MAPs in isolated blood-perfused porcine hearts with the stimulating electrode, a multi-electrode recording array, and the reference electrode in different geographical configurations. Their results indicate that signals are recorded at both the exploring and the reference electrode, which leads to confusion and controversy.

Coronel et al(Coronel et al., 2006) showed that there are two components recorded by an MAP: a local electrogram and a remote component. Location of the reference electrode in relation to the exploring electrode, as well as orientation of the reference electrode and exploring electrode to the location of the stimulus affects the recorded signal morphology. Superimposing the two components of the MAP signal has been at the root of the confusion as to which electrode is recording the MAP. Coronel et al contend that a MAP is bipolar recording, which is in agreement with Franz and Vigmond(Franz, 1983; Vigmond, 1999), and that the monophasic component is recorded at the depolarizing electrode, and conclude that MAPs should be recorded with the two electrodes positioned as closely as possible, as proposed by Franz(Franz, 2005).

Subsequent work by Zhang and Mazgalev(Zhang & Mazgalev, 2009) showed that the MAP signal was complex and consisted of components from both electrodes. Their simplistic approach to the solution was to place one recording pole on the atria, and one recording pole on the ventricle - tissues that are not activated simultaneously and have distinct cellular action potentials. They observed that the

timing and morphology of the MAP signal derives from the tissue below the depolarizing (KCl) electrode. Further, as the indifferent electrode is placed further away from the exploring electrode, a remote component can contaminate the local component of the MAP recorded by the exploring electrode..

The importance of these findings should be taken into account when designing experimental methods to accurately record local transmural potentials from silicon microprobes.

4.5 – Materials & methods

4.5.1 – Probe fabrication

Photolithographic masks for silicon-based microprobes were custom designed. The catenary horn shape was generated by code written in Matlab and exported to L-Edit software for mask creation where the fixture arms and microprobe tips were added. Six masks were generated for patterning metal recording sites and interconnect wires, for an overlay metal ground plane, for etching the recording sites from the nitride passivation and insulation layers, an etch mask to outline the shape of the microprobe and set the thickness of the tips, a wet etch release mask, and a "dummy" mask without microprobe tips to create symmetry in the vertical plane of the microprobe.

Probes were constructed according to Xi et al. Briefly, 500μm thick, 100mm diameter silicon wafers are used as a substrate. The first step is to deposit onto the wafer via low pressure chemical vapor deposition (LPCVD) a 600nm layer of silicon

nitride which acts as electrical insulation and wet-etch mask. Then, using standard lithography techniques, a 30nm chrome adhesion layer and a 250nm platinum layer is evaporated onto the wafer to form the metal layer that will be patterned to form the electrodes, interconnect wires, and bonding pads for packaging the device. Then a 1μm insulation layer of plasma-enhanced chemical vapor deposition (PECVD) nitride is deposited onto the wafer on top of the metal features. Another 30nm Cr / 250nm Pt 'ground' layer is deposited over the electrode interconnects to reduce noise and cross talk between channels. Then a 1μm passivation layer of PECVD nitride is evaporated onto the wafer over the ground layer, and windows are etched over the recording electrodes and bonding pads. Deep Reactive Ion Etching (DRIE) is performed on the front of the wafer to define the shape and thickness of the two tips at the end of the ultrasonic horn. Then a 30% potassium hydroxide solution is used to etch through the silicon from the backside of the wafer to produce and release the microprobe.

The shape of the ultrasonic horn was designed based on an optimized geometry to transmit the ultrasonic activation down to the tips. It is 10cm long, 10mm wide at the back end, and 1mm wide at the front end. The microprobe tips at the end of the horn are of negligible mass and minimal dimensions that such that they do not significantly affect the resonance mode of the ultrasonic horn. The tips are 1cm long, 200μm wide, and 140μm thick. There are five electrodes patterned on each microprobe tip, forming a 2x5 array. Each electrode has a surface area of 40μm by 40μm for sampling local electrical activity, and is aligned along the center of the microprobe tip, with a separation between each electrode of 2mm.

The ultrasonic horn with microprobe tips is bonded to a second silicon horn without probe tips to produce symmetry in thickness of the horn above and below the plane of the tips. This arrangement ensures that the major resonance mode of the horn is in the longitudinal direction. Two piezoelectric lead zirconate titanate (PZT-4) plates 0.5mm thick are cut to size such that the $\lambda/2$ longitudinal resonance of the PZT bars matches the resonance of the silicon horn for effective actuation. These PZT-4 plates are bonded to either face of the ultrasonic horn at the half wavelength displacement node. The arms of the device, which are also at the half wavelength of the device, are then bonded onto a custom fabricated printed circuit board (PCB). The PCB has bonding pads located proximally to the bonding pads of the arms on the ultrasonic horn running to a ribbon cable connector. Wires are then bonded between the pads of the ultrasonic horn arms and the pads on the PCB. The maximum transverse displacement of the microprobes (usually 8-10um) is then calculated from the frequency response between the two PZT plates, which varies slightly but significantly due to variations in mounting location and orientation of the PZT plates. A ribbon cable transmits the local signals recorded at the electrodes to a signal processing board.

4.5.2 – Circuit construction

A 5-stage circuit (See Figure 4.2) was designed and built for each recording channel. The first stage acts as a slight (1.25x) voltage amplifier, the second as a resistor-capacitor (RC) high-pass circuit to attenuate the signal to zero at ground; specifically, the signal will fall off below 3db at 3Hz. The third stage acts as a buffer

amplifier to boost the gain from the loss at low frequency due to the RC filter, and the fourth stage acts as the primary signal amplification of 100X. The last stage is another buffer amplifier for the signal before it passes to the data acquisition card.

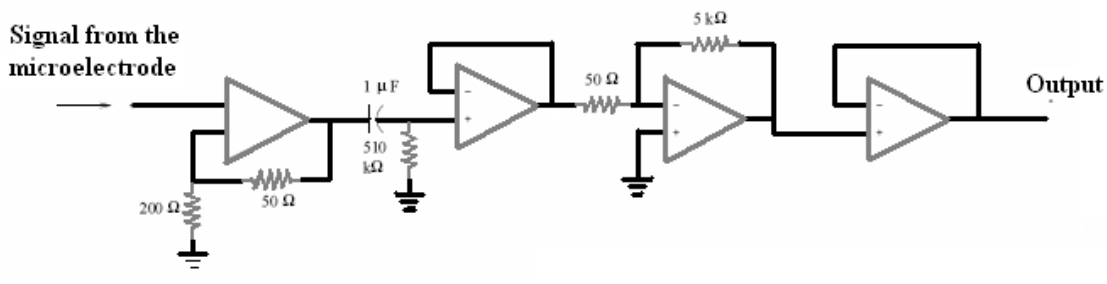

Figure 4.2: Schematic of the circuit used to pre-process the signal before recording. 5 stages exist, although the primary function is to act as a high-pass filter to attenuate the signal to zero at ground and to amplify the signal.

PCB boards were manufactured from PCB Express software, each board having 10 channels of the 5-stage circuit accommodating the 10 electrodes of each microprobe. Digikey supplied electrical components used on the circuit board.

4.5.3 – Experimental procedure

Whole hearts were excised from anesthetized adult (2-5yrs) male and female beagles. The region of the ventricular wall supplied by the left anterior descending coronary artery was identified and isolated. A section of this region was cut into preparations of size between 12cm^2 to 25cm^2 with a thickness of 0.5–1cm. The left anterior descending coronary artery was cannulated and the sample perfused with oxygenated Tyrode's solution **(**NaCl 124, KCl 4.0, $NaHCO_3$ 24, NaH_2PO_4 0.9, $CaCl_2$ 2.0, $MgCl_2$ 0.7, and glucose 5.5; pH 7.4**)** at a rate, dependent on preparation size, of between 10-20ml/min. The section of tissue was semi-immersed in a water-jacketed bath where the temperature of the bath and the perfused Tyrode's solution

was maintained at 37°C +/- 2°C. A silver-chloride wire in the bath served as a local reference or ground electrode.

During data acquisition the preparations were allowed to beat spontaneously or were paced at a constant cycle length using a bipolar stimulating electrode placed on the epicardial surface. In some experiments, to reduce muscle contraction for the purpose of alleviating stress on the microprobe tips imbedded in the tissue, the perfusion solution also contained 2,3-butanedione monoxime (BDM) or Blebbistatin (20mM/50uM respectively).

The microprobe's PCB was clamped to a mounting fixture, which was secured to a Narishige micromanipulator on a magnetic base. A ribbon cable connected the microprobe to the circuit board, which was connected to the recording computer. The ultrasonic horns were actuated at the λ/2 longitudinal resonant frequency to drive the microprobe while the probe tips were inserted in the tissue. Using a driving signal of 8Vpp, microprobes were inserted into the cardiac tissue from epicardium to endocardium. The ultrasonic actuation was then turned off after insertion to reduce noise before recording began. See Figure 4.3 for reference.

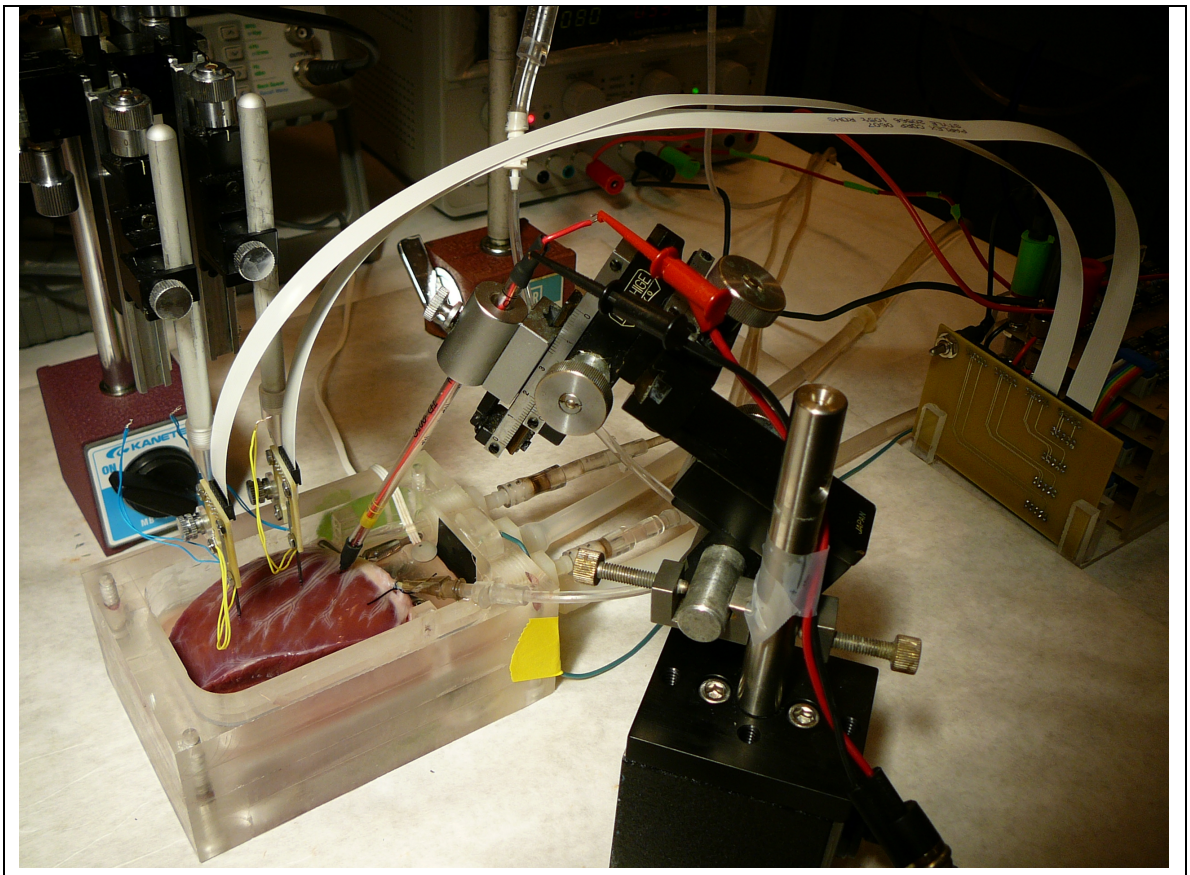

Figure 4.3 : Experimental setup. Canine LV in custom fabricated water-jacketed bath. A bipolar stimulating electrode mounted by micromanipulator stimulates the epicardial surface. Silicon microprobes mounted to a PCB and clamped to a micro-manipulator are inserted into heart from above epicardial surface. Ribbon cables provide a low-noise method of sending signals to the signal processing circuit.

4.5.4 – Data acquisition and analysis

A personal computer was used for data recording and stimulus triggering. The computer used a real-time linux kernel and a custom software suite for data acquisition with a National Instruments (N.I.) 12 bit PCI-6071E card, capable of 64 channels of simultaneous recording at 125Ms/s connected to a N.I. SCB-100 breakout board. Trigger signals for the pacing protocols were sent though the breakout board to a WPI Pulsemaster A300 pulse generator, which passed TTL

signals to a WPI A360 stimulus isolator. Current was then directed onto the epicardial surface of the tissue via a bipolar electrode to elicit an action potential / contraction of the tissue.

Paced stimulation protocols, also referred to as pacedown protocols, or simply pacedowns, consisted of 20 or 50 beats at a given cycle length to allow for reaching steady state before the cycle length was shortened. Pacedown protocols differ from paceup protocols in that slower, or longer cycle lengths always occur at the beginning of the protocol and gradually increase in frequency becoming faster and faster. The cycle lengths of pacedown protocols varied, but were used to measure APD at cycle lengths up to 10 seconds and as short as 220ms. Signals acquired from the microprobe were analyzed in MATLAB to measure APD, DI, and to create a plot of the restitution relation.

4.6 – Results

4.6.1 – Histology

To determine to what extent the probe was causing damage to the tissue, an ultrastructural evaluation of canine myocardium was conducted after a microprobe was ultrasonically actuated with 1.2 x the normal ultrasound driving voltage used for experimental purposes and inserted in the left ventricle free wall *ex vivo*. Sections of myocardium were collected from around the tip of the probe that was embedded in the tissue and were compared to myocardium harvested from untreated myocardium. No ultrastructural differences were noted between the two groups of samples, where each group displayed histological characteristics that

were typical for normal myocardium examined by transmission electron microscopy(Virágh & Challice, 1973).

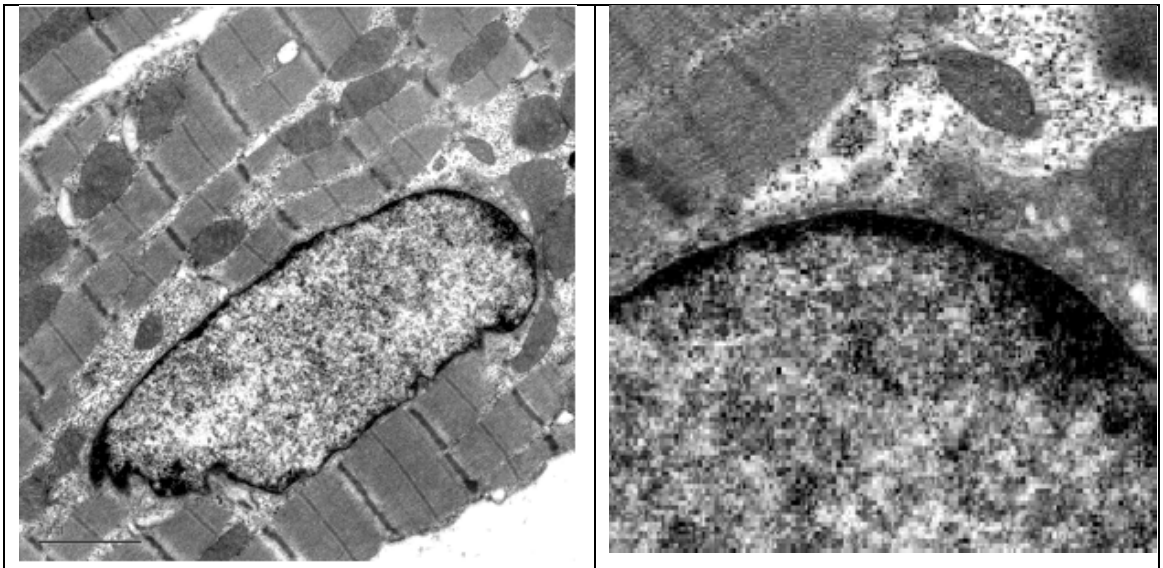

Figure 4.4 : EM scan of a cell proximal to the location of a microprobe inserted in canine myocardium shows intact nucleus of undamaged cell (left) and normal accumulation of heterochromatin around the nuclear envelope (right).

It was noted that each myocardial cell proximal to the probe's location contained a centrally located single elongate nucleus. The chromatin was uniformly dispersed and nucleoli were only observed occasionally, as seen in Figure 4.4. A small amount of heterochromatin accumulated along the nuclear envelope, which was typical in appearance. Numerous small uniform round electron dense bodies 0.5 to 1 um in diameter were clustered at the poles of the nuclei. Because of their uniform size, these particles were interpreted as glycogen granules rather than lipofuscin bodies, which are somewhat larger and more irregular. No Golgi apparatus or centrioles were observed.

Longitudinal sections of myofibers contain parallel myofibrils composed of multiple sarcomeres attached end-to-end at the electron dense Z lines (Figure 4.5).

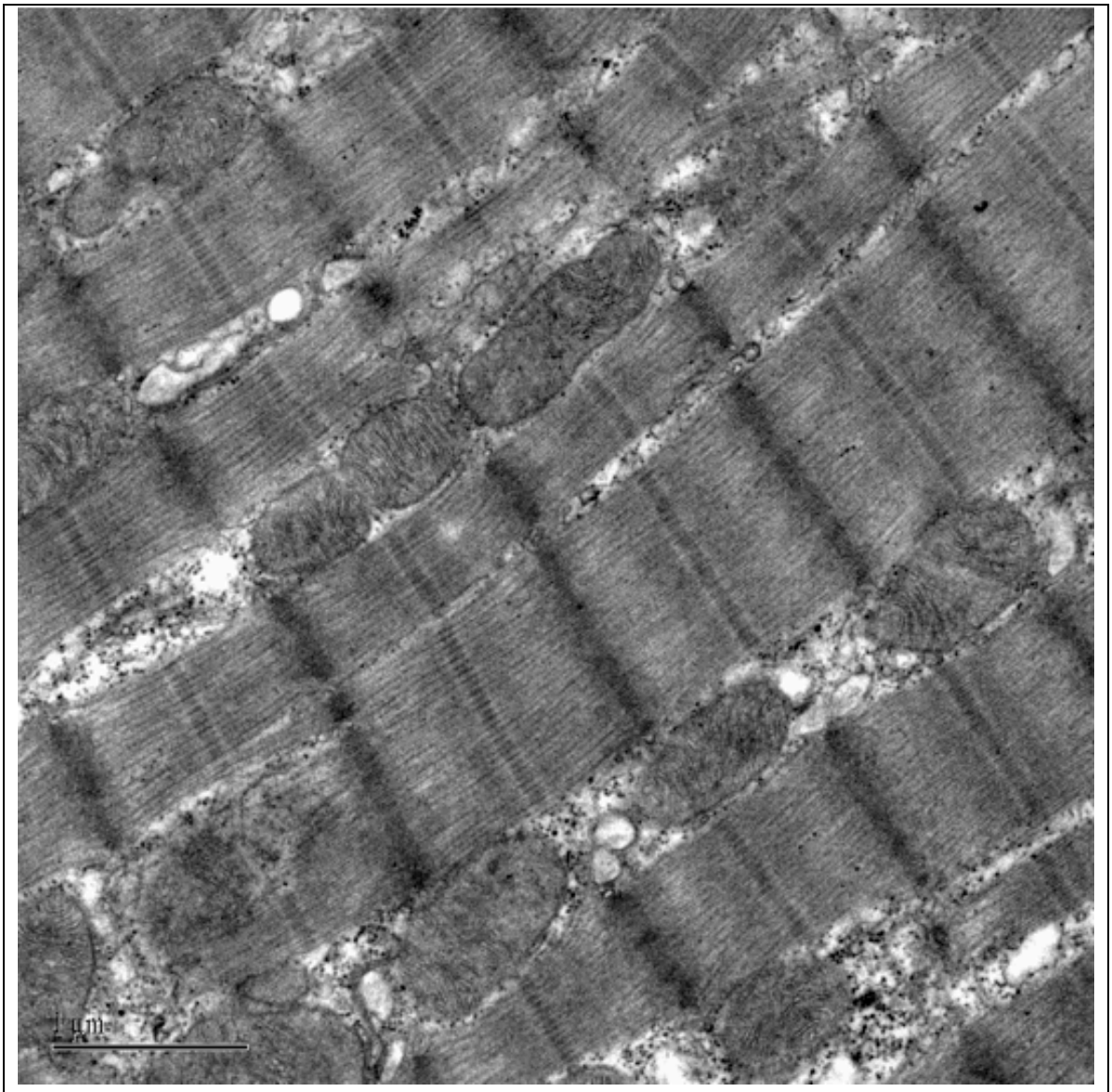

Figure 4.5 : EM scan of myofibrils

Each sarcomere had alternating I bands (isotropic; light) and A bands (anisotropic; dark). The mid-region of the I band was traversed by the Z line. The

middle of the A band had a dark M line flanked by pale H zone. Moderate myofibril width variation was noted, but was within normal limits.

Numerous mitochondria arranged in long rows were observed between the myofibrils (Figure 4.6, left) and the mitochondrial were generally plump and elongated, averaging 1.5 x 1.0 um. Each mitochondrion had an external membrane and an internal membrane that formed prominent folds (cristae). The mitochondrial matrix consisted of numerous small electron dense granules estimated to be 10 nm in diameter (Figure 4.6, right). Lipid droplets were usually 0.3 to 1.0 um in diameter and were located among the rows of mitochondria. No lipid droplets were detected in these cells. Hearts of recently exercised animals do not have lipid droplets. Stimulation of the myocardium during the experiment likely mimicked the physiological effects of exercise leading to depletion of lipid droplets.

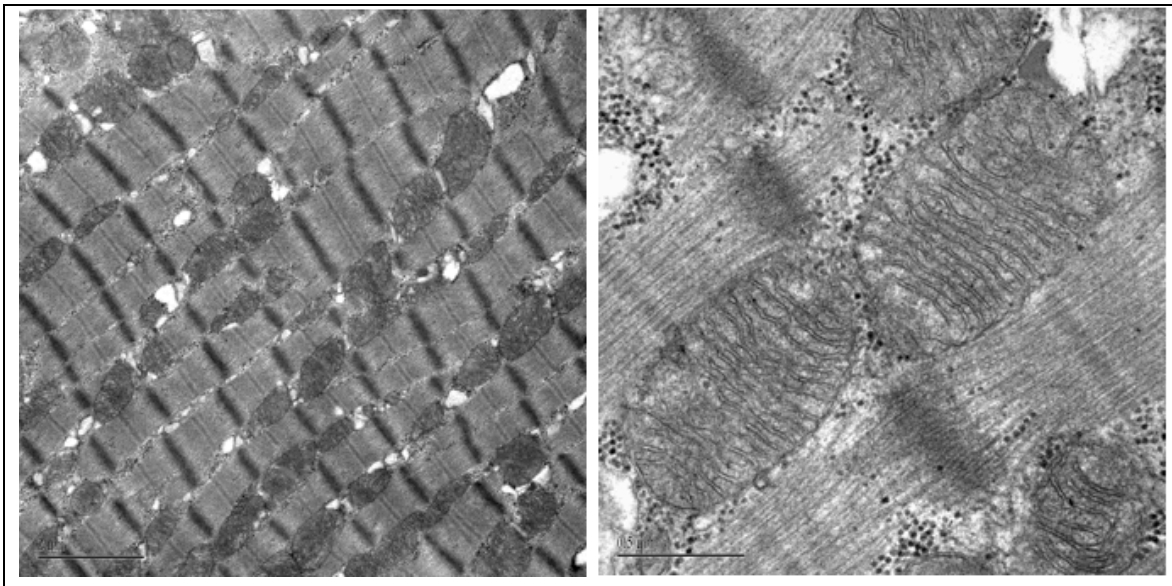

Figure 4.6 : Mitochondria and absence of lipid droplets indicate minimal damage and experiment conducted under similar physiological conditions as exercise.

The transverse tubules (T system) are best demonstrated using an extracellular marker such as horseradish peroxidase or lanthanum. However, structures interpreted as T tubules were frequently located near the Z bands of the contractile apparatus (Figure 4.7). These round membrane-bound structures, which often contained small granules, were interpreted as cross sections of transversely running tubules. No longitudinally oriented tubules were detected.

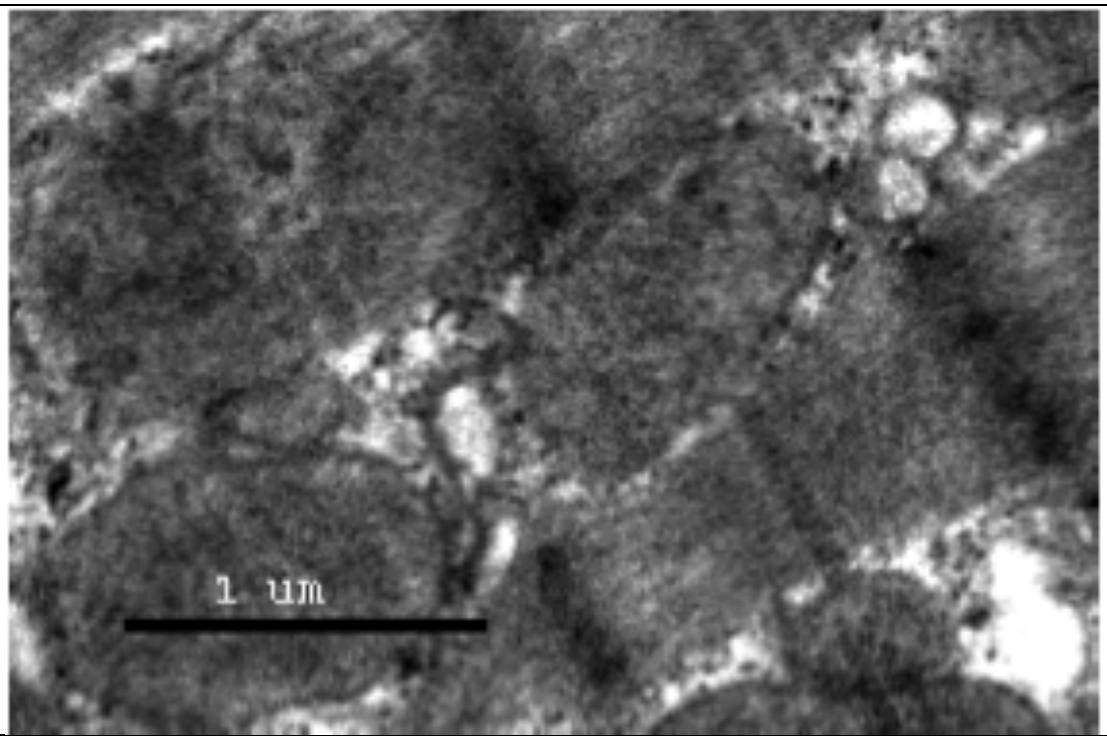

Figure 4.7 : Round, membrane-bound structures are likely cross sections of transversely running tubules.

4.6.2 – Probe & circuit signal filtering

Since accurate measurement of action potential duration of extracellular signals was of primary importance, we wanted to verify the capabilities of the noise-reduction / signal amplification circuit. The circuit response was tested by feeding a

train of action potentials recorded from an MAP electrode into the input channel of the circuit and the output from the circuit was recorded. Normalizing for the amplification of signal, the two signals are superimposed in Figure 4.8. While the signal passing through the circuit displayed a larger repolarization than the original signal and a characteristic increase in signal drift after the end of the action potential, the action potential duration was accurately measured and matched that of the original signal.

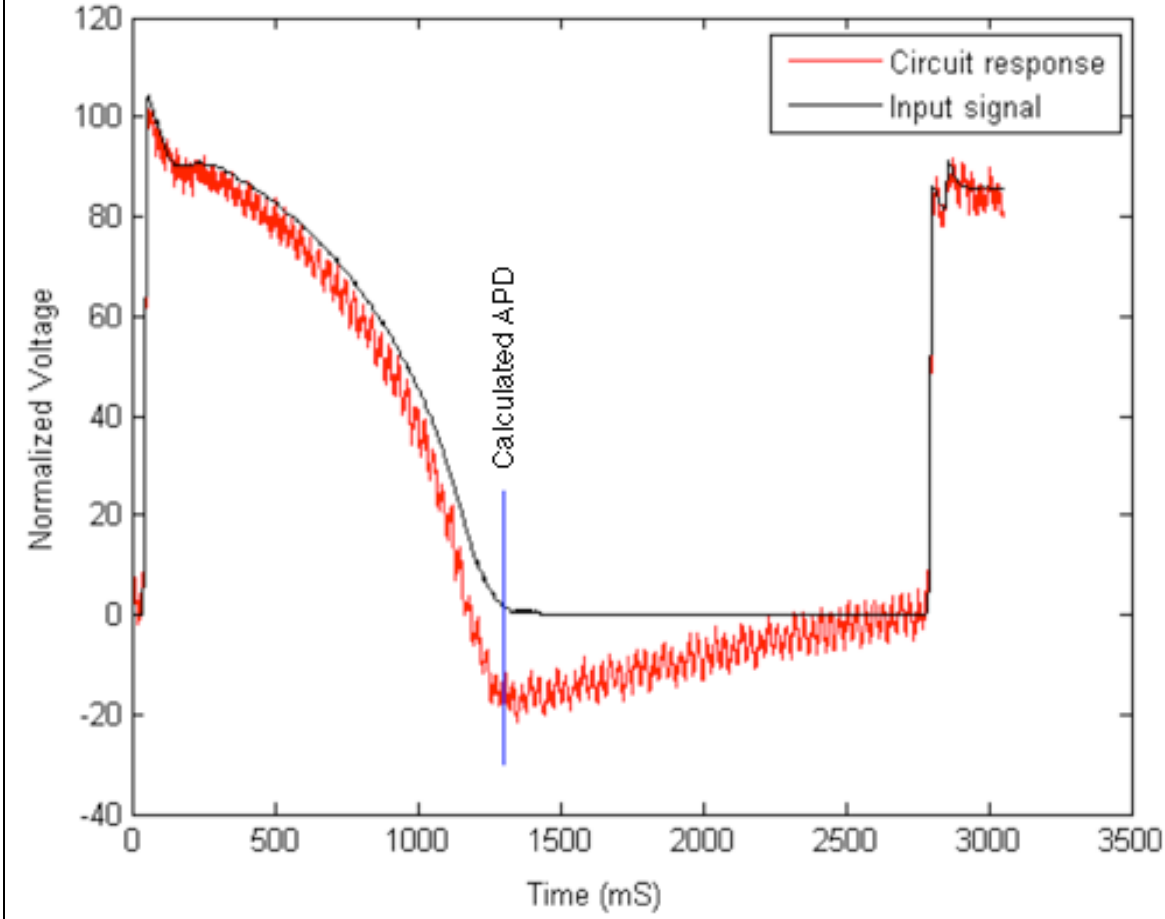

Figure 4.8 : Testing the signal processing circuit. Action potential signals were recorded from voltage clamp studies on isolated myocytes. These pre-recorded signals were passed through an Axon Instruments 1322 D/A converter directly to the signal processing circuit board.

To test the frequency response of the microprobe and circuit board in tandem, the microprobe was connected to the circuit via ribbon cable, and the microprobe tips were immersed in a beaker of Tyrode's solution. The output of the signal processing circuit was connected to an input channel of the data acquisition card. The pre-recorded action potential signal output from the signal generator was attached to a silver chloride wire inserted into the beaker of Tyrode's solution. A Teflon-coated platinum wire was inserted into the beaker of Tyrode to compare the acquired signal to that of the microprobe/circuit and was connected to a second input channel of the data acquisition card. This arrangement allowed us to compare the signal before and after being detected by the microprobe in solution and processed by the circuit. Recordings on these two channels were normalized and superimposed on each other as seen in Figure 4.9. The action potential signal as it was output from the computer through the silver chloride wire going into the beaker of Tyrode's solution is displayed in black and is listed as "Signal->Soln." The signal picked up by the platinum wire in solution, and fed back to the first input channel of the data acquisition card is displayed in blue, and is listed as "Soln -> Pt wire." These two signals closely matched. The signal as it passed through the solution, into the probe and through the circuit was recorded in red, and is listed as "Soln -> Probe -> Circuit." This signal was greatly amplified, but it was noted that noise was added to the recording and some of the action potential morphology was altered, although that action potential duration was still accurately measured.

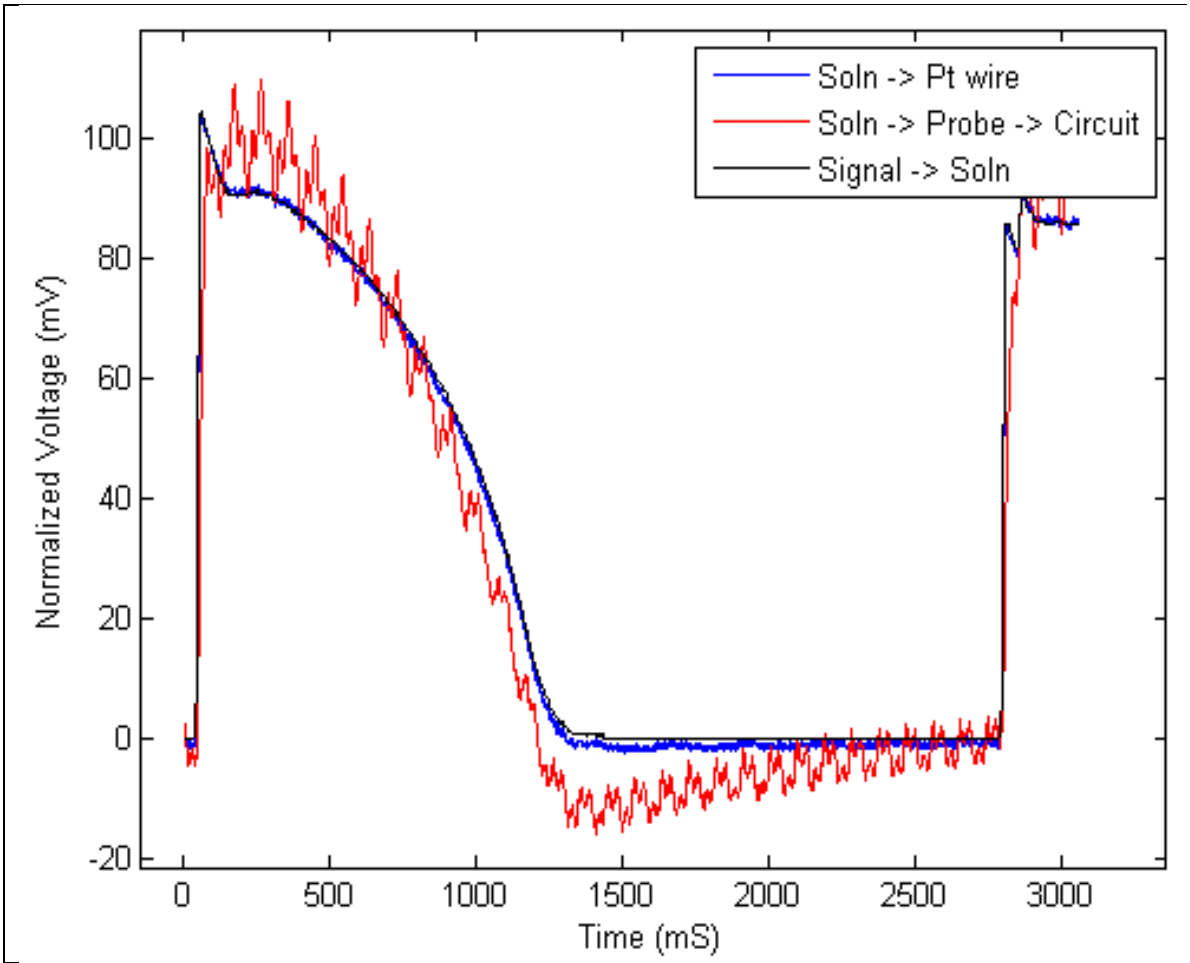

Figure 4.9 : Pre-recorded action potential signals are passed via silver-chloride wire into a beaker of Tyrode's solution, shown in black. This signal is picked up by a platinum wire also in the beaker, shown in blue, and closely matches that of the output signal. The microprobe also picked up the signal in the solution and relayed it to the signal processing circuit where it was amplified. The amplified signal was normalized to the other signals. Note the increased noise generated by the silicon microprobe, however APD is still accurately measured.

4.6.3 – Transmural restitution portraits

Pacedown experiments were performed using two protocols for a range of cycle lengths: short cycle lengths (800ms to 150ms), or long cycle lengths (10s to 700ms). The short cycle lengths were to examine the slope of the restitution relationship as it approached a steeper slope, and to determine i) if alternans

existed, and ii) the steepness of the slope at various depths through the ventricle wall. The long cycle lengths were used to probe for the existence of a subpopulation of cells that exhibited altered APD kinetics, specifically, a greater rate dependence of APD.

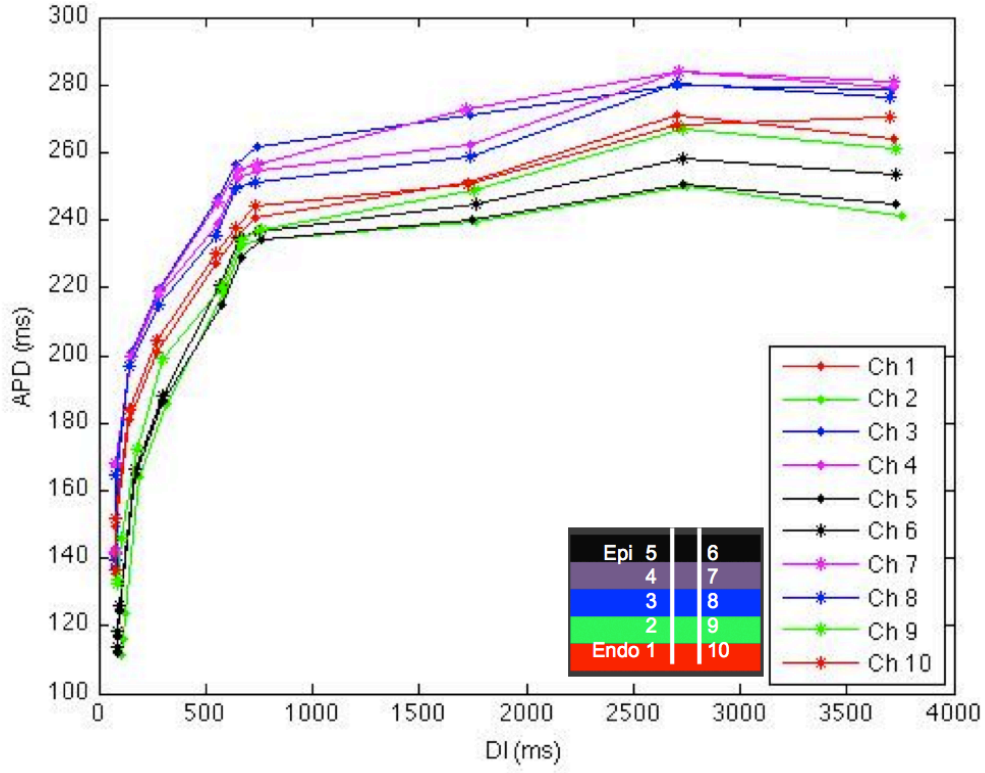

Figure 4.10: Averaged transmural restitution relationship.

Figure 4.10 shows an APD restitution plot from an adult beagle left ventricle, which was generated by a pacedown protocol from 4 seconds to 200ms. 50 beats at each cycle length were given, and the last 5 beats at a cycle length were averaged and plotted. The black trace indicates the recording closest to the epicardial surface, whereas the red trace was closest to the endocardial surface. The colors purple, blue

and green were recorded from mid-myocardial tissue. Overall, there was not a large difference in action potential duration between the surfaces and the middle layers. Generally, APD of the tissue below the surface was similar to that of the surrounding tissue, although in this particular case there was a slight prolongation of the action potential duration in the mid-myocardial layer. APD did vary somewhat in these layers between hearts and even within the same preparation, as evidenced by the fact that even though both tips of the probe were at the same depth in the tissue, APD detected on one recording pad differed from its neighboring pad at the same depth. This observation might be explained by variations in excitability, variations in temperature, or in cellular coupling of the tissue around the electrode.

Figure 4.11 illustrates the range of APD obtained from 16 pacedown protocols in 12 preparations as a function of the depth at which they were recorded. An increase in APD in the midmyocardial layers would be reflected by a rightward shift in the plots for the middle sets of data. APD in the midmyocardial layers was significantly different for the longer, but not for the shorter, pacing lengths.

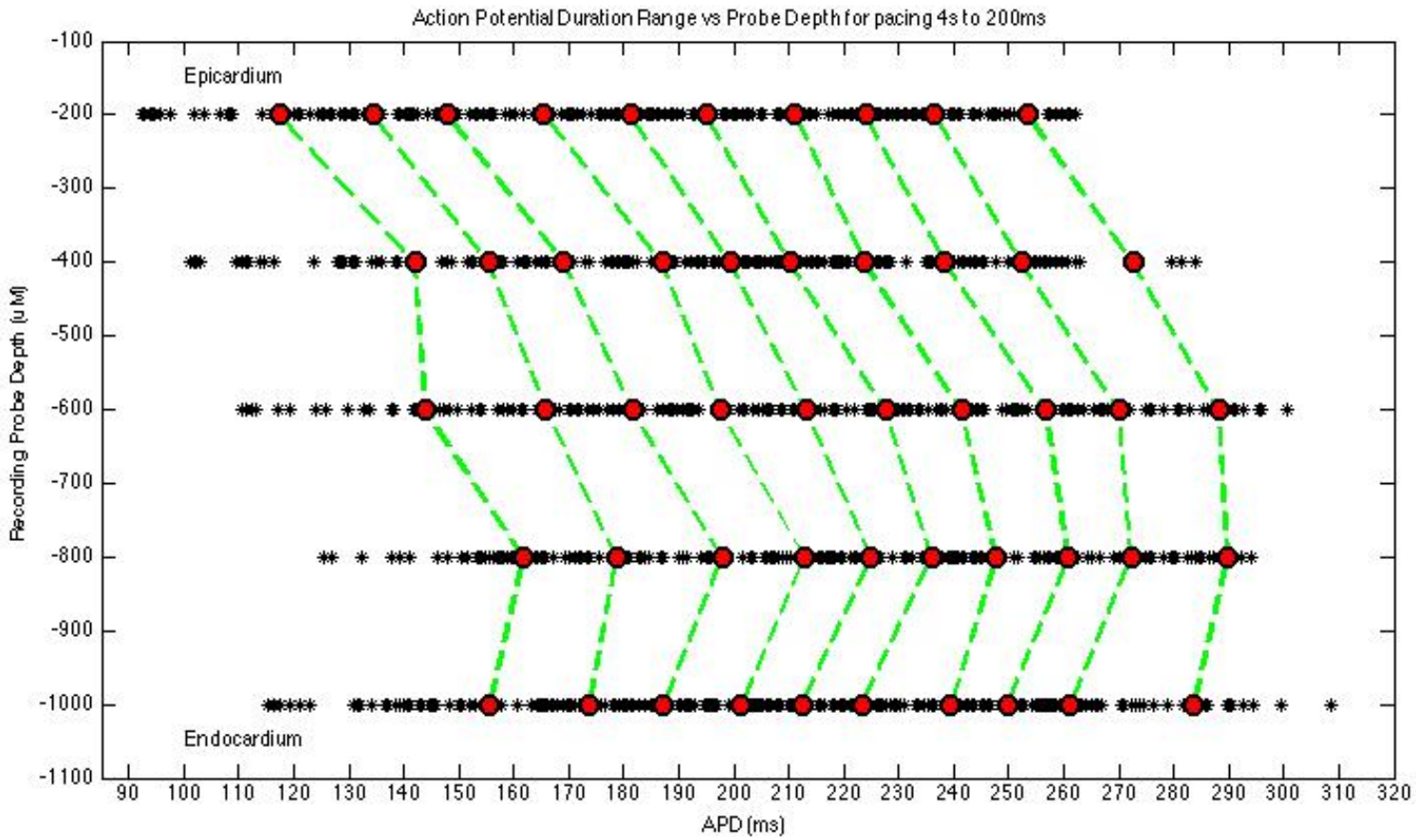

Figure 4.11 – Range of APD recorded by silicon microprobes from paced tissue at various depths through intact LV free wall. N=16 from 12 dogs. Red dots are averages for each paced cycle length between 4 seconds and 200ms. Green lines connect averages of a given CL across various recording depths.

Figure 4.12 shows the range of APD at a pacing cycle length of 4 seconds for the 16 paced protocols, where the greatest difference between APD of M-cells and other cells is expected, based on previous studies. However, the data clearly indicate that there is only a slight difference in APD between epicardium, endocardium and midmyocardium. While there is some obvious variability between experiments, and dogs, these data indicate that in a syncytium, the greater rate dependence of APD in M cells is not as apparent as in sectioned tissue or dissociated cells, indicating that electrotonic coupling may mask the contribution of M cells to transmural repolarization.

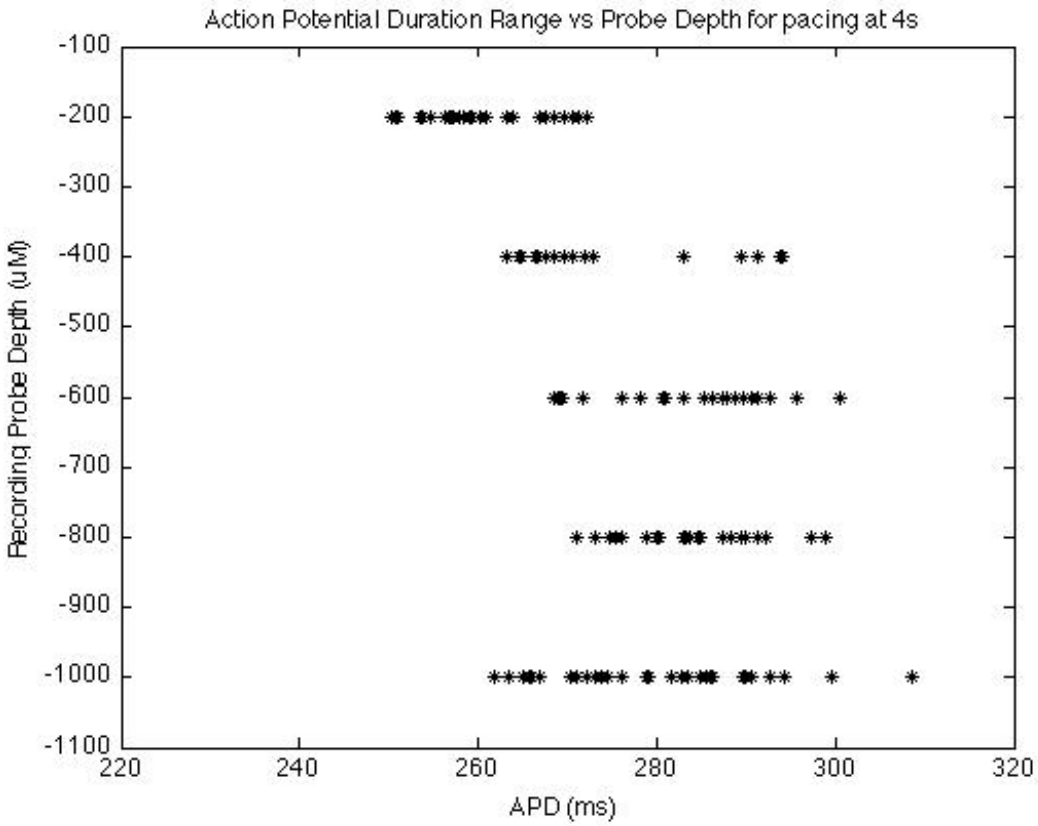

Figure 4.12 – APD recordings at 4 second pacing, where the increased rate-dependence of APD in M cells would be greatest, and one would expect to see the largest differences between the different layers.

4.6.4 – Experiments with Sotalol

Sotalol is a non-selective β-adrenergic receptor blocker that also exhibits class III antiarrhythmic properties by virtue of its inhibition of potassium channels(Bertrix, Timour-Chah, Lang, Lakhal, & Faucon, 1986; Edvardsson, Hirsch, Emanuelsson, Pontén, & Olsson, 1980). The drug was originally discovered in the 1960s(Frankl & Soloff, 1968) and became widely used clinically first as a β-blocker in the 1980s, while its function as an antiarrhythmic drug was discovered later(Antonaccio & Gomoll, 1993). Due to this dual action, Sotalol prolongs both the PR interval as well as the QT interval, and by blocking repolarizing potassium currents it increases APD. This dual action mechanism is thought to exist because of the different isomers that exist for sotalol(Gomoll & Bartek, 1986). d-sotalol is the dextrorotatory optical isomer of the racemate d,l-Sotalol, and blocks Ik_r(R. Kato, Ikeda, Yabek, & Kannan, 1986), the rapid component of the delayed-rectifier current, and lacks clinically significant beta-blocking activity(Gomoll & Bartek, 1986; Johnston, Finch, McNeill, & Shanks, 1985).

It was previously published that midmyocardial cells, specifically M cells, are more likely to display their rate dependence in the presence of Sotalol, by significantly increasing their APD(Akar et al., 2002; Shimizu & Antzelevitch, 2000; Sicouri, Moro, & Elizari, 1997).

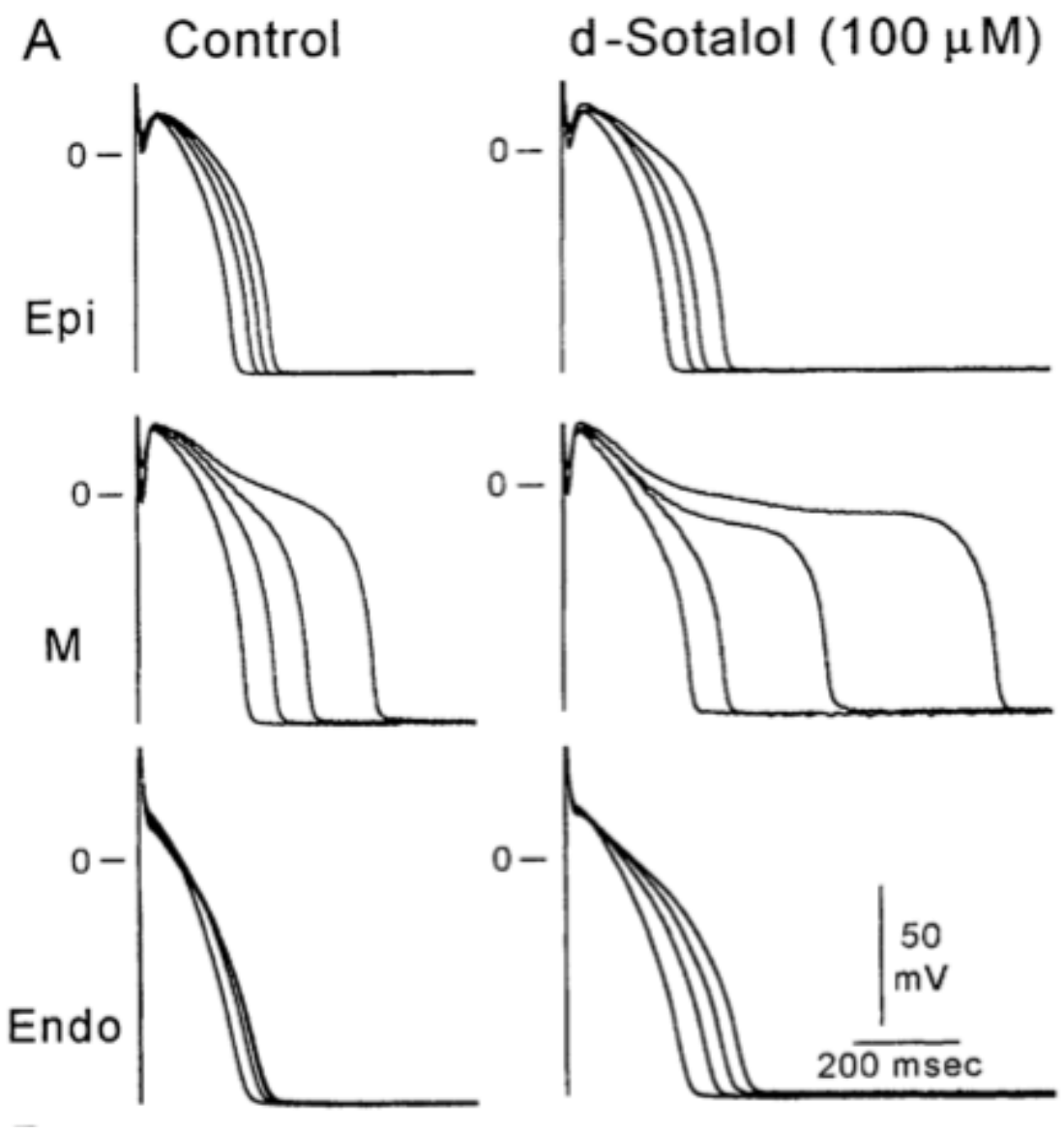

Figure 4.13 : Sicouri et al., 1997, effect of d-Sotalol on isolated transmural strips of canine cardiac muscle showing M cells having a greater rate-dependence response than epicardium or endocardium in the presence of Sotalol.

Since APD in M cells has been shown to have a greater rate dependence than epicardium or endocardium in the presence of Sotalol in isolated transmural strips

of cardiac tissue, it would be insightful to determine the rate dependence of APD during sotalol exposure in a syncytium using silicon-based microprobes.

As can be seen in figure 4.14, which shows both APD before and after application of drug, Sotalol (50 uM) increased APD, as well as the range of APD within the ventricle. At a cycle length of 4 seconds, epicardial APD increased 93ms, from 196ms to 289ms. Near the endocardial surface APD increased 124ms, from 204ms to 328ms. APD of the mid-myocardial layer 0.8cm below the epicardial surface increased 133ms, from 219ms to 352ms. These results correspond to an increase in epicardial APD of 147%, an increase of endocardial APD of 160%, and an increase of APD in the deep subendocardium of 160%.

The range of APD across the ventricular wall at a pacing cycle length of 4 seconds was 25ms during control conditions, whereas the range of APD after application of sotalol was 63ms, an increase in APD range of 252%.

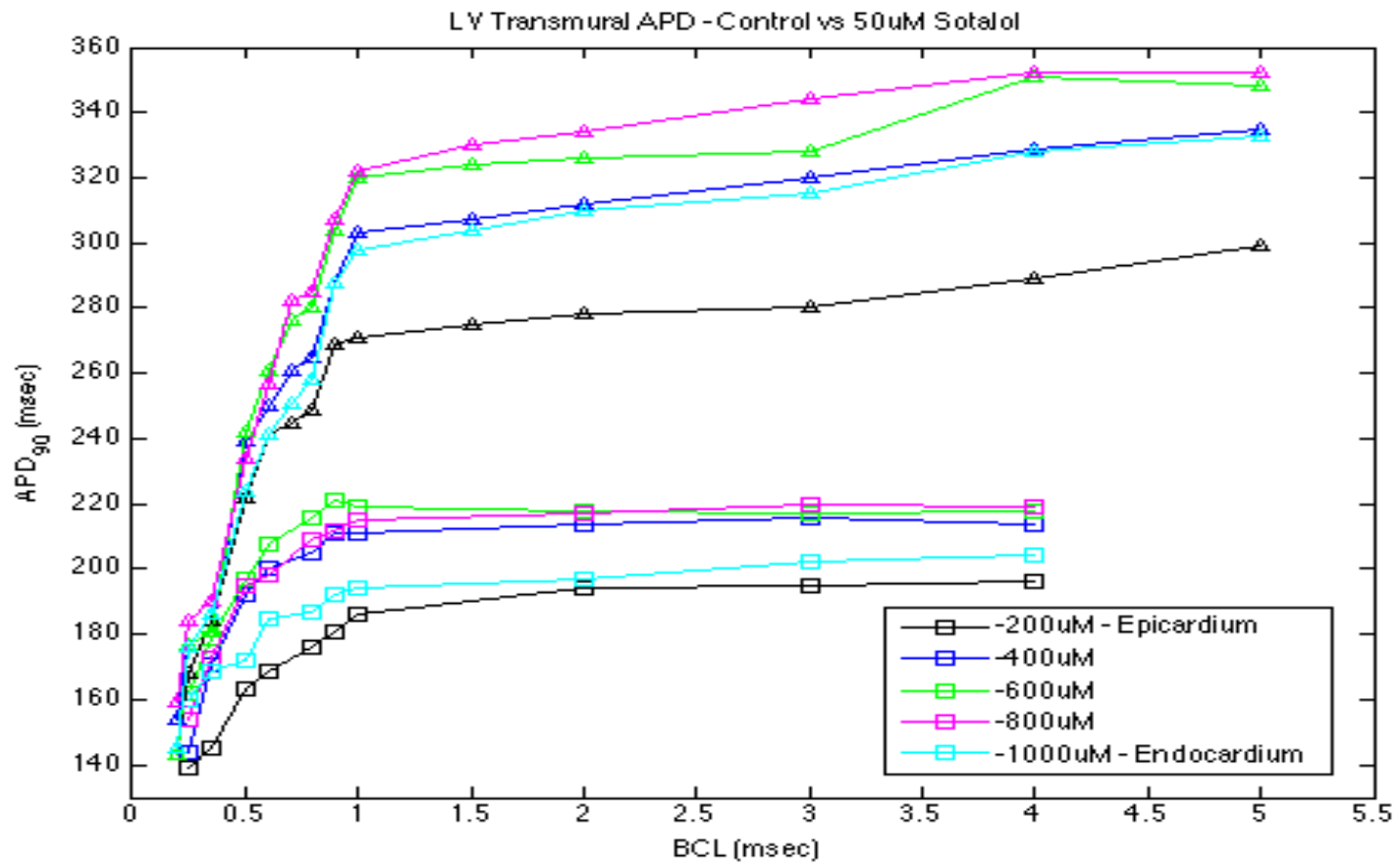

Figure 4.14 : LV transmural APD before and after application of 50uM Sotalol. Unfilled squares are control, Unfilled triangles are after drug. N=2

4.8 – Discussion

Ultrasonically actuated silicon microprobes have become a proven technique for measuring extracellular intramural activation of canine cardiac tissue. This work builds on previous studies by reducing the size of the microprobes and by recording intramural activation times to create transmural restitution plots. The purpose of this study was to evaluate if intact tissue has an intrinsic heterogeneous environment that is capable of supporting reentry and ventricular fibrillation.

Previous work shows that ultrasonic driving of the silicon microprobe tips reduces penetration force on the microprobe. A side effect may be reduction in damage to the tissue. However, some damage is obviously created, as there is visible hole on the surface of the tissue after removing a microprobe. Since there is obvious damage in some degree at the site of microprobe insertion, the extent of cell-cell coupling impairment must be evaluated. Histological examination shows minimal damage to the surrounding tissue near the insertion site of the silicon microprobe. If the microprobe is recording a local signal, it may likely be recording from well-coupled tissue.

Transmural restitution portraits of intact canine ventricle show dispersion of APD on the order of 30ms at normal physiologic cycle lengths of ~750ms, and of up to 50ms at longer pacing cycle length of 4s, with little dispersion of APD in deep sub-epicardium and deep sub-endocardium, where M cells have previously been found with greater dispersion of APD. There is notably less dispersion of APD in the mid myocardium and deep sub-endocardium compared with endocardium, however

there is some small amount of dispersion of APD between the deep sub-endocardium and epicardium. These data suggest that in well coupled tissue there is less dispersion of APD compared to areas of damage, where cell-cell coupling is impaired, such as by MI or by sectioning tissue into wedge preps, and the greater rate-dependence of the M-cells may play a larger role in creating dispersion of APD in disease conditions or areas of injury.

Sotalol, which blocks IK_r, increased APD in all layers of the heart. The increase was equivalent in the midmyocardial layers and in the deep sub-endocardium, but was not as pronounced in the sub-epicardial layer. While dispersion of APD increased across the ventricle, the degree of dispersion was less than that reported in previous studies(Sicouri & Antzelevitch, 1991), nor were M-cells as obvious at longer cycle lengths.

In these experiments, fibrillation occasionally occurred spontaneously, but occurred more often at fast pacing cycle lengths, suggesting that the amount of intrinsic dispersion of APD and refractoriness present is sufficient to support reentry. Unfortunately, because the tissue was likely to fibrillate at faster pacing cycle lengths, measurement of discordant alternans, which has been shown previously to be an important determinant of the development of VF, was difficult in the mid myocardium.

The Purkinje fiber network

Although previous studies have shown that VF is perpetuated by reentry or spiral waves, recent data suggest the role of specific sources in triggering this arrhythmia(P. Chen, 2000; Gray et al., 1995; Jalife, 2000). The Purkinje fiber system, which plays a critical role in the harmonious myocardial contraction and relaxation via its efficient propagation properties and unique geometrical distribution(Matsuda, Kamiyama, & Hoshi, 1967), has been hypothesized to play a role in the initiation and/or maintenance of VF(Berenfeld & Jalife, 1998; Dosdall et al., 2008; L. Li, Jin, Huang, Cheng, & Ideker, 2008; Tabereaux et al., 2007).

5.1 – History & characterization

Johannes Purkinje (1787–1869), a Czech anatomist and physiologist, first discovered the peripheral component of the Purkinje system in 1839 (Jay, 2000) as spindly, vacuolated cardiac muscle fibers. However, although Purkinje was the first to describe the fibers, their function was later established by others. A related structure, the Bundle of His, was described initially by Wilhelm His Jr, in 1893, who also noted “specialized muscle fibers” that were the only direct connection between the atria and the ventricles(HIS, 1949). His was the first to show that severing the “His bundle” could result in atrioventricular dissociation(Roguin, 2006). In 1906, Tawara discovered the right and left bundle branches and correctly addressed the role of the ventricular specialized conduction system in mediating the rapid spread of electrical excitation from the His bundle throughout the ventricles (Suma, 2001).

Purkinje fibers differ in numerous ways from myocardial cells. The relative sizes of Purkinje and myocardial cells are species-dependent(Sheets, January, & Fozzard, 1983; Shimada, Kawazato, Yasuda, Ono, & Sueda, 2004; Stankovicová, Bito, Heinzel, Mubagwa, & Sipido, 2003; Verkerk et al., 1999). In general, Purkinje cells are larger than myocardial cells and are distinguishable histologically(Stankovicová et al., 2003). Purkinje cells lack the prominent transverse tubules that are present in myocardial cells(Sommer & Johnson, 1968). Moreover, the amount of glycogen in Purkinje fibers is much higher than in myocardial cells(Friedman, Stewart, Fenoglio, & Wit, 1973b). The glycogen can be metabolized anaerobically, which may make Purkinje cells more resistant to hypoxia than working myocardial cells(Friedman, Stewart, Fenoglio, & Wit, 1973b), although some evidence suggests that the opposite is true(Schnabel et al., 1991).

The conduction velocity of electrical impulses is much higher in Purkinje fibers (2–3 m/s) than in myocardial cells (0.3–0.4 m/s)(Durrer et al., 1970). The rapid propagation is partially due to the different connexins in the gap junctions in these cells. The amount of Cx40, a connexin protein that causes high conductance channels, is at least three-fold greater in Purkinje fibers than in myocardial cells(Kanter, Laing, Beau, Beyer, & Saffitz, 1993). Another reason Purkinje fibers have a higher conduction velocity is that they exhibit a larger maximal upstroke velocity (V_{max}) than ventricular muscle. V_{max} is a function of sodium conductance(DRAPER & Weidmann, 1951). In the heart, the relationship between V_{max} and available sodium conductance (gNa) can be strongly non-linear, even under relatively favorable circumstances(Cohen, Bean, & Tsien, 1984), but in

general, increasing sodium conductance will increase conduction velocity. However, there does exist an optimal density of sodium channels for maximal conduction(Hodgkin, 1975) because as membrane capacitance increases, it slows conduction velocity. The desnsity of sodium channels may be lower in smaller fibers to reduce the quantity of sodium entering the cell per impulse, which needs to be pumped out by a process that consumes metabolic energy. Therefore smaller fibers are at a disadvantage, due to their higher surface area to volume ratio(Aidley, 1998).

As part of the conduction system, the Purkinje cells have the potential for automaticity, although Purkinje fiber automaticity normally suppressed by the faster pacemaker activity of the sinoatrial node(Irisawa, Brown, & Giles, 1993). Isolated cardiac Purkinje fibers usually have relatively slow spontaneous discharge rates, whereas atrial and ventricular muscle are quiescent. However, depolarization of these tissues by disease processes, such as myocardial ischemia, can induce spontaneous activity, in the form of enhanced automaticity. Enhanced automaticity refers to the accelerated generation of an action potential by either normal pacemaker tissue (enhanced normal automaticity) or by abnormal tissue within the myocardium (abnormal automaticity), such as depolarized Purkinje fibers and atrial or ventricular myocytes. (Elharrar & Zipes, n.d.). Abnormal automaticity is not suppressed by overdrive pacing(Grant & Katzung, 1976; Imanishi & Surawicz, 1976), is more easily suppressed by calcium channel blockade than sodium channel blockade(Imanishi, 1971; Katzung, 1975), and is accelerated by beta-adrenergic agonists(Katzung, 1978; Pappano & Carmeliet, 1979).

Acceleration of Purkinje fiber automaticity can also be augmented by the elevated levels of catecholamines and increased sympathetic tone which occurs during ischemia(Ceremuzyński, Staszewska-Barczak, & Herbaczynska-Cedro, 1969). In addition, Purkinje fibers surviving myocardial infarction appear to be more sensitive to the positive chronotropic effects of catecholamines than normal Purkinje fibers(Barber, Mueller, Henry, Felten, & Zipes, 1983; Cameron & Han, 1982; Cameron, Dersham, & Han, 1982).

Although Purkinje fibers may exhibit spontaneous activity, their main function is to distribute activation to ventricular myocardium, a process that involves impulse transmission across the junctions between Purkinje myocytes and ventricular muscle myocytes (Purkinje-muscle junctions; PMJs). Transitional cells between Purkinje cells and myocytes were identified both histologically and with intracellular recordings by Martinez-Palomo et al.(Martinez-Palomo, Alanis, & Benitez, 1970) The cells were characterized as having shorter action potential duration, a decreased resting potential, and a notch in the upstroke. Other investigators showed that Purkinje fibers connected via thin branches to sheets of transitional cells that were also connected to ventricular cells(Overholt, Joyner, Veenstra, Rawling, & Wiedmann, 1984; Veenstra, Joyner, & Rawling, 1984). The studies by Tranum-Jensen et al(Tranum-Jensen, Wilde, Vermeulen, & Janse, 1991) clarified this relationship. They showed the insertion of fine strands of Purkinje fibers into the transitional cell layer and in turn the connection of the transitional cell layer via thin branches to ventricular muscle, as drawn in Figure 5.1. The apparent function of transitional cells is to offer an appropriate resistance to allow

for current amplification to excite the myocardium from a Purkinje source.

The PMJ sites on the endocardial surface are a discrete groups of cells and have a characteristic delay of conduction from the Purkinje system into the adjacent muscle that suggests significant discontinuity of conduction, as compared with conduction either within the Purkinje system or the ventricular muscle layers(R. Weidmann, Tan, & Joyner, 1996).

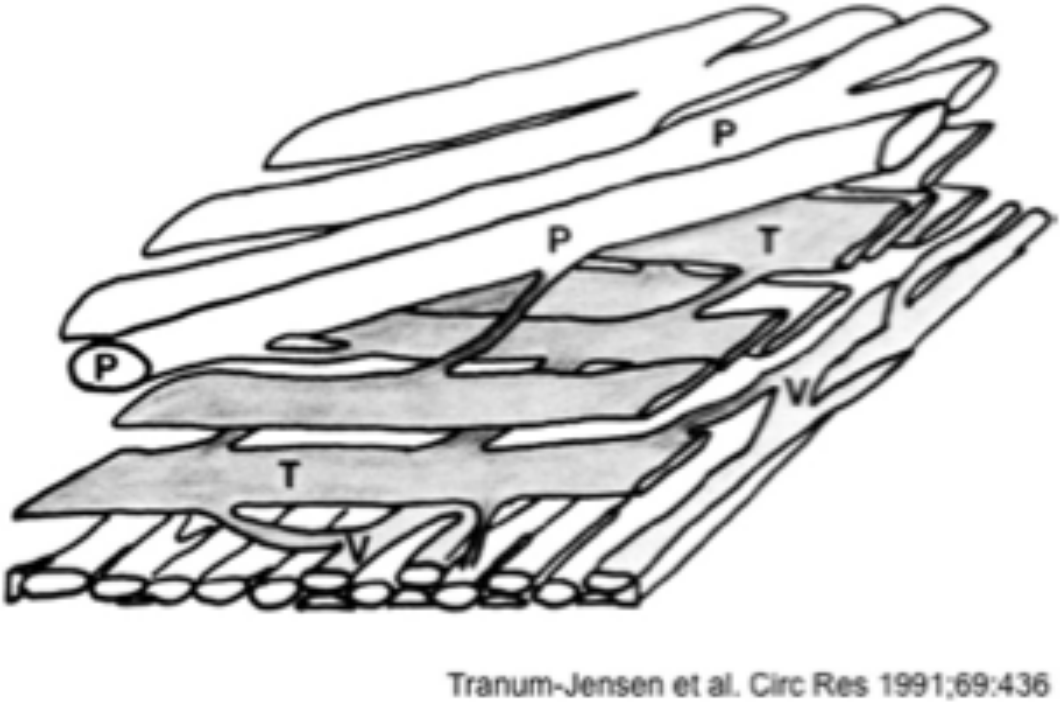

Figure 5.1 : Drawing of PMJ illustrating the connection between Purkinje and muscle fibers.

Researchers in several laboratories have studied the nature of the impulse propagation across the PMJ(Joyner, Veenstra, Rawling, & Chorro, 1984; Mendez, Mueller, & Urguiaga, 1970; Morley et al., 2005; Rawling, Joyner, & Overholt, 1985; Rohr, Kucera, Fast, & Kleber, 1997; Veenstra et al., 1984). They noted that there is a

relative lack of cell-to-cell coupling in the PMJ region(Martinez-Palomo et al., 1970). From these observations, the concept of a conduction delay occurring across the PMJ was developed(Myerburg, Stewart, & Hoffman, 1970). Evidence from canine studies, where impulse propagation across PMJs are technically feasible, indicates that propagation across only a subset of those junctions normally is successful(Mendez et al., 1970; Veenstra et al., 1984).

Progressive uncoupling in a uniform network will result in a slowing of conduction velocity following the square root relationship, but this does not necessarily have to be the case for non-uniform networks, i.e., where the size of a given excited region supplying depolarizing current ('current source') is ill matched to the amount of depolarizing current necessary to excite the regions ahead ('current sink'). An example of such a source-to-sink mismatch is represented by the PMJ, where a small source (Purkinje fiber) is coupled to a large sink (mass of ventricular tissue) (Joyner, 1982; Mendez et al., 1970; Overholt et al., 1984). Depending on the size of the mismatch, this results in either local conduction delay, or, if the mismatch is large enough, unidirectional conduction block at the junction during anterograde conduction.

In contrast to the effect of coupling on propagation in uniform tissue, partial uncoupling in such non-uniform networks can actually be accompanied by a paradoxical increase in safety and velocity of conduction(Rohr, 2004). In that regard, computer simulations of the characteristics of propagation across such expansions suggested that, contrary to intuition, partial gap junctional uncoupling might

improve conduction and remove unidirectional conduction block(Fast & Kleber, 1995; Leon & Roberge, 1991). This counter-intuitive behavior can be explained by differences in the dimensionality of the effect of gap junctional uncoupling on the source (strand) and the sink (expansion). Partial uncoupling of the essentially linear source will reduce its size in a linearly proportional manner, whereas equal uncoupling of the two-dimensional sink will reduce the size following a square function. Thus, a reduction of coupling at the PMJ improves the source-to-sink mismatch up to the point of successful anterograde conduction. Therefore, one possible explanation for why certain areas of cardiac muscle are routinely excited ahead of other areas could be explained by differences in coupling at the PMJ of those regions in comparison to other regions. This conjecture would be in agreement with experiments that show a range of conduction delays measured at the PMJ of less than 5ms(Matsuda et al., 1967) to 20ms(Alanis, Benitez, & PILAR, 1961).

Source-sink mismatches also are likely to be present in the border zone of healed infarcts(Ursell, Gardner, Albala, Fenoglio, & Wit, 1985) or in fibrotic tissue of the aged and/or hypertrophied myocardium(SPACH & Dolber, 1986). Partial gap junctional uncoupling at these regions might reduce unidirectional conduction block and therefore eliminate one of the key components of reentrant arrhythmias. Similarly, as Rohr et al. point out(Rohr, 2004), while improvement of gap junctional coupling in structurally diseased myocardium might be expected to act in an anti-arrhythmogenic manner by reducing the incidence of slowly conducting pathways,

it might at the same time provoke arrhythmias by unmasking potential regions of unidirectional conduction block.

Differences in the type and density of the ionic currents that mediate are the action potential waveforms of Purkinje and ventricular muscle cells also may contribute to unidirectional block at the PMJs(Huelsing, Spitzer, Cordeiro, & Pollard, 1998). In particular, the transient outward potassium current (I_{to}) is more prominent in Purkinje fibers than in myocardial cells(Irisawa et al., 1993). I_{to} is responsible for the rapid repolarization during phase 1 repolarization, typical of Purkinje action potentials(Nerbonne & Kass, 2005). On the other hand, the density of the inward rectifier current (I_{K1}) and the L-type Ca2+ current ($I_{Ca\text{-}L}$) are significantly higher in myocardial cells than in Purkinje fibers(Cordeiro, Spitzer, & Giles, 1998; Verkerk et al., 1999). The density of calcium currents in these cells is explained by their respective roles with respect to impulse propagation versus myocardial contraction.

Action potential duration varies continuously along the specialized conduction system(Myerburg et al., 1970). The local refractory periods of the multiple branches of the distal A-V conducting system progressively increase from proximal to distal(Myerburg et al., 1970), reaching a maximum a few millimeters proximal to the termination of a given tract of conducting tissue in muscle, and progressively decreasing beyond the point of maximum duration(Mendez, Mueller, Merideth, & Moe, 1969). The region of longest action potential duration also coincides with the region of longest refractory period. Myerburg et al. suggested the multiple areas of maximum local refractory periods function collectively to provide a limiting

segment, or “gate”, which determines the functional refractory period of preparations of large segments of A-V conducting tissue(Myerburg, GELBAND, & Hoffman, 1973).

From this point of view it seems the main role of the gating mechanism is to protect the heart against VF. In a majority of instances Myerburg et al. found that action potential duration and refractoriness were longer in the peripheral distribution of the right bundle branch than the left. They suggested that block at these peripheral sites was the electrophysiological mechanism of right bundle branch block.

This idea has been questioned for the control state in the *in vivo* conduction system, since Myereburg’s experiments were done *in vitro* with only part of the conduction system(Bailey, Lathrop, & Pippenger, 1977; Lazzara, El-Sherif, & Scherlag, 1975). Bailey et al. noted the observation that removal of the distal parts of the left bundle branch and, thus, a majority of PMJs, prolongs proximal left bundle branch APD and refractoriness comparable to those obtained for the proximal right bundle branch by Myerburg et al. Because the PMJs are of low ohmic resistance(Mendez et al., 1970), and their proximity to the bundle branch is closer in the left bundle branch than in the right bundle branch, they permit electrotonic effects between septal muscle and the proximal left bundle branch. Bailey et al. proposed that the prolongation of left bundle branch APD and refractoriness is due to loss of electrotonic effect of septal muscle on the left bundle due to transection of those PMJs. Therefore the Myerburg “gate” hypothesis could be due to an artifact of the methods used for the experiment

5.2 – PF role in arrhythmogenesis

In the last twenty years increasing experimental evidence has accumulated that indicates that the Purkinje system provides the underlying mechanism for many ventricular tachyarrhythmias, either as a trigger for arrhythmia initiation or as a substrate for arrhythmia maintenance(Elharrar & Zipes, 1977; Friedman, Stewart, & Wit, 1973a; Friedman, Stewart, Fenoglio, & Wit, 1973b; Gilmour & Zipes, 1980; Janse et al., 1980; Moak & Rosen, 1984; Nogami, 2011; Scherlag et al., 1974). More recently, mapping studies in humans have shown that Purkinje fibers can initiate VF in some patients with structurally normal hearts(Haïssaguerre, Shoda, Jaïs, & Nogami, 2002), Brugada syndrome(Häissaguerre et al., 2003), Long QT syndrome(Häissaguerre et al., 2003), myocardial infarction(Bänsch et al., 2003), ischemic cardiomyopathy(Bode et al., 2008; Marchlinski et al., 2005; Marrouche et al., 2004; Nogami, Kubota, Adachi, & Igawa, 2009; Okada et al., 2007; Szumowski et al., 2004), as well as non-ischemic cardiomyopathy(Sinha et al., 2009), providing clinical validation of the experimental studies. Although these studies imply an active role for Purkinje fibers in the development of ventricular arrhythmias, the exact mechanism by which Purkinje fibers may initiate and/or maintain VF remains a mystery.

With respect to triggering mechanisms, afterdepolarizations have been suggested as a possible cause of cardiac arrhythmias that cannot be explained adequately by reentry or by abnormal automaticity(Ferrier, 1977; Hoffman & Rosen, 1981; Rosen & Reder, 1981; Rosen et al., 1980; Rosen, Moak, & Damiano, 1984; Zipes, Arbel, Knope, & Moe, 1974; Zipes, Foster, Troup, & Pedersen, 1979). Delayed

afterdepolarizations (DADs) are oscillations of the membrane potential that follow complete repolarization of the action potential, whereas early afterdepolarizations (EADs)(Cranefield, n.d.) are depolarizing afterpotentials that interrupt or delay normal repolarization of the cardiac action potential. Both of these afterdepolarizations generate a subset of arrhythmias referred to as triggered(Cranefield, n.d.). Triggered activity is thought to be a potential arrhythmogenic mechanism in the intact heart(Ferrier, Saunders, & Mendez, 1973; Rosen, GELBAND, & Hoffman, 1973a) and has been well characterized in isolated cardiac tissue(Ferrier et al., 1973; Rosen, GELBAND, Merker, & Hoffman, 1973b).

A variety of interventions have been shown to generate DADs, the common factor of which is an increase in free intracellular calcium and/or an adjustment in the operation of the Na-Ca exchanger, which induces oscillations in membrane potential via induction of a transient inward current(Cranefield, n.d.; Wit & Rosen, n.d.). EADs have been induced in isolated cardiac tissues under a variety of conditions that increase inward current or reduce repolarizing current.

Although reentry has been thought to underlie early VT(Pogwizd & Corr, 1987; Xing et al., 2003) and VF, transmural activation studies have indicated that focal mechanisms in endocardial and Purkinje tissue may be the cause of VT(Arnar et al., 1997; Arnar, Xing, Lee, & Martins, 2001; Janse et al., 1980; Janse, Kleber, CAPUCCI, Coronel, & Wilms-Schopman, 1986; Pogwizd & Corr, 1987; G. Wu et al., 1995). In vitro models of acute ischemia involving Purkinje tissue have suggested that triggered activity (TA) due to DADs may explain these focal VTs(Coetzee & Opie,

1987; Z. Y. Li, Wang, Maldonado, & Kupersmith, 1994; Pogwizd, Onufer, Kramer, Sobel, & Corr, 1986; Wit, Cranefield, & Hoffman, 1972). PMJ cells may be particularly susceptible to TA, especially when Purkinje action potentials are prolonged(Z. Y. Li et al., 1994).

In support of a triggering role for Purkinje tissue, Purkinje fiber potentials have been shown to precede ventricular muscle activity on intramural electrograms during premature ventricular complexes in early ischemia, suggesting a Purkinje origin(BAGDONAS, STUCKEY, PIERA, AMER, & Hoffman, 1961; JANSE, KLEBER, CAPUCCI, Coronel, & WILMSSCHOPMAN, 1986). Moreover, studies of patients with polymorphic VT following myocardial infarction Szumowski et al.(Szumowski et al., 2004) showed that Purkinje signals preceded every premature beat, while ablation of the sites of the Purkinje signals eliminated all premature beats and no arrhythmia occurred in the following months. Szumowski et al. and Marrouche et al.(Marrouche et al., 2004) therefore suggested the importance of the role of the Purkinje fibers along the border zone of scar in the mechanism of polymorphic VT or VF post MI. Bogun then showed that the Purkinje system may play a role in post-infarction monomorphic VT(Bogun et al., 2006).

Purkinje fibers also may contribute to the development of a permissive substrate for VF. In that regard, the VF threshold (VFT), expressed by the amount of electrical stimulation to induce VF, has been used to quantify the susceptibility of the heart to VF(R. J. Damiano et al., 1986; Horowitz, Spear, & Moore, 1981; Posel, Noakes, Kantor, Lambert, & Opie, 1989). Horowitz et al reported a significant

difference between endocardial and epicardial VFTs in the left ventricle(Horowitz et al., 1981). They considered that the coexistence of ordinary myocardium with shorter repolarization characteristics and Purkinje fibers with a long refractory period in the endocardium facilitated the induction of VF.

Canine studies by Worley et al(Worley, Swain, Colavita, Smith, & Ideker, 1985) revealed an endocardial-to-epicardial activation rate gradient during VF. As VF continued over 20 minutes, the rate of VF slowed, primarily toward the epicardium, so that the endocardial activation rate increasingly outpaced that near the epicardium. The leading explanations for this observation are that Purkinje fibers are more resistant than the myocardium to the effects of ischemia, as shown in several studies, and that the Purkinje fibers are less ischemic because they receive oxygen by diffusion from the immobile blood in the ventricular cavities during VF(BAGDONAS et al., 1961; Friedman, Stewart, Fenoglio, & Wit, 1973b; Gilmour & Zipes, 1980).

Purkinje fibers are known to be so resistant to ischemia that they survive and continue to function even during long-lasting VF(Friedman, Fenoglio, & Wit, 1975), which may explain why VF terminates spontaneously in hearts with subendocardial chemical ablation, and suggests that Purkinje fibers play a significant role in the maintenance of VF(Dosdall et al., 2008).

It is presumed that during myocardial infarction (MI) the Purkinje fibers are relatively resistant to ischemia as they are supplied by cavital blood, and the amount of glycogen in Purkinje fibers is much higher than that in myocardial cells(Friedman, Stewart, Fenoglio, & Wit, 1973b). The glycogen can be metabolized anaerobically,

which may make Purkinje cells more resistance to hypoxia than working myocardial cells.

It also has been shown that subendocardial Purkinje fibers can survive in the infarcted area even after coronary artery occlusion. However, these Purkinje fibers display a lower maximum diastolic potential, reduced AP amplitude, depressed maximum rate of depolarization and prolonged APD when compared to normal Purkinje fibers(Friedman, Stewart, Fenoglio, & Wit, 1973b; Lazzara, El-Sherif, & Scherlag, 1973). Individually isolated Purkinje cells 24h and 48h after infarction show reduced resting potentials, AP amplitudes, and V_{max} when compared with controls(Boyden, Albala, & Dresdner, 1989), as well as exhibit reduced T-type and L-type calcium currents. This loss in calcium channel function could contribute to the abnormal transmembrane potentials of these myocytes surviving in the infarcted heart(Boyden & Pinto, 1994).

Studies have also shown a reduction in the transient outward current I_{to} and altered kinetics 48h after infarction(Jeck, Pinto, & Boyden, 1995). In addition, enhanced automaticity and triggered activity have been observed in surviving Purkinje fibers in the infarcted area(El-Sherif, Gough, Zeiler, & Mehra, 1983), which, when coupled with prolongation of the action potential duration in this region, may result in the necessary conditions for polymorphic VT/VF(Berenfeld & Jalife, 1998; Chialvo et al., 1990; Friedman, Stewart, Fenoglio, & Wit, 1973b; Kupersmith, Li, & Maldonado, 1994). It has therefore been suggested that ventricular arrhythmias seen after MI or coronary artery occlusion may originate from these Purkinje fibers

that survive infarction(Fenoglio, Karagueuzian, Friedman, Albala, & Wit, 1979; Friedman et al., 1975; Horowitz, Spear, & Moore, 1976).

Additional support for a role of Purkinje fibers in VF comes from canine heart studies in which the sub-endocardium was ablated by painting the endocardium with either Lugol's solution or phenol. In the mid 1980's Damiano et al attempted to clarify the role of the Purkinje network on ventricular vulnerability(R. J. Damiano et al., 1986). In their study, the baseline VFT increased after total ablation of the endocardial surface by applying Lugol's solution. This observation was in agreement with the findings of Janse et al.(Janse et al., 1986) in a similar study, as well as with Horowitz. In a study by Chen et al(P. S. Chen, Wolf, Cha, Peters, & Topham, 1993) in the early 1990's, VF occurred after subendocardial ablation by the flushing of Lugol's solution in *in situ* canine hearts and VF thresholds remained relatively unchanged, despite ablation of the endocardium with Lugol's solution. However, an explanation for this result may be that some Purkinje fibers may have not been ablated by this procedure, because Purkinje fiber potentials can be recorded at a depth of 2 mm in the left ventricular free wall(SPACH, HUANG, & AYERS, 1963), whereas application of Lugol's solution produces necrosis at a level of only 0.5 mm(P. S. Chen et al., 1993; R. J. Damiano et al., 1986).

These studies reveal that chemical ablation of the PF endocardial layer in canine hearts dramatically elevated the threshold for the onset of VF. More recently, it has been shown that radiofrequency ablation of the Purkinje fiber potentials observed on the endocardium resulted in noninducibility of VF(Haïssaguerre et al., 2002; Nogami, Sugiyasu, Kubota, & Kato, 2005). Other experimental and clinical

studies in humans also have revealed that catheter ablation of the Purkinje system can terminate VF and prevent VF induction(Kim et al., 1999; Pak et al., 2006; 2008; 2006; 2003). In 2002, Haıssaguerre et al. reported that idiopathic VF could be suppressed by catheter ablation of triggers originating from the Purkinje system(Häissaguerre et al., 2002; Haïssaguerre et al., 2002). In 2003, Bansch et al. reported that in patients with repetitive VF following an acute myocardial infarction (MI), Purkinje signals preceded every ventricular premature beat (VPB); ablation of the sites of the Purkinje signals eliminated all VPBs, and no VF recurred during the follow-up(Bänsch et al., 2003). In addition, Bode et al.(Bode et al., 2008) and Enjoji et al.(Enjoji et al., 2009) have reported the successful ablation of the Purkinje-related VF associated with acute coronary syndrome. Many investigators demonstrated the same approach with good results in remote MI or ischemic cardiomyopathy patients(Marchlinski et al., 2005; Marrouche et al., 2004; Nogami et al., 2009; Okada et al., 2007; Szumowski et al., 2004).

In recent studies, Pak et al(Pak et al., 2008) demonstrated the differences in the effect of Purkinje ablation and the distribution of the Purkinje network in dogs and swine(Pak et al., 2006; 2008). While the ability to induce VF was decreased by catheter ablation targeting the left ventricular endocardium in dogs, the same ablation procedure did not reduce the ability to induce VF in swine. In contrast to the canine Purkinje network, which is mostly localized to the sub-endocardium, the swine Purkinje network extends to the sub-epicardial layer with a higher density(Holland & Brooks, 1976).

Allison et al examined transmural activation mapping during long-duration VF

in swine and canines and documented that the difference in the Purkinje distribution had a significant impact on the transmural VF activation pattern(Allison et al., 2007). In pigs, the activation rate slowed from 2 to 10 minutes of VF, but continued at a similar rate transmurally as the VF continued. In dogs, the activation rate slowed near the epicardium more than near the endocardium. Conduction block in the dog first occurred toward the epicardium and progressed with time toward the endocardium. This transmural mapping during VF explains why the Purkinje system ablation from the endocardium in swine did not reduce the ability to induce VF in the experiments by Pak et al. (Pak et al., 2006; 2008)

Dosdall et al. demonstrated that the Purkinje system is active during early post shock activation cycles in pigs(Dosdall et al., 2007) and the ablation of the Purkinje system by Lugol's solution hastened spontaneous VF termination(Dosdall et al., 2008).

Other studies have shown that the Purkine system plays a role in arrhythmias after electrical shock defibrillation(H. G. Li, Jones, Yee, & Klein, 1993). In a study using isolated rabbit hearts by Wu et al(T.-J. Wu, Lin, Hsieh, Chiu, & Ting, 2009), optical mapping of endocardial and epicardial activations demonstrated the close relationship between the maintenance of VF and repetitive endocardial focal discharges; re-initiation of VF after unsuccessful electrical defibrillation was apparently caused by endocardial focal discharges.

The results of the work by Wu et al. are similar to a previous study of defibrillation from 1981. Ouyang et al reported the defibrillation threshold in open-chest dogs with reversible ten-minute coronary occlusions(Ouyang, Brinker, Bulkley,

Jugdutt, & Varghese, 1981). They found that twice as much energy was required for defibrillation of VF caused by occlusion or reperfusion but without electrical stimulation. They considered that electrically induced VF and spontaneous VF do not share identical metabolic or pathologic mechanisms. Their observation suggests that a certain triggering factor is present during spontaneous VF that hampers electrical defibrillation. Because detailed analysis of activation in the ventricles was not available at the time, the difference between electrically induced VF and ischemia-related spontaneous VF was unknown. Based on the observations in the study by Wu et al(T.-J. Wu et al., 2009), repetitive endocardial focal discharges during VF offer a plausible reason for the observations by Ouyang et al.

More recent optical mapping studies in dogs and pigs have provided additional evidence that Purkinje fibers contribute to the maintenance VF by giving rise to activation that propagates through the PMJs to stimulate the working myocardium(Allison et al., 2007; L. Li et al., 2008; Tabereaux et al., 2007). Tabereaux et al investigated the activation pattern during VF(Tabereaux et al., 2007) and found that Purkinje fibers are highly active even ten minutes after the onset of VF. In addition to anterograde (orthodromic) propagation from the Purkinje fibers to the working ventricular myocardium, they noticed retrograde (antidromic) propagation also occurred from the working ventricular myocardium to the Purkinje fibers. Although orthodromic propagation was seen less commonly than antidromic conduction, this may be due to conduction block during ischemia being more likely anterograde than retrograde through PMJs because of increased load in the anterograde direction.

The finding of Tabereaux showing that activation is propagating through the PF system throughout the first 10 minutes of VF raises the question of whether the PF activation is actively contributing to the maintenance of VF or whether it is a bystander, responding to wavefronts that originate from the working myocardium. To address this issue, Newton et al(Newton, Smith, & Ideker, 2004) used plunge needles in the left ventricular free wall of canines to show that after 2 minutes of VF, the endocardium is activating more rapidly, with conduction block occurring more commonly at the epicardium. On the basis of their findings, no apparent conducting wave fronts propagate from intramural regions toward the endocardium, consistent with activations arising from the PF system.

Although these studies strongly suggest His-Purkinje system involvement in the maintenance of VF, experimental limitations have prevented direct confirmation of the mechanism by which the His-Purkinje system has this effect.

5.3 – Structure of the His-Purkinje system

Since the His–Purkinje system plays an important role in both normal ventricular excitation and life threatening ventricular arrhythmias, accurate modeling of the His–Purkinje system is essential for a realistic computer model of the ventricle(Tusscher & Panfilov, 2008). In perhaps the most simplistic design, the His-Purkinje system could consist of a bundle of wires, all with a common starting point at the AV node, and all with different end points, connecting through PMJs with working myocardium. And in fact, early models of the Purkinje system only considered straight, isolated, un-branching strands subject to electric

fields(Krassowska, 2003; Plonsey & Barr, 1986a; 1986b). In 1990 Pollard and Barr described a simplified model of the Purkinje system that contained 35,000 individual cylindrical elements, each of whose physical dimensions approximated unit bundles of Purkinje and atrioventricular nodal cells(Pollard & Barr, 1990), which was a more geometrically realistic Purkinje system to study propagation, but only in an isolated tree. Interaction with ventricular tissue has also been studied, but in a geometrically simple model(Monserrat, Saiz, Ferrero, Ferrero, & Thakor, 2000).

Using a more complex 3-dimensional model of the ventricles, Berenfeld et al.(Berenfeld & Jalife, 1998) tested the hypothesis that reentry involving the Purkinje muscle junction may be a mechanism of focal subendocardial activation during polymorphic VT. The Purkinje system was shown to give rise to initial reentry, which led to the establishment of intra-myocardial reentry independent of the Purkinje network. Also, the reentry was terminated if the Purkinje system was disconnected from the muscle before it reached a relative steady state of VF. Their model supported the possibility that Purkinje fibers are involved in the evolution and maintenance of reentry during polymorphic VT and VF.

These simple, non-branching systems may be unrealistically simple, however. As an alternative, the complexity involved in the Purkinje system conducting a signal from a singular starting point and disseminating it to thousands of locations in the ventricle is often modeled as a fractal. Using a geometrically realistic computer model of the rabbit ventricles with a topologically realistic fractal Purkinje network, Deo et al(Deo, Boyle, Plank, & Vigmond, 2009) systematically studied the role of the Purkinje network during the onset and maintenance of

arrhythmias. They used a branching Purkinje network based on Vigmond's earlier model(Vigmond & Clements, 2007), developed using schematics and pictures of the conduction system, text descriptions of heart anatomy, and excitation mappings of the heart(Berenfeld & Jalife, 1998; Durrer et al., 1970). They found that reentry was successfully induced by all protocols, and that the Purkinje network was active throughout reentry and exhibited both anterograde and retrograde conduction at PMJs.

Another possibility regarding the structure of the Purkinje network is that it has interconnecting fibers that join different sections to form loops. Loops can be beneficial functionally: if a serial connection exists everywhere in the network, where a parent branch divides into two daughter branches, then if ever that connection fails or is damaged everything downstream is effectively disconnected. If the network is based on parallel circuits, there exists redundancy, or a backup system, and protection in case of damage. However, if not properly configured these loops could create a substrate for reentry.

The macroscopic configuration of the Purkinje network was first revealed by the seminal work of Durrer et al(Durrer et al., 1970). Although the Purkinje network covers much of the left ventricular endocardium, he noted that three specific endocardial areas were synchronously excited 0 to 5 msec after the start of the left ventricular cavity potential. These activated areas increased rapidly in size during the next 5 to 10 msec, becoming confluent at 15 to 20 msec after the onset of excitation. Therefore, the network preferentially activates certain areas of tissue

first, either by converging many of the PMJs on these specific areas, which seems irrational given that the Purkinje system covers much of the endocardial surface, or by influencing the delay at specific PMJs. If the PMJs in these specific areas have a lower conduction latency across them into the muscle than the PMJs located elsewhere on the endocardium, these areas would be activated sooner.

5.4 – Is the Purkinje network fractal in nature?

The term fractal defines a ubiquitous class of geometric shapes, traditionally thought to be merely irregular, whose subunits replicate the structure of the larger unit in accord with the principle of self-similarity(Mandelbrot, 1983). Fractals occur naturally, and are nature's way of optimizing distribution systems. One of the most fundamental (and desirable) aspects of fractals is that they optimize the relationship between the size of the distribution system and the size of the tissue being served by that system. The obvious optimization for the cardiac conduction system would be to allow the most amount of signal dissemination in the least amount of space.

Since the early 1980's it was assumed that the Purkinje network, like so many other biological systems, was fractal in nature. This assumption stemmed from Goldberger's hypothesis(Goldberger, Bhargava, West, & Mandell, 1985) based on the broad-band nature of Fourier analysis of the QRS complex of a normal electrocardiogram. Goldberger believed that the general appearance of the His-Purkinje network was of a highly complex fractal network that demonstrates self-similar structure over progressively smaller scales.

Goldberger argued that activation through a branching structure provides "electrical stability"(Goldberger et al., 1985). Lewis and Guevara(Lewis & Guevara, 1991) rejected the reasoning of Goldberger, but concluded that one simply needs a mechanism to rapidly and synchronously spread the wave of activation to the ventricular muscle, a task to which a branching network is well suited. The rapid sequential activation of a major part of the endocardium allows the wave of activation to travel in an approximately one-dimensional fashion from the endocardium outwards to the epicardium(SPACH et al., 1963), which may prohibit the collision of wave fronts and "the evolution of refractoriness-activation profiles leading to the possible formation of reentrant rhythms resulting in ventricular arrhythmias."

To test Goldberger's hypothesis, Chialvo & Jalife compared the frequency domain of a human QRS complex to a frog's QRS complex(Chialvo & Jalife, 1991). They expected the comparison to be constructive, since a frog heart does not have a His-Purkinje system. They showed that the spectral features of a frog's QRS complex closely resembled a human's QRS complex. They therefore concluded that a fractal His-Purkinje network plays no role in the spectral characteristic of the QRS complex, and that there exists no proof that the Purkinje network is fractal in nature. Their results are in agreement with the arguments of Lewis and Guevara(Lewis & Guevara, 1991), who argued that the particular spectral decay of the QRS complex is related to its (large scale) pulse-like shape, and not to a fractal anatomical substrate of the His-Purkinje system.

While Chialvo & Jalife's study disproved a connection between an anatomically fractal His-Purkinje network and a broad-band power spectrum of the QRS complex, it did not disprove the existence of a fractal Purkinje network in larger mammalian hearts. To address that question more directly, researchers have recently examined the structure of Purkinje system and PMJs in rabbit hearts using high-resolution confocal microscopy(Romero, Sachse, Sebastian, & Frangi, 2011). They showed that the Purkinje network forms plexus structures, with star-like arrangements of cells where a junction has two or more paths, indicating that the Purkinje system may be more complex than a fractal. The importance of the Purkinje system to realistic modeling has been demonstrated(Romero et al., 2010; Tusscher & Panfilov, 2008), and yet this discovery has not been considered in modeling approaches of the Purkinje tree to date(Ijiri et al., 2008; Tusscher & Panfilov, 2008).

Most recently, in 2011, researchers mapped the left and right ventricular His-Purkinje conduction network in rabbit(Atkinson et al., 2011). Unstained, the Purkinje network can be difficult to identify. Middle neurofilament (NF-M) is a positive marker for the cardiac conduction system in the rabbit(Dobrzynski et al., 2005). Using immunoenzyme-histochemistry, Atkinson et al. stained NF-M to label His-Purkinje tissue. They then outlined and segmented the His-Purkinje network into a pseudo 2-D network of 5 layers (to account for overlapping fibers) and 8.8 million grid nodes to superimpose on a 3D model of the rabbit heart. Although the authors were able to create a detailed network map of the His-Purkinje system, they

were not able to identify PMJ locations, nor were they able to determine whether the network was in fact overlapping, or if it formed closed-circuit loops.

In summary, the Purkinje fiber network has been shown to be susceptible to enhanced automaticity, abnormal automaticity, and triggered activity. The Purkinje fiber network connects to the working myocardium via Purkinje muscle junctions, where there is a delay before the signal enters the working myocardium. The delay at the PMJs varies by location over a range of time from 2ms to 25ms, and likely explains why specific regions routinely initiate the depolarization sequence on the endocardial surface. The PF network seems to have an intimate relationship with the generation and/or maintenance of VF, and ablation of all of the network, or those areas showing Purkinje potentials before PVCs has been shown to lower the inducibility of VF. The dispersion of APD and refractoriness between the muscle and the Purkinje fibers, coupled with a delay at the PMJ, could be responsible for a mechanism of reentry by allowing retrograde (antidromic) conduction. The likely interconnected nature of the Purkinje network sends the signal back through the network and across other PMJs that originally blocked and re-enters the tissue, possibly creating a micro-reentrant excitation, masquerading as a focal origin.

- Hypothesis: If the Purkinje fiber network is fractal in nature, it would provide a different mechanism for the spread of signal than a network that incorporates loop circuits.

To accurately model the network, high resolution imaging of the Purkinje system is necessary.

5.6 – Materials & methods

5.6.1 – Experimental procedure

Whole hearts were excised from adult (2-5yrs) male and female beagle dogs euthanized with Fatal-Plus (86 mg/kg intravenously) and their hearts were rapidly excised. For LV endocardial imaging, after excision the LV free wall was bifurcated midway between the left anterior descending and circumflex coronary arteries, as seen in Figure 5.2.

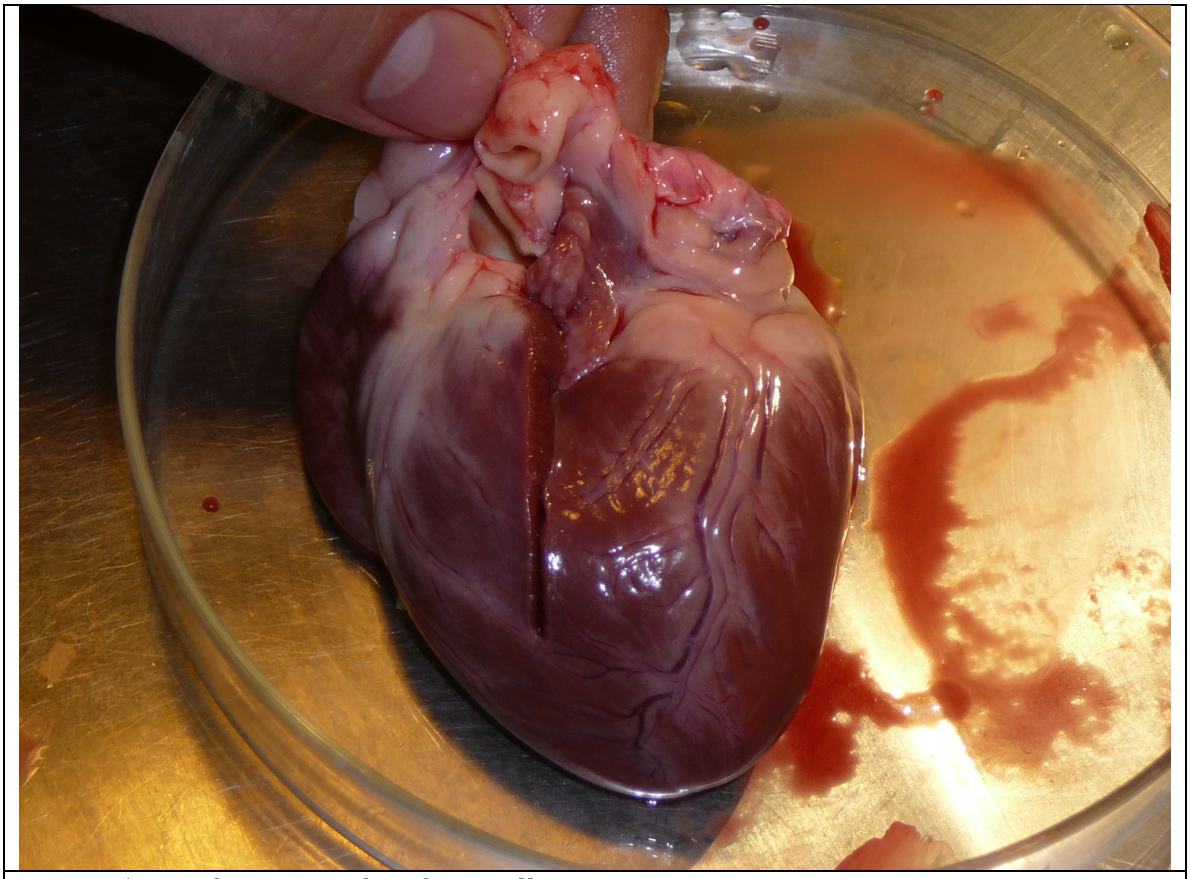

Figure 5.2 : Bifurcation of LV free wall

The left and right coronary and circumflex arteries were cannulated using polyethylene tubing as seen in Figure 5.3, and perfused with normal Tyrode solution bubbled with 95% O_2, 5% CO_2 at pO_2 400–600 mm Hg, pH 7.35 ± 0.05 and temperature 20.0-22.0 °C. The flow rates of the perfusates were 20 ml /min at a perfusion pressure of 50–80 mm Hg. After 15–30 min of equilibration, the preparation was stained with the voltage-sensitive dye di-4-ANEPPS (10 µM/L bolus). Blebbistatin (10 µM/L constant infusion over 30–40 min) was added to prevent motion artifacts. A bipolar stimulator was used to stimulate either the atria or free-floating Purkinje fibers.

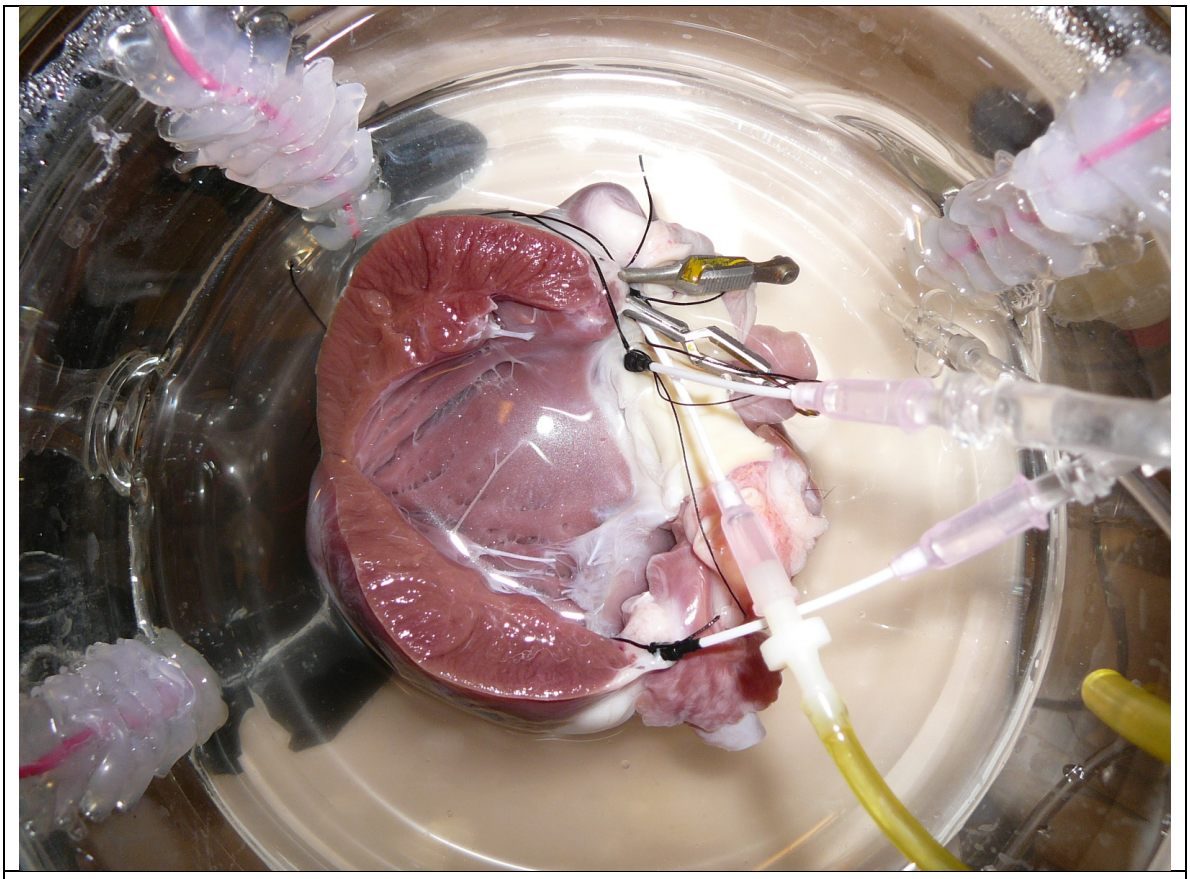

Figure 5.3 : LV bifurcated to image LV endocardium. Note the three cannulas supplying oxygenated Tyrode's solution to the heart. The heart rests in a custom fabricated water-jacketed bath.

5.6.2 – Optical fluorescence imaging

Illumination was provided by LEDs (Luxeon, 5 W, 530 nm). High-numerical-aperture lenses (F-number 0.95, focal length 50 mm) were fitted with long-wavelength-pass emission filters (580 nm). Activation of the endocardium was imaged using an EMCCD camera (electron multiplied charge coupled device, Photometrics Cascade 128+, 128 × 128 pixels, 16-bit, 511 frames /s). A personal computer running custom software was used to record and analyze data.

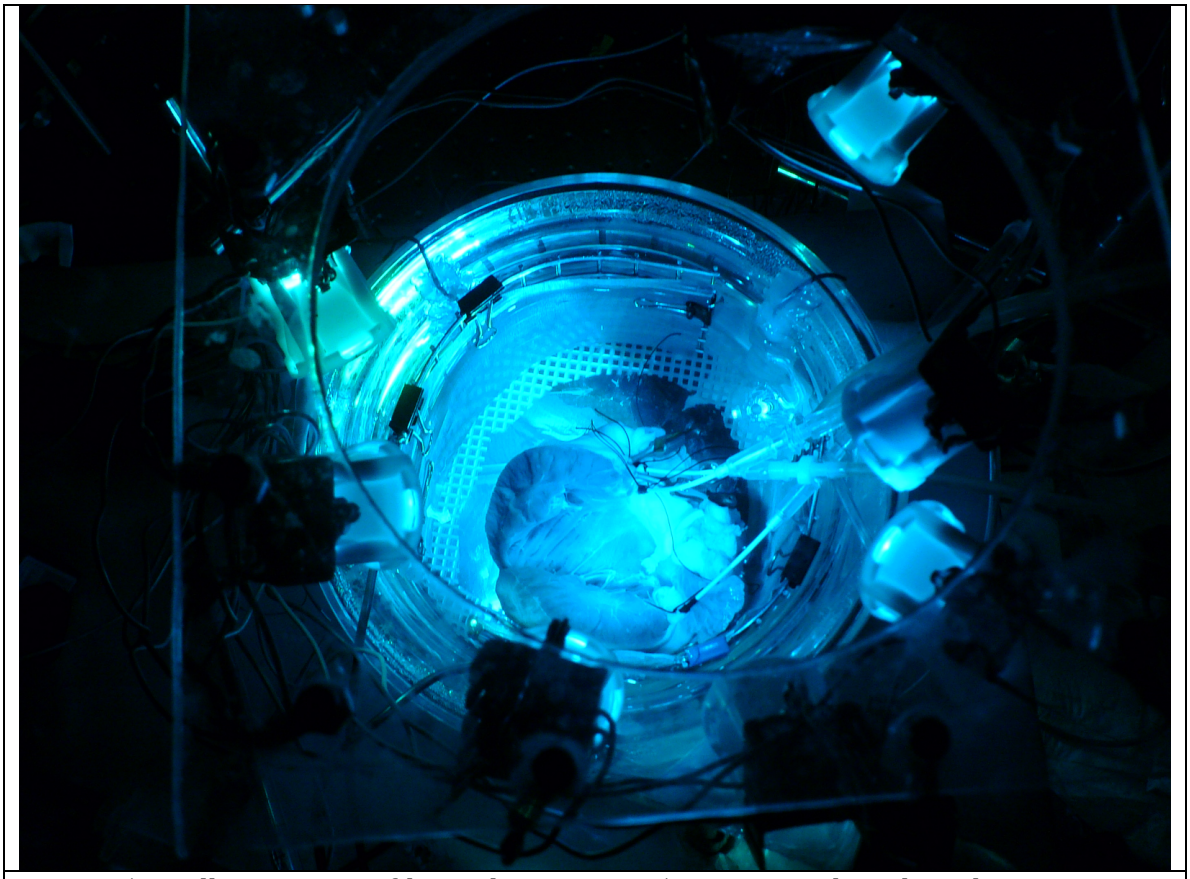

Figure 5.4 : Illumination of heart by LEDs at 530nM wavelength. Voltage sensitive dye will emit at 580nM when membrane potential depolarizes and be detected by high-speed cameras.

After optical mapping with voltage sensitive dyes, hearts were either treated with Lugol's solution, as in Figure 5.5, which preferentially stains the Purkinje fibers

for generating overlap maps via visual composite images, or with an acetylcholinesterase stain for micro CT imaging.

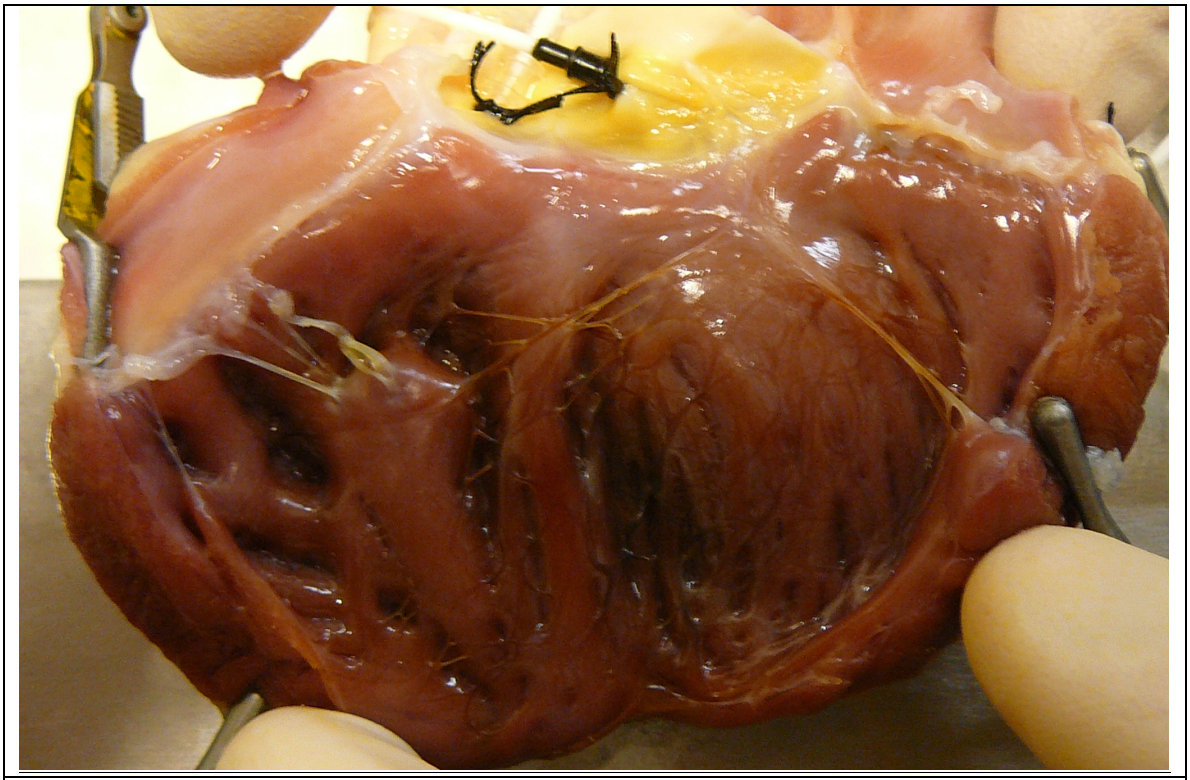

Figure 5.5 : Lugol's iodine stain of Purkinje fibers. High concentrations of glycogen (starch) in Purkinje fibers cause them to preferentially stain dark brown on the endocardial surface.

5.6.3 – Iodine staining & network mapping

Endocardial surfaces were painted with Lugol's Iodine solution to visually stain the Purkinje network. A dissecting microscope with variable magnification (10-40X) and a digital camera attachment were used to take 50-200 images of the endocardium. AutoPanoGiga software assembled the images into a composite high-resolution planar image. Manual tracing of the Purkinje network in Adobe

Photoshop and exporting the paths as scalable vector graphics (SVG) was used to create a coordinate-based network map.

5.6.4 – MicroCT imaging

Acetylcholinesterase (AChE) staining of the Purkinje fiber network was accomplished following the protocol of Sola et al(Sola et al., n.d.). Briefly, the AChE staining solution was prepared by adding in sequence the following chemical mixture to 500ml of distilled water: Na_2HPO_4(3.76g), NaH_2PO_4(10.15g), Glycine(1.5g), Acetylthiocholine Iodide(.73g), $CuSO_4 \bullet 5H_2O$ (1.04g). The heart was submerged in the staining solution for 5-7 days, and then imaged on a GE microCT 120 at a resolution of 25um or on an Xradia nanoCT at a resolution of 7um. Image analysis was performed using OsiriX software.

5.7 – Results

5.7.1 – Optical mapping

Optical maps were created to observe the activation sequence of myocardium by the Purkinje network via electrical stimulation of the right atria. At lower temperatures than physiological conditions the conduction speed of propagation through the AV node and Purkinje network was slowed so the activation sequence of endocardium was accurately recorded. As can be seen in Figure 5.6 which depicts the endocardial activation sequence, there are at least four regions that are depolarized by the Purkinje network and spread the activation sequence to the surrounding myocardium. Of note, the apex of the septum is

activated first, followed by the apex of the LV free wall, followed by the apex of the septum, and then an area between these regions is depolarized.

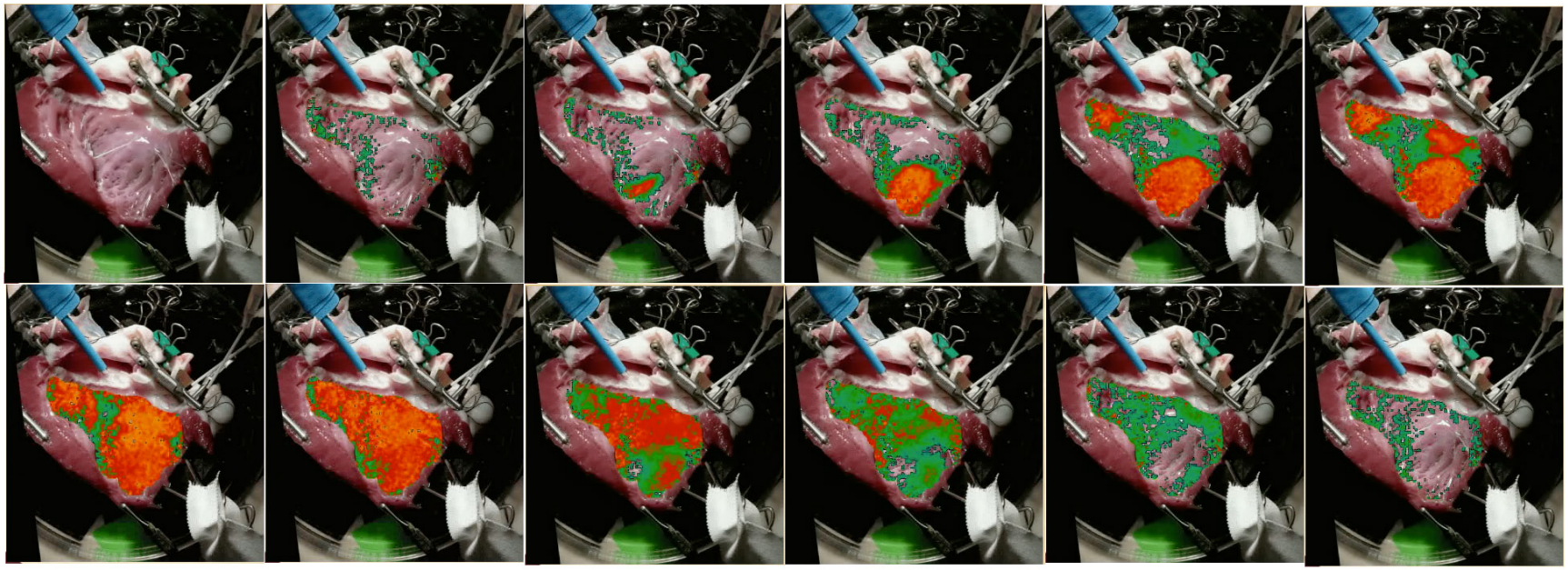

Figure 5.6 : LV endocardial activation sequence by Purkinje network. Areas in green are baseline/quiescent, while areas in red are depolarized and activated. Four distinct regions are identified as being activated by the Purkinje network.

5.7.2 – Iodine stained network maps

Hearts were treated with Lugol's solution on the endocardium to stain Purkinje fibers and using computer software to assemble individual images into a single composite image created high-resolution composite-image maps. This image was then imported into Adobe Photoshop and fibers paths were traced onto individual layer masks starting at the His Bundle and terminating at various locations on the endocardium. The paths for the Purkinje fibers were exported as SVG coordinate arrays to be later imported into modeling software. In a single composite image over 750 fiber paths were drawn to create an accurate network map of Purkinje fibers on the endocardium, as seen in Figure 5.7. The advantage to these data is that an accurate digital map is created to model the network. However, the method is time-consuming and PMJ sites are not identified by this method.

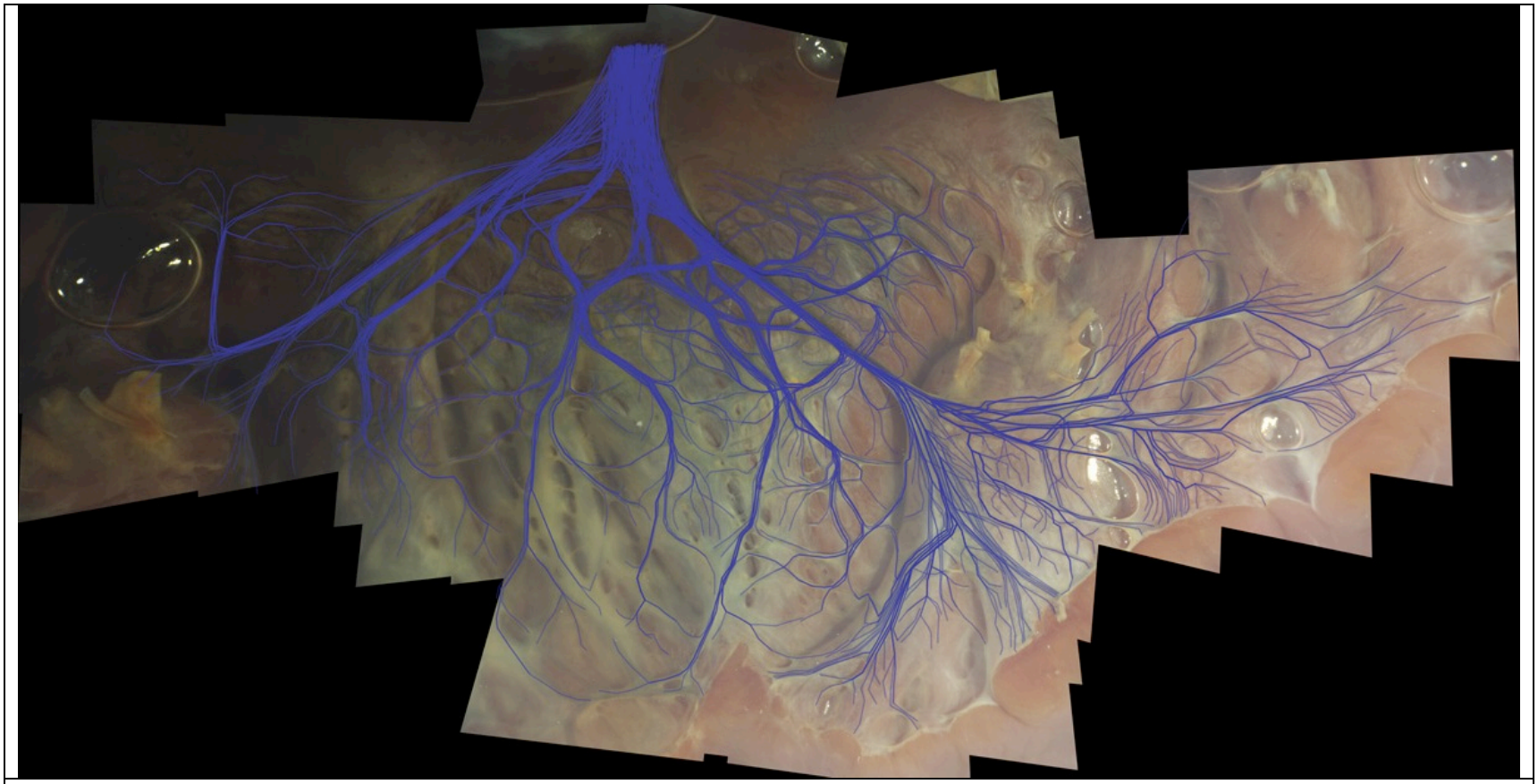

Figure 5.7 : Lugols-stained LV endocardium, high-resolution composite image, with over 750 network fiber paths traced in blue from bundle of His to termini.

5.7.3 - AChE staining

After application of Lugols and imaging the endocardium for network path analysis acetylcholinesterase (AChE) staining began. After 5 days of the heart being suspended in AChE staining solution a preferential staining of Purkinje fibers was observed, although the pliability of the tissue was significantly decreased. AChE provides a strong contrast agent for computer tomography imaging by preferentially marking Purkinje fibers with iodine. The stained Purkinje fiber network appears in high-contrast white to the naked eye, as seen in Figure 5.8, but is selectively visualized from the surrounding soft tissue during microCT or nanoCT.

Figure 5.8 : AChE stained canine LV endocardium. Note the Purkinje network is stained white.

In Figure 5.9, a magnified selection of the previous figure, it is apparent that the fibers cross over themselves multiple times, and in some instances seem to reconnect forming loop circuits. The extent to which the fibers reconnect or simply overlap is an important question to answer, as well as whether the fibers form loops and, if so, the purpose of these loops.

Figure 5.9 – Magnified view of AChE-stained Purkinje network. Note that the bundle of His (arrow) is composed of more than one fiber, in disagreement with the tenet that the Purkinje network is fractal in nature.

5.7.4 - CT imaging

Purkinje fibers were preferentially stained, compared to surrounding soft tissue, yielding a detailed network map of the entire Purkinje network, as seen in Figure 5.10. Although the Purkinje network does descend into the myocardium, it was noted that the AChE stain was mostly confined to the surface of the endocardium, and did not stain fibers below the surface, as can be seen in Figure 5.11. Unfortunately, the combination of contrast agent and resolution of the micro CT, which was on the order of 25uM, as well as the nano CT, as seen in Figure 5.12, which scanned at a resolution of 7uM, was not sufficient to discriminate individual Purkinje cells within the bundles or to assess electrical connections at the bifurcation/joining points of the fiber network.

Figure 5.10 : MicroCT image of the AChE stained Purkinje network which shows preferential Purkinje staining and allows examination of network map to determine whether fibers are reconnecting to form loops.

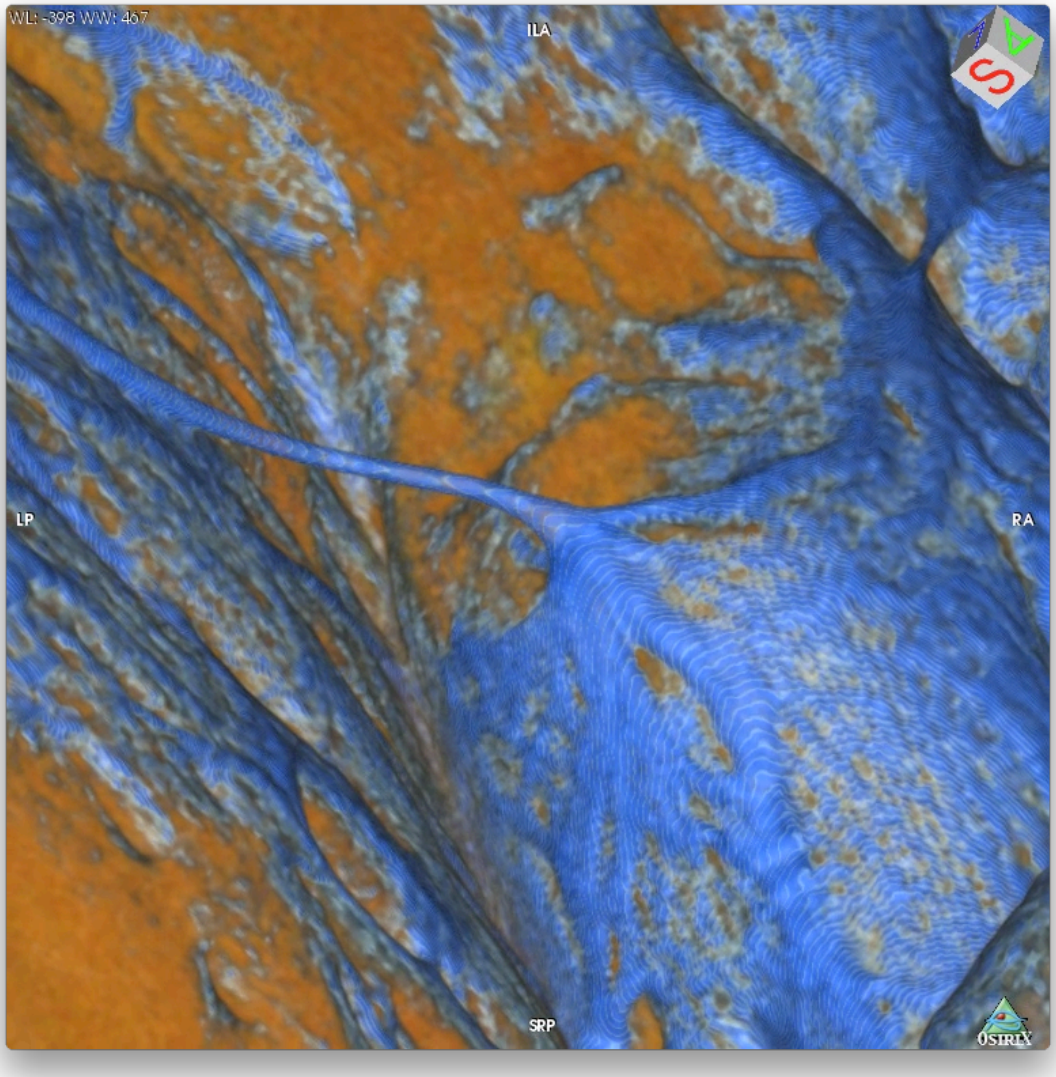

Figure 5.11 : False color magnification of 25uM MicroCT scan of Purkinje network, which shows good surface staining, but lack of sub-surface stain.

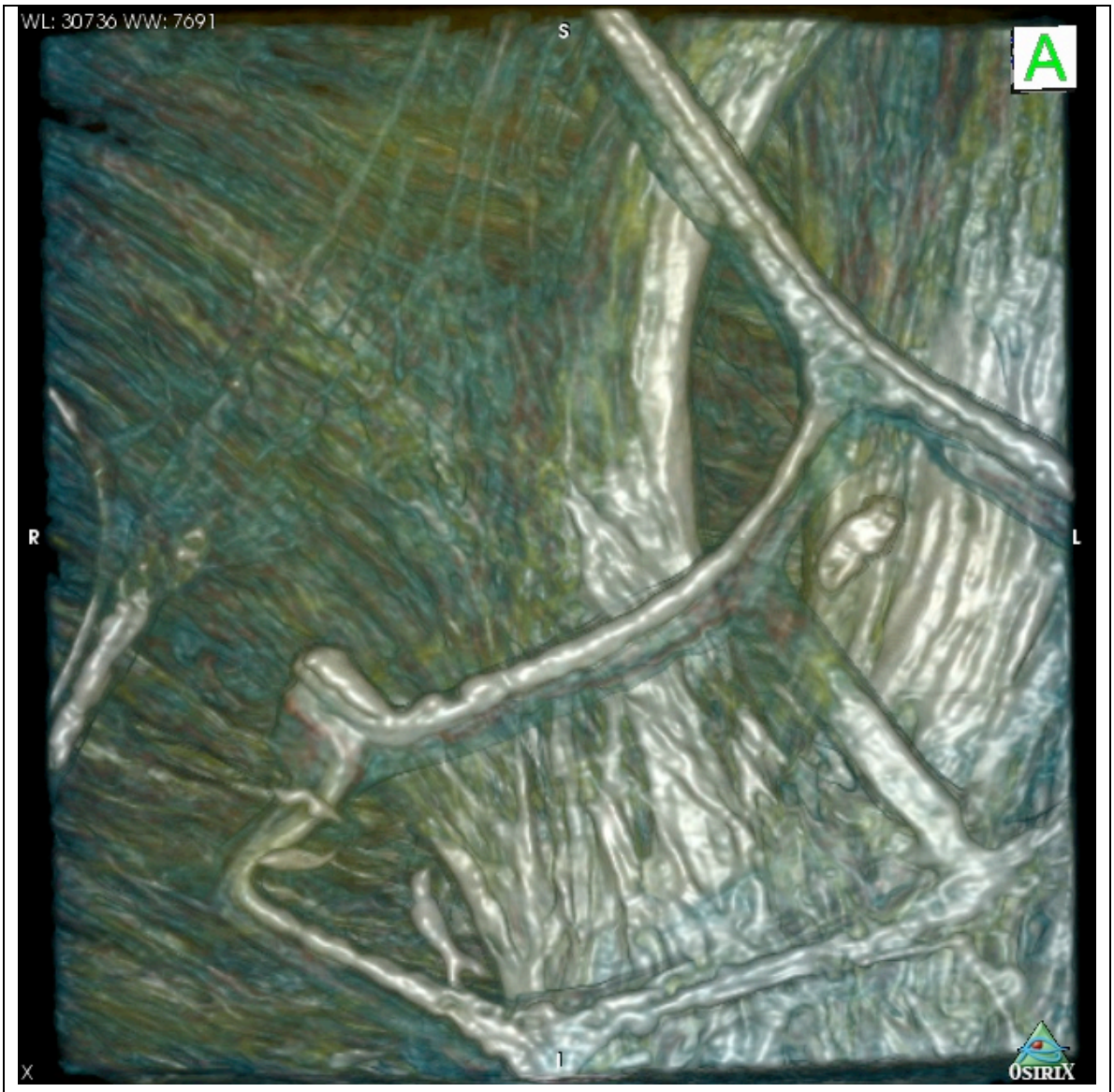

Figure 5.12 : False color image of nanoCT image with 6.5uM resolution. While it becomes possible to see reconnecting fiber paths, resolution by CT is insufficient to see individual Purkinje cells or to determine electrical connections at these locations.

5.8 – Discussion

As mentioned previously, the Purkinje network has often been characterized as a fractal and represented by a tree structure in computer models. However, high-resolution imaging of a stained network indicates that this representation is likely a misconception. Evidence in support of this argument is that the bundle of His appears to be made up of perhaps hundreds of individual fibers, each comprised of several Purkinje cells, and not a single fiber that branches repeatedly. This observation makes sense from a functional standpoint, since a perpetual division of signal from a parent branch into daughter branches would present a great source-sink mismatch for current drain in the Purkinje network. Such a situation could make it more difficult to disseminate a signal throughout the network. A more likely configuration is that the bundle of His resembles a bundle of individual wires, each leading to a different location.

A new direction for future work would be to determine if each fiber in the bundle of His acts like a fractal, branching in a tree structure, or if each fiber is electrically isolated along its entire path from AV node to its terminus in the endocardium. Higher resolution imaging solutions such as confocal microscopy might help solve this problem, but a target antibody to label Purkinje in canine currently is not available. Some work has already been done in rabbit by Romero et al(Romero et al., 2011), which indicates that a single Purkinje cell can be electrically connected to several branches at a bifurcation node. However, the bifurcation nodes they examined via high resolution confocal microscopy were distant from the

bundle of His, and may not be indicative of all bifurcation locations. A more thorough study of multiple junctional sites near and far from the bundle of His would be useful to assess the interaction between fibers throughout the network.

Optical mapping experiments of activation patterns on the endocardium by the Purkinje network allude to the possibility that either some Purkinje muscle junctions have a shorter delay time, or more likely that there exists a greater density of Purkinje muscle junctions at certain locations [this conflicts with what you said earlier in the intro]. While activation sequences are useful to locate these regions of higher density, it would also be useful to know how many PMJs are in these regions, as well as in the surrounding areas. One possible experiment to verify whether PMJs exist everywhere or in specific areas is to image the areas of primary activation of the muscle and then chemically ablate or selectively cool those regions to see if the muscle is activated in other regions instead. The answers to these questions will be useful for building more accurate computer models, and future work to determine PMJ population density should target these regions of initial myocardial activation.

On the macroscopic level, the Purkinje fiber structure does appear tree-like, with a central trunk comprised of the bundle of His, and two main branches (the left and right bundle branches) that further bifurcate along the inner walls of the heart. But closer examination by CT imaging of this network, which was thought to simply have overlapping fibers, shows these fibers form loop circuits. The purpose of these loops is not clear, but one possible explanation is that, unlike in a simple tree

structure, they act as a protective mechanism so that if an area becomes damaged and electrically disconnected, loss of signal is not guaranteed since there may be alternate pathways to route a signal.

Another hypothesis is that areas of myocardium which are activated first during normal heart rhythm have a greater number of loops with Purkinje muscle junctions present that allow more current to be routed to that area. By increasing the ratio of current source, the Purkinje network, to current sink, the myocardium, certain areas would be preferentially activated. This scenario could explain why certain areas of endocardium are repeatedly activated in the same sequence, but that idea remains to be tested experimentally.

REFERENCES

Aidley, D. J. (1998). *The physiology of excitable cells*. Cambridge University Press.

Akar, F. G., & Rosenbaum, D. S. (2003). Transmural electrophysiological heterogeneities underlying arrhythmogenesis in heart failure. *Circulation research*, *93*(7), 638–645. doi:10.1161/01.RES.0000092248.59479.AE

Akar, F. G., Yan, G.-X., Antzelevitch, C., & Rosenbaum, D. S. (2002). Unique topographical distribution of M cells underlies reentrant mechanism of torsade de pointes in the long-QT syndrome. *Circulation*, *105*(10), 1247–1253.

Alanis, J., Benitez, D., & PILAR, G. (1961). A functional discontinuity between the Purkinje and ventricular muscle cells. *Acta physiologica latino americana*, *11*, 171–183.

Allessie, M., Bonke, F., & Schopman, F. (1973). Circus movement in rabbit atrial muscle as a mechanism of tachycardia. *Circulation research*, *33*(1), 54–62.

Allessie, M., Bonke, F., & Schopman, F. (1976). Circus movement in rabbit atrial muscle as a mechanism of tachycardia. *Circulation research*, II. The role of nonuniform recovery of excitability in the occurrence of unidirectional block, as studied with multiple microelectrodes, *39*(2), 168–177.

Allessie, M., Bonke, F., & Schopman, F. (1977). Circus movement in rabbit atrial muscle as a mechanism of tachycardia. *Circulation research*, III. The "leading circle" concept: a new model of circus movement in cardiac tissue without the involvement of an anatomical obstacle, *41*(1), 9–18.

Allison, J. S., Qin, H., Dosdall, D. J., Huang, J., Newton, J. C., Allred, J. D., Smith, W. M., et al. (2007). The transmural activation sequence in porcine and canine left ventricle is markedly different during long-duration ventricular fibrillation. *Journal of cardiovascular electrophysiology*, *18*(12), 1306–1312. doi:10.1111/j.1540-8167.2007.00963.x

Antonaccio, M. J., & Gomoll, A. (1993). Pharmacologic basis of the antiarrhythmic and hemodynamic effects of sotalol. *The American journal of cardiology*, *72*(4), 27A–37A.

Antzelevitch, C. (2000). Electrical heterogeneity, cardiac arrhythmias, and the sodium channel. *Circulation research*.

Antzelevitch, C., & Shimizu, W. (1999). The M cell. *Journal of ….*

Antzelevitch, C., Sicouri, S., & Litovsky, S. (1991a). Heterogeneity within the ventricular wall. Electrophysiology and pharmacology of epicardial, endocardial, and M cells. *Circulation*.

Antzelevitch, C., Sicouri, S., Litovsky, S. H., Lukas, A., Krishnan, S. C., Di Diego, J. M., Gintant, G. A., et al. (1991b). Heterogeneity within the ventricular wall. Electrophysiology and pharmacology of epicardial, endocardial, and M cells. *Circulation research*, *69*(6), 1427–1449.

Arnar, D. O., Bullinga, J. R., & Martins, J. B. (1997). Role of the Purkinje system in spontaneous ventricular tachycardia during acute ischemia in a canine model. *Circulation*, *96*(7), 2421–2429.

Arnar, D. O., Xing, D., Lee, H., & Martins, J. B. (2001). Prevention of ischemic ventricular tachycardia of Purkinje origin: role for alpha(2)-adrenoceptors in Purkinje? *American journal of physiology Heart and circulatory physiology*, *280*(3), H1182–90.

Atkinson, A., Inada, S., Li, J., Tellez, J. O., Yanni, J., Sleiman, R., Allah, E. A., et al. (2011). Anatomical and molecular mapping of the left and right ventricular His-Purkinje conduction networks. *Journal of Molecular and Cellular Cardiology*, *51*(5), 689–701. doi:10.1016/j.yjmcc.2011.05.020

BAGDONAS, A. A., STUCKEY, J. H., PIERA, J., AMER, N. S., & Hoffman, B. F. (1961). Effects of ischemia and hypoxia on the specialized conducting system of the canine heart. *American Heart Journal*, *61*, 206–218.

Bailey, J. C., Lathrop, D. A., & Pippenger, D. L. (1977). Differences between proximal left and right bundle branch block action potential durations and refractoriness in the dog heart. *Circulation research*, *40*(5), 464–468.

Barber, M. J., Mueller, T. M., Henry, D. P., Felten, S. Y., & Zipes, D. P. (1983). Transmural myocardial infarction in the dog produces sympathectomy in noninfarcted myocardium. *Circulation*, *67*(4), 787–796.

Bartocci, E., Singh, R., Stein, von, F. B., Amedome, A., Caceres, A. J. J., Castillo, J., Closser, E., et al. (2011). Teaching cardiac electrophysiology modeling to undergraduate students: laboratory exercises and GPU programming for the study of arrhythmias and spiral wave dynamics. *Advances in physiology education*, *35*(4), 427–437. doi:10.1152/advan.00034.2011

Bänsch, D., Oyang, F., Antz, M., Arentz, T., Weber, R., Val-Mejias, J. E., Ernst, S., et al. (2003). Successful catheter ablation of electrical storm after myocardial infarction. *Circulation*, *108*(24), 3011–3016. doi:10.1161/01.CIR.0000103701.30662.5C

Belousov, B. (1959). *A periodic reaction and its mechanism* (Vol. 147). Compilation of Abstracts on Radiation Medicine.

Berenfeld, O., & Jalife, J. (1998). Purkinje-muscle reentry as a mechanism of polymorphic ventricular arrhythmias in a 3-dimensional model of the ventricles. *Circulation research*, *82*(10), 1063–1077.

Bertrix, L., Timour-Chah, Q., Lang, J., Lakhal, M., & Faucon, G. (1986). Protection against ventricular and atrial fibrillation by sotalol. *Cardiovascular research*, *20*(5), 358–363.

Bode, K., Hindricks, G., Piorkowski, C., Sommer, P., Janousek, J., Dagres, N., & Arya, A. (2008). Ablation of polymorphic ventricular tachycardias in patients with structural heart disease. *Pacing and Clinical Electrophysiology*, *31*(12), 1585–1591. doi:10.1111/j.1540-8159.2008.01230.x

Bogun, F., Good, E., Reich, S., Elmouchi, D., Igic, P., Tschopp, D., Dey, S., et al. (2006). Role of Purkinje fibers in post-infarction ventricular tachycardia. *Journal of the American College of Cardiology*, *48*(12), 2500–2507. doi:10.1016/j.jacc.2006.07.062

Bonometti, C., Hwang, C., Hough, D., Lee, J. J., Fishbein, M. C., Karagueuzian, H. S., & Chen, P. S. (1995). Interaction between strong electrical stimulation and reentrant wavefronts in canine ventricular fibrillation. *Circulation research*, *77*(2), 407–416.

Boyden, P. A., & Pinto, J. M. (1994). Reduced calcium currents in subendocardial Purkinje myocytes that survive in the 24- and 48-hour infarcted heart. *Circulation*, *89*(6), 2747–2759.

Boyden, P. A., Albala, A., & Dresdner, K. P. (1989). Electrophysiology and ultrastructure of canine subendocardial Purkinje cells isolated from control and 24-hour infarcted hearts. *Circulation research*, *65*(4), 955–970.

Burdon-Sanderson, J., & Page, F. (1883). *On the electrical phenomena of the excitatory process in the heart of the frog and of the tortoise, as investigated photgraphically. J. Physiol. London* (1883rd ed. pp. 327–338). J Phsiol.

Cameron, J. S., & Han, J. (1982). Effects of epinephrine on automaticity and the incidence of arrhythmias in Purkinje fibers surviving myocardial infarction. *The Journal of pharmacology and experimental therapeutics*, *223*(2), 573–579.

Cameron, J. S., Dersham, G. H., & Han, J. (1982). Effects of epinephrine on the electrophysiologic properties of Purkinje fibers surviving myocardial infarction. *American Heart Journal*, *104*(3), 551–560.

Cao, J., Qu, Z., Kim, Y., Wu, T., & Garfinkel, A. (1999). Spatiotemporal heterogeneity in the induction of ventricular fibrillation by rapid pacing:... - Abstract - UK PubMed Central. *Circulation*.

Ceremuzyński, L., Staszewska-Barczak, J., & Herbaczynska-Cedro, K. (1969). Cardiac rhythm disturbances and the release of catecholamines after acute coronary occlusion in dogs. *Cardiovascular research*, *3*(2), 190–197.

Chen, J., Mandapati, R., Berenfeld, O., Skanes, A. C., & Jalife, J. (2000). High-frequency periodic sources underlie ventricular fibrillation in the isolated rabbit heart. *Circulation research*, *86*(1), 86–93.

Chen, P. (2000). Electrode mapping of ventricular fibrillation. (D. Zipes & J. Jalife, Eds.)*Cardiac electrophysiology: from cell to bedside*, 395–404.

Chen, P. S., Wolf, P. D., Dixon, E. G., Danieley, N. D., Frazier, D. W., Smith, W. M., & Ideker, R. E. (1988). Mechanism of ventricular vulnerability to single premature stimuli in open-chest dogs. *Circulation research*, *62*(6), 1191–1209.

Chen, P. S., Wolf, P. L., Cha, Y. M., Peters, B. B., & Topham, S. L. (1993). Effects of subendocardial ablation on anodal supernormal excitation and ventricular vulnerability in open-chest dogs. *Circulation*, *87*(1), 216–229.

Chen, X., Lal, A., & Riccio, M. (2004). Silicon based ultrasonic microprobes for cardiac signal recording. *IEEE Ultrasonics Symposium*, 618–621.

Chen, X., Lal, A., Riccio, M. L., & Gilmour, R. F. (2006). Ultrasonically Actuated Silicon Microprobes for Cardiac Signal Recording. *IEEE transactions on bio-medical engineering*, *53*(8), 1665–1671. doi:10.1109/TBME.2006.877808

Cherry, E. M., & Fenton, F. H. (2004). Suppression of alternans and conduction blocks despite steep APD restitution: electrotonic, memory, and conduction velocity restitution effects. *American journal of physiology Heart and circulatory physiology*, *286*(6), H2332–41. doi:10.1152/ajpheart.00747.2003

Chialvo, D. R., & Jalife, J. (1991). 1/f Power spectral density of the cardiac QRS complex is not associated with a fractal Purkinje system. *Biophysical journal*, *60*(5), 1303–1305.

Chialvo, D. R., Michaels, D. C., & Jalife, J. (1990). Supernormal excitability as a mechanism of chaotic dynamics of activation in cardiac Purkinje fibers. *Circulation research*, *66*(2), 525–545.

CHURNEY, L., & OHSHIMA, H. (1964). AN IMPROVED SUCTION ELECTRODE FOR RECORDING FROM THE DOG HEART IN SITU. *Journal of applied physiology*, *19*, 793–798.

Coetzee, W. A., & Opie, L. H. (1987). Effects of components of ischemia and metabolic inhibition on delayed afterdepolarizations in guinea pig papillary muscle. *Circulation research*, *61*(2), 157–165.

Cohen, C. J., Bean, B. P., & Tsien, R. W. (1984). Maximal upstroke velocity as an index of available sodium conductance. Comparison of maximal upstroke velocity and voltage clamp measurements of sodium current in rabbit Purkinje fibers. *Circulation research*, *54*(6), 636–651.

Cole, K. S. (1939). Electric impedance of the squid giant axon during activity. *The Journal of general physiology*, *22*(5), 649–670. doi:10.1085/jgp.22.5.649

Coraboeuf, E., & Weidmann, S. (1949). *Potentials d'action du muscle cardiaque obtenus à l'aide de microelectrodes intracelulaires. Présence d'une inversion de potentiel.* (1949th ed. pp. 1360–1361). Car Soc Biol Paris.

Cordeiro, J. M., Spitzer, K. W., & Giles, W. R. (1998). Repolarizing K+ currents in rabbit heart Purkinje cells. *The Journal of physiology*, *508 (Pt 3)*, 811–823.

Coronel, R., de Bakker, J. M. T., Wilms-Schopman, F. J. G., Opthof, T., Linnenbank, A. C., Belterman, C. N., & Janse, M. J. (2006). Monophasic action potentials and activation recovery intervals as measures of ventricular action potential duration: experimental evidence to resolve some controversies. *Heart rhythm : the official journal of the Heart Rhythm Society*, *3*(9), 1043–1050. doi:10.1016/j.hrthm.2006.05.027

Cranefield, P. (n.d.). *The conduction of the cardiac impulse: The slow response and cardiac arrhythmias* (1975th ed.). Futura Pub. Co. Mount Kisco, N.Y.

Cranefield, P. (n.d.). *Cardiac arrhythmias: the role of triggered activity and other mechanisms* (1988th ed.). Futura Pub. Co. Mount Kisco, N.Y.

Damiano, R. J., Smith, P. K., Tripp, H. F., Asano, T., Small, K. W., Lowe, J. E., Ideker, R. E., et al. (1986). The effect of chemical ablation of the endocardium on ventricular fibrillation threshold. *Circulation*, *74*(3), 645–652.

Davidenko, J. M., Pertsov, A. V., Salomonsz, R., Baxter, W., & Jalife, J. (1992). Stationary and drifting spiral waves of excitation in isolated cardiac muscle. *Nature*, *355*(6358), 349–351. doi:10.1038/355349a0

Deo, M., Boyle, P., Plank, G., & Vigmond, E. (2009). Arrhythmogenic mechanisms of the Purkinje system during electric shocks: a modeling study. *Heart rhythm : the official journal of the Heart Rhythm Society*, *6*(12), 1782–1789. doi:10.1016/j.hrthm.2009.08.023

Dobrzynski, H., Li, J., Tellez, J., Greener, I. D., Nikolski, V. P., Wright, S. E., Parson, S. H., et al. (2005). Computer three-dimensional reconstruction of the sinoatrial node. *Circulation*, *111*(7), 846–854. doi:10.1161/01.CIR.0000152100.04087.DB

Dosdall, D. J., Cheng, K.-A., Huang, J., Allison, J. S., Allred, J. D., Smith, W. M., & Ideker, R. E. (2007). Transmural and endocardial Purkinje activation in pigs before local myocardial activation after defibrillation shocks. *Heart rhythm : the official journal of the Heart Rhythm Society*, *4*(6), 758–765. doi:10.1016/j.hrthm.2007.02.017

Dosdall, D. J., Tabereaux, P. B., Kim, J. J., Walcott, G. P., Rogers, J. M., Killingsworth, C. R., Huang, J., et al. (2008). Chemical ablation of the Purkinje system causes early termination and activation rate slowing of long-duration ventricular fibrillation in dogs. *American journal of physiology Heart and circulatory physiology*, *295*(2), H883–9. doi:10.1152/ajpheart.00466.2008

Downar, E., Harris, L., Mickleborough, L. L., Shaikh, N., & Parson, I. D. (1988). Endocardial mapping of ventricular tachycardia in the intact human ventricle: evidence for reentrant mechanisms. *Journal of the American College of Cardiology*, *11*(4), 783–791.

DRAPER, M. H., & Weidmann, S. (1951). Cardiac resting and action potentials recorded with an intracellular electrode. *The Journal of physiology*, *115*(1), 74–94.

Durrer, D., & Van Der Tweel, L. H. (1953). Spread of activation in the left ventricular wall of the dog. I. *American Heart Journal*, 683–691.

Durrer, D., van Dam, R. T., Freud, G. E., Janse, M. J., Meijler, F. L., & Arzbaecher, R. C. (1970). Total excitation of the isolated human heart. *Circulation*, *41*(6), 899–912.

Echebarria, B., & Karma, A. (2002). Instability and spatiotemporal dynamics of alternans in paced cardiac tissue. *Physical Review Letters*, *88*(20), 208101.

Edvardsson, N., Hirsch, I., Emanuelsson, H., Pontén, J., & Olsson, S. B. (1980). Sotalol-induced delayed ventricular repolarization in man. *European heart journal*, *1*(5), 335–343.

Efimov, I., Sidorov, V., & Cheng, Y. (1999). Evidence of Three-Dimensional Scroll Waves with Ribbon-Shaped Filament as a Mechanism of Ventricular Tachycardia in the Isolated Rabbit Heart. *J Cardiovasc Res*, *10*(11), 1452–1462.

El-Sherif, N. (1988). Reentry Revisited. *Pacing and Clinical Electrophysiology*, *11*(9), 1358–1368. doi:10.1111/j.1540-8159.1988.tb04000.x

El-Sherif, N., Caref, E. B., Yin, H., & Restivo, M. (1996). The electrophysiological mechanism of ventricular arrhythmias in the long QT syndrome. Tridimensional mapping of activation and recovery patterns. *Circulation research*, *79*(3), 474–492.

El-Sherif, N., Gough, W. B., Zeiler, R. H., & Mehra, R. (1983). Triggered ventricular rhythms in 1-day-old myocardial infarction in the dog. *Circulation research*, *52*(5), 566–579.

Elharrar, V., & Zipes, D. (n.d.). *The Slow inward current and cardiac arrhythmias*. (V. Elharrar, D. Zipes, & J. Bailey, Eds.)Voltage modulation of automaticity in cardiac Purkinje fibers (1980th ed. p. 357). Martinus Nijhoff, The Hague.

Elharrar, V., & Zipes, D. P. (1977). Cardiac electrophysiologic alterations during myocardial ischemia. *The American journal of physiology*, *233*(3), H329–45.

Enjoji, Y., Mizobuchi, M., Muranishi, H., Miyamoto, C., Utsunomiya, M., Funatsu, A., Kobayashi, T., et al. (2009). Catheter ablation of fatal ventricular tachyarrhythmias storm in acute coronary syndrome--role of Purkinje fiber network. *Journal of interventional cardiac electrophysiology : an international journal of arrhythmias and pacing*, *26*(3), 207–215. doi:10.1007/s10840-009-9394-7

Ensell, G., Banks, D. J., Ewins, D. J., Balachandran, W., & Richards, P. R. (1996). Silicon-based microelectrodes for neurophysiology fabricated using a gold metallization/nitride passivation system. *Journal of Microelectromechanical Systems*, *5*(2), 117–121. doi:10.1109/84.506199

Fast, V. G., & Kleber, A. G. (1995). Block of impulse propagation at an abrupt tissue expansion: evaluation of the critical strand diameter in 2- and 3-dimensional computer models. *Cardiovascular research*, *30*(3), 449–459.

Fast, V. G., Sharifov, O. F., Cheek, E. R., Newton, J. C., & Ideker, R. E. (2002). Intramural virtual electrodes during defibrillation shocks in left ventricular wall assessed by optical mapping of membrane potential. *Circulation*, *106*(8), 1007–1014.

Fenoglio, J. J., Karagueuzian, H. S., Friedman, P. L., Albala, A., & Wit, A. L. (1979). Time course of infarct growth toward the endocardium after coronary occlusion. *The American journal of physiology*, *236*(2), H356–70.

Ferrier, G. R. (1977). Digitalis arrhythmias: role of oscillatory afterpotentials. *Progress in cardiovascular diseases*, *19*(6), 459–474.

Ferrier, G. R., Saunders, J. H., & Mendez, C. (1973). A cellular mechanism for the generation of ventricular arrhythmias by acetylstrophanthidin. *Circulation research*, *32*(5), 600–609.

Fox, J. J., Riccio, M. L., Hua, F., Bodenschatz, E., & Gilmour, R. F. (2002a). Spatiotemporal transition to conduction block in canine ventricle. *Circulation research*, *90*(3), 289–296.

Fox, J., Gilmour, R., & Bodenschatz, E. (2002b). Conduction Block in One-Dimensional Heart Fibers. *Physical Review Letters*, *89*(19). doi:10.1103/PhysRevLett.89.198101

Frankl, W. S., & Soloff, L. A. (1968). Sotalol: A new, safe beta adrenergic receptor blocking agent∗. *The American journal of cardiology*, *22*(2), 266–272. doi:10.1016/0002-9149(68)90233-6

Franz, M. (2005). What is a monophasic action potential recorded by the Franz contact electrode? *Cardiovascular research*.

Franz, M. R. (1983). Long-term recording of monophasic action potentials from human endocardium. *The American journal of cardiology*, *51*(10), 1629–1634.

Franz, M. R., Burkhoff, D., Spurgeon, H., Weisfeldt, M. L., & Lakatta, E. G. (1986). In vitro validation of a new cardiac catheter technique for recording monophasic action potentials. *European heart journal*, *7*(1), 34–41.

Frazier, D. W., Krassowska, W., Chen, P. S., Wolf, P. D., Danieley, N. D., Smith, W. M., & Ideker, R. E. (1988). Transmural activations and stimulus potentials in three-dimensional anisotropic canine myocardium. *Circulation research*, *63*(1), 135–146.

Friedman, P. L., Fenoglio, J. J., & Wit, A. L. (1975). Time course for reversal of electrophysiological and ultrastructural abnormalities in subendocardial Purkinje fibers surviving extensive myocardial infarction in dogs. *Circulation research*, *36*(1), 127–144.

Friedman, P. L., Stewart, J. R., & Wit, A. L. (1973a). Spontaneous and induced cardiac arrhythmias in subendocardial Purkinje fibers surviving extensive myocardial infarction in dogs. *Circulation research*, *33*(5), 612–626.

Friedman, P. L., Stewart, J. R., Fenoglio, J. J., & Wit, A. L. (1973b). Survival of subendocardial Purkinje fibers after extensive myocardial infarction in dogs. *Circulation research*, *33*(5), 597–611.

Garfinkel, A., Chen, P. S., Walter, D. O., Karagueuzian, H. S., Kogan, B., Evans, S. J., Karpoukhin, M., et al. (1997). Quasiperiodicity and chaos in cardiac fibrillation. *The Journal of clinical investigation*, *99*(2), 305–314. doi:10.1172/JCI119159

Garrey, W. (1912). The nature of fibrillary contraction of the heart. *American Journal of Physiology-- ...*, Its relation to tissue mass and form. Retrieved December 18, 2011, from http://ajplegacy.physiology.org/content/33/3/397.extract

Gelzer, A. R., Koller, M. L., Otani, N. F., Fox, J. J., Enyeart, M. W., Hooker, G. J., Riccio, M. L., et al. (2008). Dynamic Mechanism for Initiation of Ventricular Fibrillation In Vivo. *Circulation*, *118*(11), 1113–1114. doi:10.1161/CIRCULATIONAHA.108.190525

Gilmour, R. F. (2004). The anatomy of an arrhythmia. *The Journal of clinical investigation*, *113*(5), 662–664. doi:10.1172/JCI21223

Gilmour, R. F. (2009). Restitution, heterogeneity and unidirectional conduction block: New roles for old players. *Heart rhythm : the official journal of the Heart Rhythm Society*, *6*(4), 544–545. doi:10.1016/j.hrthm.2009.01.036

Gilmour, R., & Zipes, D. (1980). Different electrophysiological responses of canine endocardium and epicardium to combined hyperkalemia, hypoxia, and acidosis. *Circulation research*. Retrieved January 16, 2012, from http://circ.ahajournals.org/cgi/ijlink?linkType=PDF&journalCode=circresaha&resid=46/6/814

Glukhov, A. V., Fedorov, V. V., Lou, Q., Ravikumar, V. K., Kalish, P. W., Schuessler, R. B., Moazami, N., et al. (2010). Transmural dispersion of repolarization in failing and nonfailing human ventricle. *Circulation research*, *106*(5), 981–991. doi:10.1161/CIRCRESAHA.109.204891

Goldberger, A. L., Bhargava, V., West, B. J., & Mandell, A. J. (1985). On a mechanism of cardiac electrical stability. The fractal hypothesis. *Biophysical journal*, *48*(3), 525–528. doi:10.1016/S0006-3495(85)83808-X

Gomez-Gesteria, M., & Fernández-Garcia, G. (1994). Vulnerability in excitable Belousov-Zhabotinsky medium: from 1D to 2D. *Physica D: Nonlinear Phenomena*, *76*, 359–368.

Gomoll, A. W., & Bartek, M. J. (1986). Comparative beta-blocking activities and electrophysiologic actions of racemic sotalol and its optical isomers in anesthetized dogs. *European journal of pharmacology*, *132*(2-3), 123–135.

Gorelova, N. A., & Bures, J. (1983). Spiral waves of spreading depression in the isolated chicken retina. *Journal of neurobiology*, *14*(5), 353–363. doi:10.1002/neu.480140503

Grant, A. O., & Katzung, B. G. (1976). The effects of quinidine and verapamil on electrically induced automaticity in the ventricular myocardium of guinea pig. *The Journal of pharmacology and experimental therapeutics*, *196*(2), 407–419.

Gray, R. A., Jalife, J., Panfilov, A. V., Baxter, W. T., Cabo, C., Davidenko, J. M., & Pertsov, A. M. (1995). Mechanisms of cardiac fibrillation. *Science*, *270*(5239), 1222–3; author reply 1224–5.

Gray, R. A., Pertsov, A. M., & Jalife, J. (1998). Spatial and temporal organization during cardiac fibrillation. *Nature*, *392*(6671), 75–78. doi:10.1038/32164

Guevara, M., Alonso, F., & Jeandupeux, D. (1989). Alternans in periodically stimulated isolated ventricular myocytes: experiment and model. *Cell to Cell signaling …*.

Guyton, A. C. (1985). Handbook of Physiology-The Cardiovascular System. *Critical Care Medicine*, *13*(5), 449.

Häissaguerre, M., Extramiana, F., Hocini, M., Cauchemez, B., Jaïs, P., Cabrera, J. A., Farré, J., et al. (2003). Mapping and ablation of ventricular fibrillation associated with long-QT and Brugada syndromes. *Circulation*, *108*(8), 925–928. doi:10.1161/01.CIR.0000088781.99943.95

Häissaguerre, M., Shah, D. C., Jaïs, P., Shoda, M., Kautzner, J., Arentz, T., Kalushe, D., et al. (2002). Role of Purkinje conducting system in triggering of idiopathic ventricular fibrillation. *Lancet*, *359*(9307), 677–678. doi:10.1016/S0140-6736(02)07807-8

Haïssaguerre, M., Shoda, M., Jaïs, P., & Nogami, A. (2002). Mapping and Ablation of Idiopathic Ventricular Fibrillation. *Circulation*.

HIS, W. (1949). The story of the atrioventricular bundle with remarks concerning embryonic heart activity. *Journal of the history of medicine and allied sciences*, *4*(3), 319–333.

Hodgkin, A. (1975). The optimum density of sodium channels in an unmyelinated nerve. *Philosophical transactions of the Royal Society of London. Series B, Biological sciences*, *270*(908), 297–300.

Hoffman, B. F. (2000). *Monophasic Action Potentials*. (M. Franz, Ed.)Bridging Cell and Bedside. Futura Publishing Co.

Hoffman, B. F., & Rosen, M. R. (1981). Cellular mechanisms for cardiac arrhythmias. *Circulation research*, *49*(1), 1–15.

Hoffman, B., & Cranefield, P. (1959). Comparison of cardiac monophasic action potentials recorded by intracellular and suction electrodes. *American Journal of …*.

Holden, A., Mironov, S., & Pertsov, A. (1999). Three-dimensional aspects of re-entry in experimental and numerical models of ventricular fibrillation. *… Journal of Bifurcation …*.

Holland, R. P., & Brooks, H. (1976). The QRS complex during myocardial ischemia. An experimental analysis in the porcine heart. *The Journal of clinical investigation*, *57*(3), 541–550. doi:10.1172/JCI108309

Hooks, D. A., LeGrice, I. J., Harvey, J. D., & Smaill, B. H. (2001). Intramural multisite recording of transmembrane potential in the heart. *Biophysical journal*, *81*(5), 2671–2680. doi:10.1016/S0006-3495(01)75910-3

Horowitz, L. N., Spear, J. F., & Moore, E. N. (1976). Subendocardial origin of ventricular arrhythmias in 24-hour-old experimental myocardial infarction. *Circulation*, *53*(1), 56–63.

Horowitz, L. N., Spear, J. F., & Moore, E. N. (1981). Relation of the endocardial and epicardial ventricular fibrillation thresholds of the right and left ventricle. *The American journal of cardiology*, *48*(4), 698–701.

Huelsing, D. J., Spitzer, K. W., Cordeiro, J. M., & Pollard, A. E. (1998). Conduction between isolated rabbit Purkinje and ventricular myocytes coupled by a variable resistance. *The American journal of physiology*, *274*(4 Pt 2), H1163–73.

Huizar, J. F., Warren, M. D., Shvedko, A. G., Kalifa, J., Moreno, J., Mironov, S., Jalife, J., et al. (2007). Three distinct phases of VF during global ischemia in the isolated blood-perfused pig heart. *American journal of physiology Heart and circulatory physiology*, *293*(3), H1617–28. doi:10.1152/ajpheart.00130.2007

Ideker, R. E., Klein, G. J., Harrison, L., Smith, W. M., Kasell, J., Reimer, K. A., Wallace, A. G., et al. (1981). The transition to ventricular fibrillation induced by reperfusion after acute ischemia in the dog: a period of organized epicardial activation. *Circulation*, *63*(6), 1371–1379.

Ideker, R. E., Rogers, J., & Huang, J. (2004). Types of ventricular fibrillation: 1,2,4,5, or 3000,000? *Journal of cardiovascular electrophysiology*, *15*(12), 1441–1443. doi:10.1046/j.1540-8167.2004.04589.x

Ijiri, T., Ashihara, T., Yamaguchi, T., Takayama, K., Igarashi, T., Shimada, T., Namba, T., et al. (2008). A procedural method for modeling the purkinje fibers of the heart. *The*

journal of physiological sciences : JPS, *58*(7), 481–486. doi:10.2170/physiolsci.RP003208

Imanishi, S. (1971). Calcium-sensitive discharges in canine Purkinje fibers. *The Japanese journal of physiology*, *21*(4), 443–463.

Imanishi, S., & Surawicz, B. (1976). Automatic activity in depolarized guinea pig ventricular myocardium. Characteristics and mechanisms. *Circulation research*, *39*(6), 751–759.

Irisawa, H., Brown, H. F., & Giles, W. (1993). Cardiac pacemaking in the sinoatrial node. *Physiological reviews*, *73*(1), 197–227.

Jalife, J. (1990). Mathematical approaches to cardiac arrhythmias. *Annals of the New York Academy of Sciences*, *591*, –.

Jalife, J. (2000). Ventricular fibrillation: mechanisms of initiation and maintenance. *Annual review of physiology*, *62*, 25–50. doi:10.1146/annurev.physiol.62.1.25

Jalife, J., Delmar, M., & Davidenko, J. (1999). *Basic Cardiac Electrophysiology for the Clinician* (2nd ed.). Wiley-Blackwell.

Janse, M. J., Kleber, A. G., CAPUCCI, A., Coronel, R., & Wilms-Schopman, F. (1986). Electrophysiological basis for arrhythmias caused by acute ischemia. Role of the subendocardium. *Journal of Molecular and Cellular Cardiology*, *18*(4), 339–355.

Janse, M. J., van Capelle, F. J., Morsink, H., Kleber, A. G., Wilms-Schopman, F., Cardinal, R., d'Alnoncourt, C. N., et al. (1980). Flow of "injury" current and patterns of excitation during early ventricular arrhythmias in acute regional myocardial ischemia in isolated porcine and canine hearts. Evidence for two different arrhythmogenic mechanisms. *Circulation research*, *47*(2), 151–165.

JANSE, M., KLEBER, A., CAPUCCI, A., Coronel, R., & WILMSSCHOPMAN, F. (1986). Electrophysiological basis for arrhythmias caused by acute ischemiaRole of the subendocardium. *Journal of Molecular and Cellular Cardiology*, *18*(4), 339–355. doi:10.1016/S0022-2828(86)80898-7

Jay, V. (2000). *The extraordinary career of Dr Purkinje. Archives of pathology & laboratory medicine* (Vol. 124, pp. 662–663). doi:10.1043/0003-9985(2000)124<0662:TECODP>2.0.CO;2

Jeck, C., Pinto, J., & Boyden, P. (1995). Transient outward currents in subendocardial Purkinje myocytes surviving in the infarcted heart. *Circulation*, *92*(3), 465–473.

Johnston, G. D., Finch, M. B., McNeill, J. A., & Shanks, R. G. (1985). A comparison of the cardiovascular effects of (+)-sotalol and (+/-)-sotalol following intravenous administration in normal volunteers. *British journal of clinical pharmacology*, *20*(5), 507–510.

Joyner, R. W. (1982). Effects of the discrete pattern of electrical coupling on propagation through an electrical syncytium. *Circulation research*, *50*(2), 192–200.

Joyner, R. W., Veenstra, R., Rawling, D., & Chorro, A. (1984). Propagation through electrically coupled cells. Effects of a resistive barrier. *Biophysical journal*, *45*(5), 1017–1025. doi:10.1016/S0006-3495(84)84247-2

Kanter, H. L., Laing, J. G., Beau, S. L., Beyer, E. C., & Saffitz, J. E. (1993). Distinct patterns of connexin expression in canine Purkinje fibers and ventricular muscle. *Circulation research*, *72*(5), 1124–1131.

Karma, A. (1994). Electrical alternans and spiral wave breakup in cardiac tissue. *Chaos (Woodbury, NY)*, *4*(3), 461–472. doi:10.1063/1.166024

Kato, R., Ikeda, N., Yabek, S., & Kannan, R. (1986). Electrophysiologic effects of the levo- and dextrorotatory isomers of sotalol in isolated cardiac muscle and their in vivo pharmacokinetics. *JACC*, *7*(1), 116–125.

Katzung, B. G. (1975). Effects of extracellular calcium and sodium on depolarization-induced automaticity in guinea pig papillary muscle. *Circulation research*, *37*(1), 118–127.

Katzung, B. G. (1978). Automaticity in cardiac cells. *Life sciences*, *23*(13), 1309–1315.

Kerber, R., Spencer, K., Kallok, M., & Birkett, C. (1994). Overlapping sequential pulses. A new waveform for transthoracic defibrillation. *Circulation*.

Kewley, D., Hills, M., & Borkholder, D. (1997). Plasma-etched neural probes. *Sensors and Actuators A …*, *58*, 27–35.

Kim, Y. H., Xie, F., Yashima, M., Wu, T. J., Valderrábano, M., Lee, M. H., Ohara, T., et al. (1999). Role of papillary muscle in the generation and maintenance of reentry during ventricular tachycardia and fibrillation in isolated swine right ventricle. *Circulation*, *100*(13), 1450–1459.

Koller, M. L., Riccio, M. L., & Gilmour, R. F. (1998). Dynamic restitution of action potential duration during electrical alternans and ventricular fibrillation. *The American journal of physiology*, *275*(5 Pt 2), H1635–42.

Kondo, M., Nesterenko, V., & Antzelevitch, C. (2004). Cellular basis for the monophasic action potential. Which electrode is the recording electrode? *Cardiovascular research*, *63*(4), 635–644. doi:10.1016/j.cardiores.2004.05.003

Kovacs, G. (1994). *Enabling Technologies for Cultured Neural Networks*. (D. Stenger & T. McKenna, Eds.)Ch 7: Introduction to the Theory, Design, and Modeling of Thin-Film Microelectrodes for Neural Interfaces. (pp. 121–165). Academic Press.

Krassowska, W. (2003). Field stimulation of cardiac fibers with random spatial structure. *IEEE transactions on bio-medical engineering*, *50*(1), 33–40. doi:10.1109/TBME.2002.807324

Kupersmith, J., Li, Z. Y., & Maldonado, C. (1994). Marked action potential prolongation as a source of injury current leading to border zone arrhythmogenesis. *American Heart Journal*, *127*(6), 1543–1553.

Lal, A. (1998). *Silicon-based surgical tools*. Proceedings of the IEEE EMBS conference.

Lazzara, R., El-Sherif, N., & Scherlag, B. J. (1973). Electrophysiological properties of canine Purkinje cells in one-day-old myocardial infarction. *Circulation research*, *33*(6), 722–734.

Lazzara, R., El-Sherif, N., & Scherlag, B. J. (1975). Disorders of cellular electrophysiology produced by ischemia of the canine His bundle. *Circulation research*, *36*(3), 444–454.

Leon, L. J., & Roberge, F. A. (1991). Directional characteristics of action potential propagation in cardiac muscle. A model study. *Circulation research*, *69*(2), 378–395.

Lewis, T. J., & Guevara, M. R. (1990). Chaotic dynamics in an ionic model of the propagated cardiac action potential. *Journal of theoretical biology*, *146*(3), 407–432.

Lewis, T. J., & Guevara, M. R. (1991). 1/f alpha power spectrum of the QRS complex does not imply fractal activation of the ventricles. *Biophysical journal*, *60*(5), 1297–1305. doi:10.1016/S0006-3495(91)82165-8

Li, H. G., Jones, D. L., Yee, R., & Klein, G. J. (1993). Defibrillation shocks produce different effects on Purkinje fibers and ventricular muscle: implications for successful defibrillation, refibrillation and postshock arrhythmia. *Journal of the American College of Cardiology*, *22*(2), 607–614.

Li, L., Jin, Q., Huang, J., Cheng, K.-A., & Ideker, R. E. (2008). Intramural foci during long duration fibrillation in the pig ventricle. *Circulation research*, *102*(10), 1256–1264. doi:10.1161/CIRCRESAHA.107.170399

Li, Z. Y., Wang, Y. H., Maldonado, C., & Kupersmith, J. (1994). Role of junctional zone cells between Purkinje fibres and ventricular muscle in arrhythmogenesis. *Cardiovascular research*, *28*(8), 1277–1284.

Liu, D. W., Gintant, G. A., & Antzelevitch, C. (1993). Ionic bases for electrophysiological distinctions among epicardial, midmyocardial, and endocardial myocytes from the free wall of the canine left ventricle. *Circulation research*, *72*(3), 671–687.

Mandelbrot, B. B. (1983). *The fractal geometry of nature* (pp. 14–58;247–256). W.H. Freeman.

Marchlinski, F., Garcia, F., Siadatan, A., Sauer, W., Beldner, S., Zado, E., Hsia, H., et al. (2005). Ventricular tachycardia/ventricular fibrillation ablation in the setting of ischemic heart disease. *Journal of cardiovascular electrophysiology*, *16 Suppl 1*, S59–70. doi:10.1111/j.1540-8167.2005.50210.x

Marrouche, N. F., Verma, A., Wazni, O., Schweikert, R., Martin, D. O., Saliba, W., Kilicaslan, F., et al. (2004). Mode of initiation and ablation of ventricular fibrillation storms in patients with ischemic cardiomyopathy. *Journal of the American College of Cardiology*, *43*(9), 1715–1720. doi:10.1016/j.jacc.2004.03.004

Martinez-Palomo, A., Alanis, J., & Benitez, D. (1970). Transitional cardiac cells of the conductive system of the dog heart. Distinguishing morphological and electrophysiological features. *The Journal of cell biology*, *47*(1), 1–17.

Matsuda, K., Kamiyama, A., & Hoshi, T. (1967). Configuration of the transmembrane potential of the Purkinje-ventricular fiber junction and its analysis. (T. Sano, V. Mizuhira, & K. Matsuda, Eds.)*Electrophysiology and ultrastructure of the heart*, 177–187.

McWilliam, J. A. (1888). On the Rhythm of the Mammalian Heart. *The Journal of physiology*, *9*(2-3), 167–212.9.

Mendez, C., Mueller, W. J., & Urguiaga, X. (1970). Propagation of impulses across the Prukinje fiber-muscle junctions in the dog heart. *Circulation research*, *26*(2), 135–150.

Mendez, C., Mueller, W. J., Merideth, J., & Moe, G. K. (1969). Interaction of transmembrane potentials in canine Purkinje fibers and at Purkinje fiber-muscle junctions. *Circulation research*, *24*(3), 361–372.

Mines, G. R. (1914). On circulating excitations in heart muscles and their possible relation to tachycardia and fibrillation.

Moak, J. P., & Rosen, M. R. (1984). Induction and termination of triggered activity by pacing in isolated canine Purkinje fibers. *Circulation*, *69*(1), 149–162.

Moe, G. (1964). A computer model of atrial fibrillation. *American Heart Journal*, *67*(2), 200–220. doi:10.1016/0002-8703(64)90371-0

Monserrat, M., Saiz, J., Ferrero, J. M., Ferrero, J. M., & Thakor, N. V. (2000). Ectopic activity in ventricular cells induced by early afterdepolarizations developed in Purkinje cells. *Annals of biomedical engineering*, *28*(11), 1343–1351.

Morley, G. E., Danik, S. B., Bernstein, S., Sun, Y., Rosner, G., Gutstein, D. E., & Fishman, G. I. (2005). Reduced intercellular coupling leads to paradoxical propagation across the Purkinje-ventricular junction and aberrant myocardial activation. *Proceedings of the National Academy of Sciences of the United States of America*, *102*(11), 4126–4129. doi:10.1073/pnas.0500881102

Myerburg, R. J., GELBAND, H., & Hoffman, B. F. (1973). Confinement of premature impulses in functional compartments of regions of the A-V conducting system. *Cardiovascular research*, *7*(1), 69–81. doi:10.1093/cvr/7.1.69

Myerburg, R. J., Stewart, J. W., & Hoffman, B. F. (1970). Electrophysiological properties of the canine peripheral A-V conducting system. *Circulation research*, *26*(3), 361–378.

Nagy-Ungvarai, Z., Ungvarai, J., & Müller, S. C. (1993). Complexity in spiral wave dynamics(a)). *Chaos (Woodbury, NY)*, *3*(1), 15–19. doi:10.1063/1.165973

Najafi, K. (1986). An implantable multielectrode array with on-chip signal processing. *Solid-State Circuits*, *21*(6), 1035–1044.

Najafi, K., Wise, K. D., & Mochizuki, T. (1985). A high-yield IC-compatible multichannel recording array. *IEEE Transactions on Electron Devices*, *32*(7), 1206–1211. doi:10.1109/T-ED.1985.22102

Nerbonne, J. M., & Kass, R. S. (2005). Molecular physiology of cardiac repolarization. *Physiological reviews*, *85*(4), 1205–1253. doi:10.1152/physrev.00002.2005

Newton, J. C., Smith, W. M., & Ideker, R. E. (2004). Estimated global transmural distribution of activation rate and conduction block during porcine and canine ventricular fibrillation. *Circulation research*, *94*(6), 836–842. doi:10.1161/01.RES.0000120860.01645.17

Nogami, A. (2011). Purkinje-related arrhythmias part ii: polymorphic ventricular tachycardia and ventricular fibrillation. *Pacing and Clinical Electrophysiology*, *34*(8), 1034–1049. doi:10.1111/j.1540-8159.2011.03145.x

Nogami, A., Kubota, S., Adachi, M., & Igawa, O. (2009). Electrophysiologic and histopathologic findings of the ablation sites for ventricular fibrillation in a patient with ischemic cardiomyopathy. *Journal of interventional cardiac electrophysiology : an international journal of arrhythmias and pacing*, *24*(2), 133–137. doi:10.1007/s10840-008-9312-4

Nogami, A., Sugiyasu, A., Kubota, S., & Kato, K. (2005). Mapping and ablation of idiopathic ventricular fibrillation from the Purkinje system. *Heart rhythm : the official journal of the Heart Rhythm Society*, *2*(6), 646–649. doi:10.1016/j.hrthm.2005.02.006

Nolasco, J. B., & Dahlen, R. W. (1968). A graphic method for the study of alternation in cardiac action potentials. *Journal of applied physiology*, *25*(2), 191–196.

Okada, T., Yamada, T., Murakami, Y., Yoshida, N., Ninomiya, Y., & Toyama, J. (2007). Mapping and ablation of trigger premature ventricular contractions in a case of electrical storm associated with ischemic cardiomyopathy. *Pacing and clinical electrophysiology : PACE*, *30*(3), 440–443. doi:10.1111/j.1540-8159.2007.00689.x

Olsson, S. (1971). *Olsson BS - Monophasic action potentials of right heart. Goteborg: Elanders, 1971*. Goteborg: Elanders.

Omichi, C., Lee, M. H., Ohara, T., Naik, A. M., Wang, N. C., Karagueuzian, H. S., & Chen, P. S. (2000). Comparing cardiac action potentials recorded with metal and glass microelectrodes. *American journal of physiology Heart and circulatory physiology*, *279*(6), H3113–7.

Ouyang, P., Brinker, J. A., Bulkley, B. H., Jugdutt, B. I., & Varghese, P. J. (1981). Ischemic ventricular fibrillation: the importance of being spontaneous. *The American journal of cardiology*, *48*(3), 455–459.

Overholt, E. D., Joyner, R. W., Veenstra, R. D., Rawling, D., & Wiedmann, R. (1984). Unidirectional block between Purkinje and ventricular layers of papillary muscles. *The American journal of physiology*, *247*(4 Pt 2), H584–95.

Pak, H.-N., Kim, G. I., Lim, H. E., Fang, Y. H., Choi, J. I., Kim, J. S., Hwang, C., et al. (2008). Both Purkinje cells and left ventricular posteroseptal reentry contribute to the maintenance of ventricular fibrillation in open-chest dogs and swine: effects of catheter ablation and the ventricular cut-and-sew operation. *Circulation journal : official journal of the Japanese Circulation Society*, *72*(7), 1185–1192.

Pak, H.-N., Kim, Y.-H., Lim, H. E., Chou, C.-C., Miyauchi, Y., Fang, Y. H., Sun, K., et al. (2006). Role of the posterior papillary muscle and purkinje potentials in the mechanism of ventricular fibrillation in open chest dogs and Swine: effects of catheter ablation. *Journal of cardiovascular electrophysiology*, *17*(7), 777–783. doi:10.1111/j.1540-8167.2006.00511.x

Pak, H.-N., Oh, Y.-S., Liu, Y.-B., Wu, T.-J., Karagueuzian, H. S., Lin, S.-F., & Chen, P.-S. (2003). Catheter ablation of ventricular fibrillation in rabbit ventricles treated with beta-blockers. *Circulation*, *108*(25), 3149–3156. doi:10.1161/01.CIR.0000104563.12408.12

Pappano, A. J., & Carmeliet, E. E. (1979). Epinephrine and the pacemaking mechanism at plateau potentials in sheep cardiac Purkinje fibers. *Pflügers Archiv : European journal of physiology*, *382*(1), 17–26.

Petrov, V., Crowley, M., & Showalter, K. (1994). Tracking unstable periodic orbits in the Belousov-Zhabotinsky reaction. *Physical Review Letters*, *72*(18), 2955–2958.

Plonsey, R., & Barr, R. C. (1986a). Effect of microscopic and macroscopic discontinuities on the response of cardiac tissue to defibrillating (stimulating) currents. *Medical & biological engineering & computing*, *24*(2), 130–136.

Plonsey, R., & Barr, R. C. (1986b). Inclusion of junction elements in a linear cardiac model through secondary sources: application to defibrillation. *Medical & biological engineering & computing*, *24*(2), 137–144.

Pogwizd, S. M., & Corr, P. B. (1987). Reentrant and nonreentrant mechanisms contribute to arrhythmogenesis during early myocardial ischemia: results using three-dimensional mapping. *Circulation research*, *61*(3), 352–371.

Pogwizd, S. M., Onufer, J. R., Kramer, J. B., Sobel, B. E., & Corr, P. B. (1986). Induction of delayed afterdepolarizations and triggered activity in canine Purkinje fibers by lysophosphoglycerides. *Circulation research*, *59*(4), 416–426.

Pollard, A. E., & Barr, R. C. (1990). The construction of an anatomically based model of the human ventricular conduction system. *IEEE transactions on bio-medical engineering*, *37*(12), 1173–1185. doi:10.1109/10.64460

Pope, A. J., Sands, G. B., Smaill, B. H., & LeGrice, I. J. (2008). Three-dimensional transmural organization of perimysial collagen in the heart. *American journal of physiology Heart and circulatory physiology*, *295*(3), H1243–H1252. doi:10.1152/ajpheart.00484.2008

Posel, D., Noakes, T., Kantor, P., Lambert, M., & Opie, L. H. (1989). Exercise training after experimental myocardial infarction increases the ventricular fibrillation threshold before and after the onset of reinfarction in the isolated rat heart. *Circulation*, *80*(1), 138–145.

Qu, Z., Garfinkel, A., & Chen, P. (2000). Mechanisms of Discordant Alternans and Induction of Reentry in Simulated Cardiac Tissue. *Circulation*.

Qu, Z., Shiferaw, Y., & Weiss, J. (2007). Nonlinear dynamics of cardiac excitation-contraction coupling: An iterated map study. *Physical Review E*, *75*(1). doi:10.1103/PhysRevE.75.011927

Rawling, D. A., Joyner, R. W., & Overholt, E. D. (1985). Variations in the functional electrical coupling between the subendocardial Purkinje and ventricular layers of the canine left ventricle. *Circulation research*, *57*(2), 252–261.

Riccio, M. L., Koller, M. L., & Gilmour, R. F. (1999). Electrical restitution and spatiotemporal organization during ventricular fibrillation. *Circulation research*, *84*(8), 955–963.

Roger, V., Go, A., Lloyd-Jones, D., & Adams, R. (2011). Heart Disease and Stroke Statistics - 2011 Update. *Circulation*, A report from the American Heart Association, *123*, e18–e209. doi:10.1161/CIR.0b013e3182009701

Roguin, A. (2006). *Wilhelm His Jr. (1863-1934)--the man behind the bundle. Heart rhythm : the official journal of the Heart Rhythm Society* (Vol. 3, pp. 480–483). doi:10.1016/j.hrthm.2005.11.020

Rohr, S. (2004). Role of gap junctions in the propagation of the cardiac action potential. *Cardiovascular research*, *62*(2), 309–322. doi:10.1016/j.cardiores.2003.11.035

Rohr, S., Kucera, J. P., Fast, V. G., & Kleber, A. G. (1997). Paradoxical improvement of impulse conduction in cardiac tissue by partial cellular uncoupling. *Science*, *275*(5301), 841–844.

Romero, D., Sachse, F., Sebastian, R., & Frangi, A. (2011). *Towards high resolution computational models of the cardiac conduction system: A pipeline for characterization of Purkinje-ventricular-junctions* (Vol. 6666, pp. 28–35). Berlin, Heidelberg: Springer Berlin Heidelberg. doi:10.1007/978-3-642-21028-0_4

Romero, D., Sebastian, R., Bijnens, B. H., Zimmerman, V., Boyle, P. M., Vigmond, E. J., & Frangi, A. F. (2010). Effects of the purkinje system and cardiac geometry on biventricular pacing: a model study. *Annals of biomedical engineering*, *38*(4), 1388–1398. doi:10.1007/s10439-010-9926-4

Rosen, M. R., & Reder, R. F. (1981). Does triggered activity have a role in the genesis of cardiac arrhythmias? *Annals of internal medicine*, *94*(6), 794–801.

Rosen, M. R., Fisch, C., Hoffman, B. F., Danilo, P., Lovelace, D. E., & Knoebel, S. B. (1980). Can accelerated atrioventricular junctional escape rhythms be explained by delayed afterdepolarizations? *The American journal of cardiology*, *45*(6), 1272–1284.

Rosen, M. R., GELBAND, H., & Hoffman, B. F. (1973a). Correlation between effects of ouabain on the canine electrocardiogram and transmembrane potentials of isolated Purkinje fibers. *Circulation*, *47*(1), 65–72.

Rosen, M. R., GELBAND, H., Merker, C., & Hoffman, B. F. (1973b). Mechanisms of digitalis toxicity. Effects of ouabain on phase four of canine Purkinje fiber transmembrane potentials. *Circulation*, *47*(4), 681–689.

Rosen, M. R., Moak, J. P., & Damiano, B. (1984). The clinical relevance of afterdepolarizations. *Annals of the New York Academy of Sciences*, *427*, 84–93.

Scherlag, B. J., El-Sherif, N., Hope, R., & Lazzara, R. (1974). Characterization and localization of ventricular arrhythmias resulting from myocardial ischemia and infarction. *Circulation research*, *35*(3), 372–383.

Schnabel, P. A., Richter, J., Schmiedl, A., Ramsauer, B., Bartels, U., Gebhard, M. M., Mall, G., et al. (1991). The ultrastructural effects of global ischaemia on Purkinje fibres compared with working myocardium: a qualitative and morphometric investigation on the canine heart. *Virchows Archiv. A, Pathological anatomy and histopathology*, *418*(1), 17–25.

Selvester, R. H., Kirk, W. L., & Pearson, R. B. (1970). Propagation velocities and voltage magnitudes in local segments of dog myocardium. *Circulation research*, *27*(4), 619–629.

Shabetai, R., Surawicz, B., & Hammill, W. (1968). Monophasic action potentials in man. *Circulation*, *38*(2), 341–352.

Shakhashiri, B. (1989). *Chemical Demonstrations: A Handbook for Teachers of Chemistry* (Vol. 1). Univ. of Wisconsin Press

Madison, WI.

Sharifov, O. F., & Fast, V. G. (2003). Optical mapping of transmural activation induced by electrical shocks in isolated left ventricular wall wedge preparations. *Journal of cardiovascular electrophysiology*, *14*(11), 1215–1222.

Shaw, R., & Rudy, Y. (1995). The Vulnerable Window for Unidirectional Block in Cardiac Tissue:. *Journal of cardiovascular electrophysiology*, Characterization and Dependence on Membrane Excitability and Intercellular Coupling, *6*(2), 115–131. doi:10.1111/j.1540-8167.1995.tb00763.x

Sheets, M. F., January, C. T., & Fozzard, H. A. (1983). Isolation and characterization of single canine cardiac purkinje cells. *Circulation research*, *53*(4), 544–548.

Shiferaw, Y., Chen, P., & Garfinkel, A. (2006). From Pulsus to Pulseless. *Circulation*.

Shimada, T., Kawazato, H., Yasuda, A., Ono, N., & Sueda, K. (2004). Cytoarchitecture and intercalated disks of the working myocardium and the conduction system in the mammalian heart. *The anatomical record. Part A, Discoveries in molecular, cellular, and evolutionary biology*, *280*(2), 940–951. doi:10.1002/ar.a.20109

Shimizu, W., & Antzelevitch, C. (2000). Differential effects of beta-adrenergic agonists and antagonists in LQT1, LQT2 and LQT3 models of the long QT syndrome. *Journal of the American College of Cardiology*, *35*(3), 778–786.

Shinbrot, T., Ditto, W., Grebogi, C., Ott, E., Spano, M., & Yorke, J. (1992). Using the sensitive dependence of chaos (the "butterfly effect") to direct trajectories in an experimental chaotic system. *Physical Review Letters*, *68*(19), 2863–2866.

Sicouri, S. (1991). A subpopulation of cells with unique electrophysiological properties in the deep subepicardium of the canine ventricle. The M cell. *Circulation research*.

Sicouri, S., & Antzelevitch, C. (1991). A subpopulation of cells with unique electrophysiological properties in the deep subepicardium of the canine ventricle. The M cell. *Circulation research*, *68*(6), 1729–1741.

Sicouri, S., Moro, S., & Elizari, M. V. (1997). d-Sotalol Induces Marked Action Potential Prolongation and Early Afterdepolarizations in M but Not Epicardial or Endocardial Cells of the Canine Ventricle. *Journal of Cardiovascular Pharmacology and Therapeutics*, *2*(1), 27–37. doi:10.1177/107424849700200104

Sinha, A.-M., Schmidt, M., Marschang, H., Gutleben, K., Ritscher, G., Brachmann, J., & Marrouche, N. F. (2009). Role of left ventricular scar and Purkinje-like potentials during mapping and ablation of ventricular fibrillation in dilated cardiomyopathy.

Pacing and clinical electrophysiology : PACE, *32*(3), 286–290. doi:10.1111/j.1540-8159.2008.02233.x

Sola, O. M., Sauvage, L. R., Kakulas, B. A., Howell, J. M. C., Shi, Q., Mungin, D. L., Salama, N. V., et al. (n.d.). Acetylcholinesterase staining of Purkinje fibers. *The Hope Heart Institute*. Retrieved July 16, 2012, from http://www.hopeheart.org/downloads/ACETYLCHOLINESTERASE%20STAINING%20OF%20PURKINJE%20FIBERS.pdf

Solberg, L. E., Singer, D. H., Eick, ten, R. E., & Duffin, E. G. (1974). Glass microelectrode studies on intramural papillary muscle cells. Description of preparation and studies on normal dog papillary muscle. *Circulation research*, *34*(6), 783–797.

Sommer, J., & Johnson, E. (1968). Cardiac muscle. *J. Cell Biol*, A comparative study of Purkinje fibers and ventricular fibers. Retrieved January 6, 2012, from http://jcb.rupress.org/content/36/3/497.long

Son, I., Lal, A., & Hubbard, B. (2001). A multifunctional silicon-based microscale surgical system. *Sensors and Actuators A: Physical*, *91*, 351–356.

SPACH, M. S., & Dolber, P. C. (1986). Relating extracellular potentials and their derivatives to anisotropic propagation at a microscopic level in human cardiac muscle. Evidence for electrical uncoupling of side-to-side fiber connections with increasing age. *Circulation research*, *58*(3), 356–371.

SPACH, M. S., HUANG, S. N., & AYERS, C. R. (1963). Electrical and anatomic study of the Purkinje system of the canine heart. *American Heart Journal*, *65*, 664–673.

Sperelakis, N. (1979). *Sperelakis N. Origin of the cardiac resting potential. In: Berne RM, et al - Eds - Handbook of Physiology, The Cardiovascular System. Bethesda, MD: American Physiological Society, 1979: 188, 193, 211, 257*. Handbook of Physiology. The ….

Stankovicová, T., Bito, V., Heinzel, F., Mubagwa, K., & Sipido, K. R. (2003). Isolation and morphology of single Purkinje cells from the porcine heart. *General physiology and biophysics*, *22*(3), 329–340.

Starmer, C. (2007). Vulnerability of cardiac dynamics. *Scholarpedia*, *2*(11), 1847. doi:10.4249/scholarpedia.1847

Steinhaus, B. M. (1989). Estimating cardiac transmembrane activation and recovery times from unipolar and bipolar extracellular electrograms: a simulation study. *Circulation research*, *64*(3), 449–462.

Suma, K. (2001). *Sunao Tawara: a father of modern cardiology. Pacing and clinical electrophysiology : PACE* (Vol. 24, pp. 88–96).

Szumowski, L., Sanders, P., Walczak, F., Hocini, M., Jaïs, P., Kepski, R., Szufladowicz, E., et al. (2004). Mapping and ablation of polymorphic ventricular tachycardia after myocardial infarction. *Journal of the American College of Cardiology*, *44*(8), 1700–1706. doi:10.1016/j.jacc.2004.08.034

Tabereaux, P. B., Dosdall, D. J., & Ideker, R. E. (2009). Mechanisms of VF maintenance: wandering wavelets, mother rotors, or foci. *Heart rhythm : the official journal of the Heart Rhythm Society*, *6*(3), 405–415. doi:10.1016/j.hrthm.2008.11.005

Tabereaux, P. B., Walcott, G. P., Rogers, J. M., Kim, J., Dosdall, D. J., Robertson, P. G., Killingsworth, C. R., et al. (2007). Activation patterns of Purkinje fibers during long-duration ventricular fibrillation in an isolated canine heart model. *Circulation*, *116*(10), 1113–1119. doi:10.1161/CIRCULATIONAHA.107.699264

Tae Hwan Yoon, Eun Jung Hwang, Dong Yong Shin, Se Ik Park, Seung Jae Oh, Sung Cherl Jung, Hyung Cheul Shin, et al. (2000). A micromachined silicon depth probe for multichannel neural recording. *IEEE transactions on bio-medical engineering*, *47*(8), 1082–1087. doi:10.1109/10.855936

Taggart, P., Sutton, P. M., Spear, D. W., Drake, H. F., Swanton, R. H., & Emanuel, R. W. (1988). Simultaneous endocardial and epicardial monophasic action potential recordings during brief periods of coronary artery ligation in the dog: influence of adrenaline, beta blockade and alpha blockade. *Cardiovascular research*, *22*(12), 900–909.

Tolkacheva, E., Schaeffer, D., Gauthier, D., & Krassowska, W. (2003). Condition for alternans and stability of the 1:1 response pattern in a “memory” model of paced cardiac dynamics. *Physical Review E*, *67*(3). doi:10.1103/PhysRevE.67.031904

Tranum-Jensen, J., Wilde, A. A., Vermeulen, J. T., & Janse, M. J. (1991). Morphology of electrophysiologically identified junctions between Purkinje fibers and ventricular muscle in rabbit and pig hearts. *Circulation research*, *69*(2), 429–437.

Tusscher, Ten, K., & Panfilov, A. (2008). Modelling of the ventricular conduction system. *Progress in biophysics and molecular biology*, *7*(26), 152–170.

Ursell, P. C., Gardner, P. I., Albala, A., Fenoglio, J. J., & Wit, A. L. (1985). Structural and electrophysiological changes in the epicardial border zone of canine myocardial infarcts during infarct healing. *Circulation research*, *56*(3), 436–451.

Vanag, V., Yang, L., Dolnik, M., Zhabotinsky, A., & Epstein, I. (2000). Oscillatory cluster patterns in a homogeneous chemical system with global feedback. *Nature*, *406*(6794), 389–391. doi:10.1038/35019038

VANDAM, R., & Durrer, D. (1961). Experimental study on the intramural distribution of the excitability cycle and on the form of the epicardial T wave in the dog heart in situ1. *American Heart Journal*, *61*(4), 537–542. doi:10.1016/0002-8703(61)90554-3

Veenstra, R. D., Joyner, R. W., & Rawling, D. A. (1984). Purkinje and ventricular activation sequences of canine papillary muscle. Effects of quinidine and calcium on the Purkinje-ventricular conduction delay. *Circulation research*, *54*(5), 500–515.

Verkerk, A. O., Tan, H. L., Kirkels, J. H., & Ravesloot, J. H. (2003). Role of Ca2+-activated Cl- current during proarrhythmic early afterdepolarizations in sheep and human ventricular myocytes. *Acta physiologica Scandinavica*, *179*(2), 143–148.

Verkerk, A. O., Veldkamp, M. W., Abbate, F., Antoons, G., Bouman, L. N., Ravesloot, J. H., & van Ginneken, A. C. (1999). Two types of action potential configuration in single cardiac Purkinje cells of sheep. *The American journal of physiology*, *277*(4 Pt 2), H1299–310.

Vigmond, E. (1999). Electrophysiological basis of mono-phasic action potential recordings. *Medical and Biological Engineering and ….*

Vigmond, E. J., & Clements, C. (2007). Construction of a computer model to investigate sawtooth effects in the Purkinje system. *IEEE transactions on bio-medical engineering*, *54*(3), 389–399. doi:10.1109/TBME.2006.888817

Virágh, S., & Challice, C. E. (1973). Origin and differentiation of cardiac muscle cells in the mouse. *Journal of ultrastructure research*, *42*(1), 1–24.

Viswanathan, P. C., Shaw, R. M., & Rudy, Y. (1999). Effects of IKr and IKs heterogeneity on action potential duration and its rate dependence: a simulation study. *Circulation*, *99*(18), 2466–2474.

Wan, X., Laurita, K. R., Pruvot, E. J., & Rosenbaum, D. S. (2005). Molecular correlates of repolarization alternans in cardiac myocytes. *Journal of Molecular and Cellular Cardiology*, *39*(3), 419–428. doi:10.1016/j.yjmcc.2005.06.004

Weidmann, R., Tan, R., & Joyner, R. (1996, October). Discontinuous conduction at Purkinje-ventricular muscle junction. *ajpheart.physiology.org*. Retrieved January 11, 2012, from http://ajpheart.physiology.org/content/271/4/H1507.abstract

Weiss, J. N., Garfinkel, A., Karagueuzian, H. S., Qu, Z., & Chen, P. S. (1999). Chaos and the transition to ventricular fibrillation: a new approach to antiarrhythmic drug evaluation. *Circulation*, *99*(21), 2819–2826.

WEISSENBURGER, J., NESTERENKO, V. V., & Antzelevitch, C. (2000). Transmural Heterogeneity of Ventricular Repolarization Under Baseline and Long QT Conditions in the Canine Heart In Vivo: Torsades de Pointes Develops with Halothane but not Pentobarbital Anesthesia. *Journal of cardiovascular electrophysiology*, *11*(3), 290–304. doi:10.1111/j.1540-8167.2000.tb01798.x

Wilson, L. D., Jennings, M. M., & Rosenbaum, D. S. (2011). Point: M cells are present in the ventricular myocardium. *Heart rhythm : the official journal of the Heart Rhythm Society*, *8*(6), 930–933. doi:10.1016/j.hrthm.2011.01.026

Winfree, A. (2001). *The Geometry of Biological Time*. (J. Marsden, S. Wiggins, & L. Sirovich, Eds.). University of Arizona

Tucson, AZ.

Wise, K. D., Angell, J. B., & Starr, A. (1970). An integrated-circuit approach to extracellular microelectrodes. *IEEE transactions on bio-medical engineering*, *17*(3), 238–247.

Wit, A. L., Cranefield, P. F., & Hoffman, B. F. (1972). Slow conduction and reentry in the ventricular conducting system. II. Single and sustained circus movement in networks of canine and bovine Purkinje fibers. *Circulation research*, *30*(1), 11–22.

Wit, A., & Rosen, M. (n.d.). *The heart and cardiovascular system*. Afterdepolarizations and triggered activity: distinction from automaticity as an arrhythmogenic mechanism (1986th ed. pp. 1449–1490). Raven Press, New York.

Witkowski, F., Leon, L., Penkoske, P., & Giles, W. (1998). Spatiotemporal evolution of ventricular fibrillation. *Nature*, *392*, 78–82.

WOODBURY, L. A., Woodbury, J. W., & Hecht, H. H. (1950). Membrane resting and action potentials of single cardiac muscle fibers. *Circulation*, *1*(2), 264–266.

Worley, S. J., Swain, J. L., Colavita, P. G., Smith, W. M., & Ideker, R. E. (1985). Development of an endocardial-epicardial gradient of activation rate during electrically induced, sustained ventricular fibrillation in dogs. *The American journal of cardiology*, *55*(6), 813–820.

Wu, G., Littmann, L., Svenson, R. H., Nanney, G. A., Tatsis, G. P., Tuntelder, J. R., Chuang, C. H., et al. (1995). Computerized three-dimensional activation mapping study of spontaneous ventricular arrhythmias during acute myocardial ischemia in dogs. Evidence against macroreentrant mechanism. *Journal of electrocardiology*, *28*(2), 115–130.

Wu, T.-J., Lin, S.-F., Hsieh, Y.-C., Chiu, Y.-T., & Ting, C.-T. (2009). Repetitive endocardial focal discharges during ventricular fibrillation with prolonged global ischemia in isolated rabbit hearts. *Circulation journal : official journal of the Japanese Circulation Society*, *73*(10), 1803–1811.

Xie, F., Qu, Z., & Garfinkel, A. (2001). Electrophysiological heterogeneity and stability of reentry in simulated cardiac tissue. *American Journal of …*

Xie, F., Qu, Z., Yang, J., Baher, A., Weiss, J. N., & Garfinkel, A. (2004). A simulation study of the effects of cardiac anatomy in ventricular fibrillation. *The Journal of clinical investigation*, *113*(5), 686–693. doi:10.1172/JCI17341

Xing, D., Kjølbye, A. L., Nielsen, M. S., Petersen, J. S., Harlow, K. W., Holstein-Rathlou, N.-H., & Martins, J. B. (2003). ZP123 increases gap junctional conductance and

prevents reentrant ventricular tachycardia during myocardial ischemia in open chest dogs. *Journal of cardiovascular electrophysiology*, *14*(5), 510–520.

Yan, G. X., Shimizu, W., & Antzelevitch, C. (1998). Characteristics and distribution of M cells in arterially perfused canine left ventricular wedge preparations. *Circulation*, *98*(18), 1921–1927.

Zhabotinsky, A. (1964). *Periodic processes of malonic acid oxidation in a liquid phase* (Vol. 9, pp. 306–311). Biofizika.

Zhang, Y., & Mazgalev, T. N. (2009). Site of origin of the monophasic action potential: which electrode, the "potassium" or the “indifferent,” records monophasic action potential? *Heart rhythm : the official journal of the Heart Rhythm Society*, *6*(4), 561–563. doi:10.1016/j.hrthm.2008.12.022

Zheng, Z. J., Croft, J. B., Giles, W. H., & Mensah, G. A. (2001). Sudden cardiac death in the United States, 1989 to 1998. *Circulation*, *104*(18), 2158–2163.

Zicha, S., Xiao, L., Stafford, S., Cha, T. J., Han, W., Varro, A., & Nattel, S. (2004). Transmural expression of transient outward potassium current subunits in normal and failing canine and human hearts. *The Journal of physiology*, *561*(Pt 3), 735–748. doi:10.1113/jphysiol.2004.075861

Zipes, D. P., Arbel, E., Knope, R. F., & Moe, G. K. (1974). Accelerated cardiac escape rhythms caused by ouabain intoxication. *The American journal of cardiology*, *33*(2), 248–253.

Zipes, D. P., Foster, P. R., Troup, P. J., & Pedersen, D. H. (1979). Atrial induction of ventricular tachycardia: reentry versus triggered automaticity. *The American journal of cardiology*, *44*(1), 1–8.